AFRL-VA-WP-TR-2001-3037

STRUCTURAL TECHNOLOGY AND ANALYSIS PROGRAM (STAP)
Delivery Order 0004: Durability Patch

Roy Ikegami
Eric Haugse
Angela Trego

Boeing Phantom Works
P.O. Box 3707
Seattle, WA 98124-2207

Lynn Rogers and Joe Maly

CSA Engineering

JUNE 2001

Final Report for 01 May 1995 – 29 June 2001

AIR VEHICLES DIRECTORATE
AIR FORCE RESEARCH LABORATORY
AIR FORCE MATERIEL COMMAND
WRIGHT-PATTERSON AIR FORCE BASE, OH 45433-7542

NOTICE

USING GOVERNMENT DRAWINGS, SPECIFICATIONS, OR OTHER DATA INCLUDED IN THIS DOCUMENT FOR ANY PURPOSE OTHER THAN GOVERNMENT PROCUREMENT DOES NOT IN ANY WAY OBLIGATE THE U.S. GOVERNMENT. THE FACT THAT THE GOVERNMENT FORMULATED OR SUPPLIED THE DRAWINGS, SPECIFICATIONS, OR OTHER DATA DOES NOT LICENSE THE HOLDER OR ANY OTHER PERSON OR CORPORATION; OR CONVEY ANY RIGHTS OR PERMISSION TO MANUFACTURE, USE OR SELL ANY PATENTED INVENTION THAT MAY RELATE TO THEM.

THIS REPORT IS RELEASABLE TO THE NATIONAL TECHNICAL INFORMATION SERVICE (NTIS). AT NTIS, IT WILL BE AVAILABLE TO THE GENERAL PUBLIC, INCLUDING FOREIGN NATIONS.

THIS TECHNICAL REPORT HAS BEEN REVIEWED AND IS APPROVED FOR PUBLICATION.

Do not return copies of this report unless contractual obligations or notice on a specific document requires its return.

David L. Banaszak, Project Engineer
Analytical Structural Mechanics Branch
Structures Division

JAMES W. ROGERS JR., MAJ, USAF
Chief, Analytical Structural Mechanics Branch
Structures Division
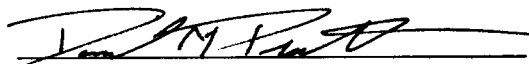
DAVID M. PRATT, PhD
Technical Advisor
Structures Division

REPORT DOCUMENTATION PAGE		*Form Approved* *OMB No. 0704-0188*

The public reporting burden for this collection of information is estimated to average 1 hour per response, including the time for reviewing instructions, searching existing data sources, searching existing data sources, gathering and maintaining the data needed, and completing and reviewing the collection of information. Send comments regarding this burden estimate or any other aspect of this collection of information, including suggestions for reducing this burden, to Department of Defense, Washington Headquarters Services, Directorate for Information Operations and Reports (0704-0188), 1215 Jefferson Davis Highway, Suite 1204, Arlington, VA 22202-4302. Respondents should be aware that notwithstanding any other provision of law, no person shall be subject to any penalty for failing to comply with a collection of information if it does not display a currently valid OMB control number. **PLEASE DO NOT RETURN YOUR FORM TO THE ABOVE ADDRESS.**

1. REPORT DATE *(DD-MM-YY)* June 2001	2. REPORT TYPE Final	3. DATES COVERED *(From - To)* 05/01/ 1995 – 06/29/2001

4. TITLE AND SUBTITLE	5a. CONTRACT NUMBER F33615-95-D-3203
STRUCTURAL TECHNOLOGY AND ANALYSIS PROGRAM (STAP) Delivery Order 0004: Durability Patch	5b. GRANT NUMBER
	5c. PROGRAM ELEMENT NUMBER 69199F

6. AUTHOR(S)	5d. PROJECT NUMBER 0AFF
Roy Ikegami (Boeing Phantom Works) Eric Haugse (Boeing Phantom Works) Angela Trego (Boeing Phantom Works)	5e. TASK NUMBER 02
Lynn Rogers (CSA Engineering) Joe Maly (CSA Engineering)	5f. WORK UNIT NUMBER 00

7. PERFORMING ORGANIZATION NAME(S) AND ADDRESS(ES)		8. PERFORMING ORGANIZATION REPORT NUMBER
Boeing Phantom Works P.O. Box 3707 Seattle, WA 98124-2207	CSA Engineering	

9. SPONSORING/MONITORING AGENCY NAME(S) AND ADDRESS(ES)	10. SPONSORING/MONITORING AGENCY ACRONYM(S) AFRL/ VASM
Air Vehicles Directorate Air Force Research Laboratory Air Force Materiel Command Wright-Patterson Air Force Base, OH 45433-7542	11. SPONSORING/MONITORING AGENCY REPORT NUMBER(S) AFRL-VA-WP-TR-2001-3037

12. DISTRIBUTION/AVAILABILITY STATEMENT
Approved for public release; distribution is unlimited.

13. SUPPLEMENTARY NOTES
Report contains color.

14. ABSTRACT *(Maximum 200 Words)*

Structural cracks in secondary structure, resulting from a high cycle fatigue (HCF) environment, are often referred to as nuisance cracks. This type of damage can result in costly inspections and repair. The repairs often do not last long because the repaired structure continues to respond in a resonant fashion to the environment. Although the use of materials for passive damping applications is well understood, there are few applications to high-cycle fatigue problems. This is because design information characterizing temperature, resonant response frequency and strain levels are difficult to determine.

The Durability Patch and Damage Dosimeter Program addressed these problems by 1) Developing a damped repair design process which includes a methodology for designing the material and application characteristics required to optimally damp the repair. 2) Designing and developing a rugged, small, and lightweight data acquisition unit called the damage dosimeter. This is a battery operated, single board computer, capable of collecting three channels of strain and one channel of temperature, processing this data by user developed algorithms written in the C programming language, and storing the processed data in resident memory. The dosimeter is used to provide flight data needed to characterize the vibration environment. The vibration environment is then used to design the damping material characteristics and repair.

The repair design methodology and dosimeter were demonstrated on B-52, C-130, and F-15 aircraft applications.

15. SUBJECT TERMS

bonded repair, damped repair, high cycle fatigue, damage dosimeter, health monitoring, aging aircraft, structural integrity

16. SECURITY CLASSIFICATION OF:			17. LIMITATION OF ABSTRACT: SAR	18. NUMBER OF PAGES 146	19a. NAME OF RESPONSIBLE PERSON (Monitor) David Banaszak
a. REPORT Unclassified	b. ABSTRACT Unclassified	c. THIS PAGE Unclassified			19b. TELEPHONE NUMBER *(Include Area Code)* (937) 904-6859

Standard Form 298 (Rev. 8-98)
Prescribed by ANSI Std. Z39-18

i

TABLE OF CONTENTS

TABLE OF CONTENTS (Continued)

LIST OF FIGURES

LIST OF FIGURES (Continued)

LIST OF TABLES

FOREWORD

This report, prepared by the Boeing Phantom Works, is the final report provided under the Structural Technology and Analysis Program (STAP) Durability Patch (Delivery Order No. 0004). Air Force funding is under Contract No. F33615-95-D-3203.

1 EXECUTIVE SUMMARY

Structural cracks in secondary structure, resulting from a high cycle fatigue (HCF) environment, are often referred to as nuisance cracks. This type of damage can result in costly inspection and repair. The repairs often do not last long because the repaired structure continues to respond in a resonant fashion to the environment. Although the use of visco-elastic materials for passive damping applications is well understood, there are few applications to high-cycle fatigue problems. This is because design information characterizing temperature, resonant response frequency and strain levels are difficult to determine. The Durability Patch and Damage Dosimeter Program tries to resolve these problems with the application of compact, stand-alone, electronics and a damped bonded repair patch.

The Durability Patch and Damage Dosimeter Program goal is to develop an optimal design methodology for repair of secondary structure. Since this structure is not flight critical, it typically does not carry very high loads and is often minimum gage. The durability patch is designed to both restore structural integrity and to increase the structure's damping in the repair region. Increased damping leads to reduced resonant response, which in turn enables the repair to survive the life of the aircraft. In order to design a repair with effective damping properties, the in-service structural strains and temperatures must be known for the in-service structure. This is because damping material properties are a function of both frequency and temperature. Additionally, to optimize the placement of the damping treatment, the strain energy distribution in the resonant mode of interest must be known. A stand-alone data acquisition system was developed to allow an engineer to easily install instrumentation on an in-service aircraft and monitor temperature and structural dynamic characteristics. This provides the information required to design a repair with optimal strength and damping effectiveness. An overview of the Durability Patch Design Process is shown in Figure 1.
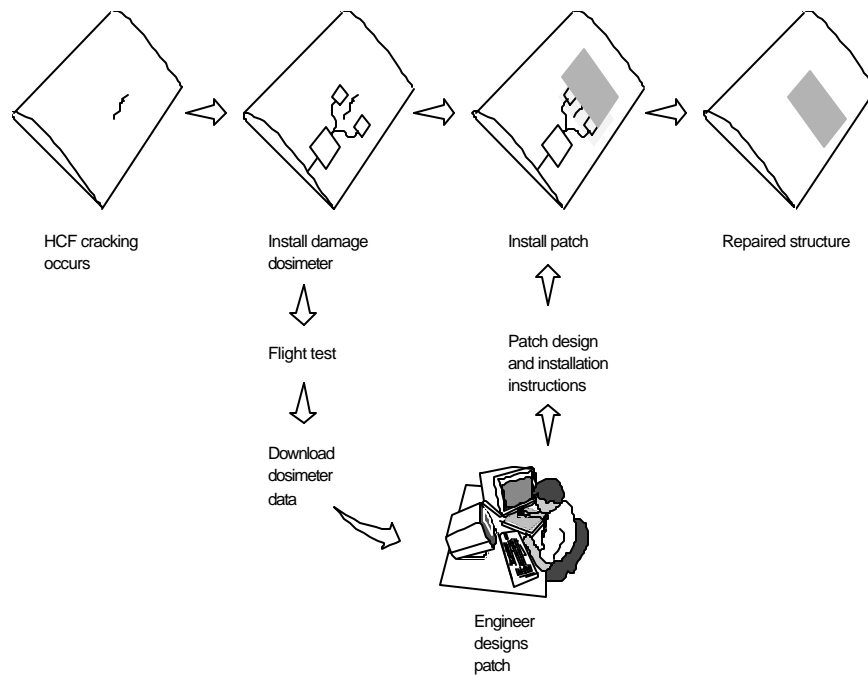
Figure 1. Durability Patch Design Process

1

The illustration shown in figure 1 identifies the steps in an idealized procedure to design and install a damped repair for secondary structure. The damage dosimeter, shown in figure 2, is the stand-alone data acquisition system developed to gather the design information (structural strain and temperature) for the repair. It also checks the effectiveness of the repair after installation. In order to minimize the impact on an aircraft's normal operations, the damage dosimeter does not require aircraft power, cooling, or access to standard aircraft data buses. This greatly reduces the amount and severity of modifications to the aircraft in order to use a damage dosimeter. It greatly reduces the amount of effort and calendar time required to fly additional instrumentation on a military aircraft. In addition to being battery powered, the damage dosimeter operates autonomously which reduces interference with the aircraft and its crew.
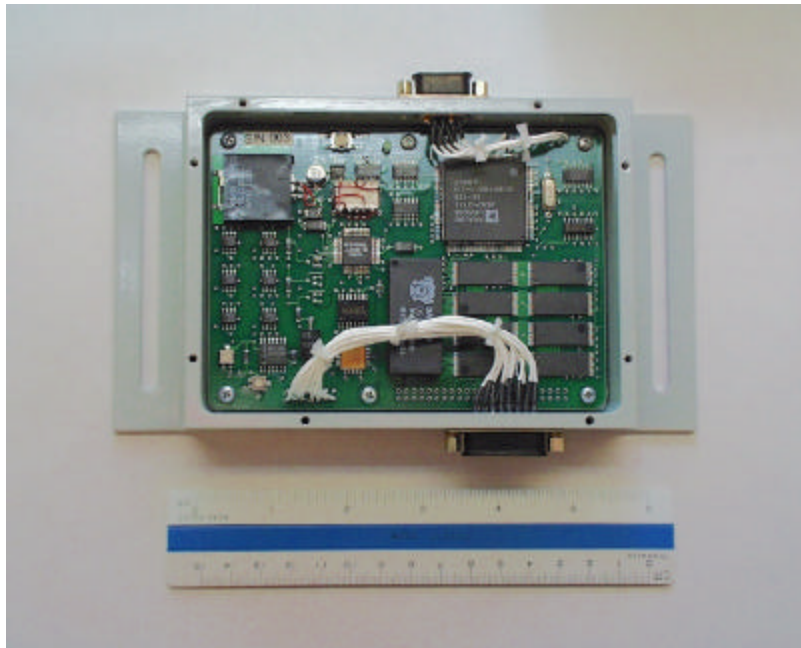
Figure 2. Damage Dosimeter

Three service applications were used to assess the damage dosimeter and durability patch design process. The first is a high-cycle fatigue application on the B-52 aircraft. It researches initially believed that this application would require a durability patch attached to the exterior fuselage. After using the damage dosimeter and discussions with the B-52 SPO, a damping treatment was installed on the interior skin of the airplane. The second application, was to evaluate the dynamic characteristics for an F-15 access panel on the underside of the airplane. This location was previously evaluated and a durability patch had been installed. The purpose of this application was to confirm performance of the damage dosimeter and patch design process with prior known data. and to evaluate the dosimeter in a relatively severe fighter environment. The third application, was to evaluate the environment on the edge of the flap well of a C-130 aircraft. This location has experienced cracking.The following sections present an introduction, a technical description of the durability patch design process, damage dosimeter development, flightline installation procedures and three aircraft service applications.

2   INTRODUCTION

The Durability Patch Program addresses the restoration of structural integrity of cracked secondary structure induced by resonant high-cycle fatigue. The program adapts technology from three basic areas: (1) bonded structural repair, (2) viscoelastic passive damping and (3) flight data instrumentation. These three areas each possess a large technology base and have a maturity sufficient to support the durability patch program.

A typical durability patch repair would be for a crack less than four inches (4 mm) long in 0.050 (1.25 mm) inch thick skin on the upper trailing edge of a wing. Typical sources of excitation include: (1) pressure pulses from engine first stage compressor, (2) jet engine exhaust, (3) disturbed air flow behind stores, (4) separated flow on upper wing, (5) air flow around open cavities, and (6) propeller tip vortices, etc.

2.1 HIGH CYCLE FATIGUE REDUCTION OF MATERIAL LIFE

Characterizing high-cycle fatigue life and crack growth rates are required to evaluate the longevity of structural repair. The methodology for calculation of resonant high-cycle fatigue (HCF), sometimes called sonic fatigue or acoustic fatigue life and associated crack growth rates is well established and consistent with standard industry practice (refs. 1, 2, 3, 4 and 5). In most cases, the HCF damage is due to linear resonant response in a single vibration mode. This implies that the vibratory stress is a narrow band random process. Usually the minimum number of cycles for high-cycle fatigue is 10^6 cycles. Fatigue consists of crack initiation, propagation and final rupture. The termination of the crack initiation phase is arbitrary since it depends on what is detectable and on what is acceptable in service.

Typical locations affected by high-cycle fatigue cracking are: (1) flap skins, (2) spoiler skins, (3) rudder skins, (4) aileron skins, (5) weapon bay doors, (6) wing trailing edges.

The basis for fatigue is the following equation relating stress to application fatigue cycles.

$$S = S_{UHCF} N^b$$

In the equation, S represents the root mean square (RMS) stress. The coefficient S_{UHCF} may be considered to be a hypothetical ultimate high-cycle fatigue (UHCF)stress which would cause failure at the first cycle, N is the fatigue life in number of cycles, and b is the Basquin parameter or exponent. This equation describes stress as a function of life and is a straight line when plotted on a log-log scale. For 2024 aluminum, the value of the Basquin parameter is 0.1772 and the value of the coefficient is 98.26 ksi. For these values, a stress improvement factor (SIF) of 2 results in a life improvement factor (LIF) of 50, and fatigue strengths of (8.5 and 2.5 ksi) at 10^6 and 10^9 cycles respectively. Other aluminum alloys are similar. Since HCF begins at 10^6 cycles, the upper threshold of interest for most aluminum is (8.5 ksi) RMS, or a strain of approximately 850 microstrain RMS. This corresponds to approximately 3000 microstrain peak. Because of stress concentrations, uncertainties in locating strain

gages, and averaging effects, measured strains are somewhat less. One objective is to reduce the stress level such that life is enhanced. Stress levels can be significantly reduced through structural enhancement using bonded repair techniques and through vibration damping using visco-elastic materials (VEM).

2.2 BONDED REPAIR

The technology base for application of bonded repairs to aircraft structure has maturity sufficient to support this effort. Structural repair materials, structural adhesives, surface preparation techniques, design methods, and installation processing and procedures are well established and documented (refs. 6, 7 and 8). There are many applications performing satisfactorily in service, for primary structures. One recommended design practice is that the repair matches the extensional membrane stiffness of the baseline structure in order to avoid load attraction or shedding. Single sided repair results in eccentricity of load and induces bending stresses.

The design concepts for patches used in bonded repair of primary structure are monolithic and laminated. Structural patch materials commonly include: (1) aluminum, (2) fiber metal laminate (FML, e.g., GLARE, an aluminum and fiber glass (FG) laminate), (3) graphite fiber/epoxy prepreg, and (4) boron fiber/epoxy prepreg.

2.3 DAMPING

RMS stress level at a resonant frequency is approximately proportional to the square root of modal damping. Consequently, damping is a very useful approach for vibratory stress reduction. Modal damping is dependent on the dynamic mechanical properties of the viscoelastic material (VEM), which in turn are dependent on service temperature and vibration frequency of the structure. It is therefore necessary to determine the vibration frequency and temperature at which damage accumulates in service. The temperature and strain time histories must be collected at the location of HCF cracking. Visco-elastic vibration damping technology has a level of maturity sufficient to support this effort (ref. 3). Conventional constrained layer damping is flying in service on external surfaces subjected to direct air flow. Some of these applications use an edge sealant and some have their perimeter adhesive bonded. The intrinsic damping in secondary structure is generally low. This fact makes the structure more susceptible to resonant HCF cracking. This fact also increases the benefits of damping because RMS stress levels are highly dependent on modal damping. High levels of damping will enhance the life of the repaired skin as well as the adjacent bays of skin and substructure. The modal strain energy (MSE) method has been established as the proper approach to calculate modal damping (refs. 9, 10 and 11).

The fundamental purpose of the Durability Patch Program was to establish a repair technique for secondary structure (or other lightly loaded structure) which consists of restoring structural integrity, with structural repair patch and increasing fatigue life with the addition of structural damping. Very importantly, the durability patch offers an attractive option (relative to conventional techniques) to the potential user, to significantly increase the service life of the structural component resulting in net cost savings with no adverse effects.

3.0 TECHNICAL DESCRIPTION

The durability patch design process includes identifying the problem, determining the flight data required to analyze the problem, collecting this data, and then analyzing and designing the repair. The following sections will discuss the Durability Patch design process and the development and testing of the damage dosimeter. Section 4.0 contains flight line installation and operating procedures. Section 5.0 will discuss three service applications of the damage dosimeter and the durability patch design process.

3.1 DURABILITY PATCH DESIGN PROCESS

3.1.1 Requirements

The following must be considered for a durability patch design process.

1. Restoration of static load capability.
2. Life enhancement.
3. Minimum quality assurance/inspection.
4. Simplified installation procedure.

The static load capability of the structure must be restored. It is well known in bonded repair that the extensional membrane stiffness of the original skin should be closely matched to avoid load attraction and load shedding. The repaired structure must be capable of carrying any applied static and dynamic loads.

The life of a properly designed and installed bonded repair should exceed the life of the undamaged baseline structure. The durability patch must withstand moisture for decades, must reduce stress intensity and consequent crack growth rate, should reduce static stresses and must reduce dynamic stresses. These points suggest three requirements for the Patch:

- no stress concentrations or hard points,
- vibration damping, and
- high tolerance to disbonds and porosity.

Since the structures under consideration are not flight-safety critical, in order to minimize costs, there should be a minimum of quality assurance and in-service inspection. The installation procedures should be simplified as much as possible to allow application by flight line personnel. The level to which this is accomplished depends on the application and direction from the Special Program Office (SPO).

3.1.2 Description of Design Methodology

The Durability Patch program investigated:
- single-sided, bonded elastic repair,
- reinforcement of sonic fatigue cracking areas, and
- simultaneous integration of viscoelastic vibration damping.

When sonic fatigue cracking has actually occurred, there is an opportunity for durability enhancement. Sonic fatigue cracking implies relatively thin and lightly loaded structure. Sonic fatigue cracks generally occur at the center of the long edge of a skin panel and run parallel to the edge; they will occur at a chem-mill land, at the edge of substructure, or in a fastener row. Regardless, there will be a length of substructure associated with the crack. The fasteners around the cracked skin panel and the fasteners of the adjoining skin panel on the opposite side of the substructure define a generic pattern shaped as a "figure 8," as shown in Figure 3.

Figure 3 shows the recommended Durability Patch design. The figure shows a cross section of a Durability Patch installed over a crack that has occurred at a row of fasteners; the generic "figure 8" of fasteners associated with two skin panels is also shown.

For installation, surface preparation is the first and most important step. Then a layer of structural adhesive film is placed on the original skin, its perimeter reaching close to the edge of the fastener "figure 8." Corners may be square or slightly rounded. The fasteners of the shared substructure are covered. The second layer is viscoelastic material (VEM) film with a perimeter 0.5 inches away from the edge of the structural adhesive and with a cutout in the location of the crack. The third layer is fiberglass (FG) prepreg of the same size as the structural adhesive. Successive layers are all fiberglass prepreg, each one smaller than the previous one, to provide a tapered edge. This installation process produces a Durability Patch that consists of three regions, shown schematically in Figure 3, an elastic repair region near the crack (associated with the cutout in the VEM layer), a damping region (associated with the location of the VEM layer around the cutout), and a bonded perimeter region.
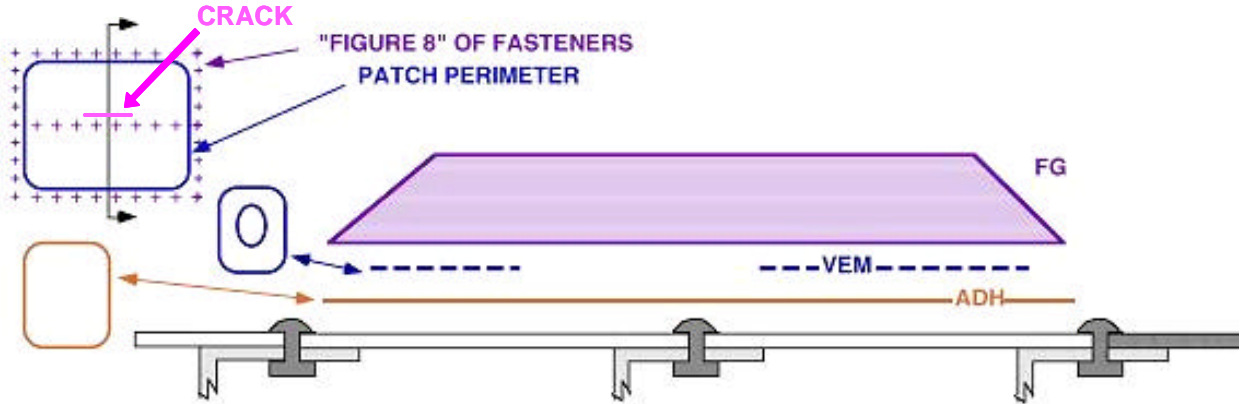
Figure 3. "Figure 8" Planform of Fasteners and Cross Section of Durability Patch

For comparison to standard bonded repair technology and definition of important terminology, Figure 4 shows a schematic cross section of a one-sided bonded repair (reference 25). In this schematic, a tensile load is shown applied to a repaired cracked structure. Deformations are exaggerated to illustrate key design quantities, designated by letters A through P. A tensile load is applied to the structure adjoining the patched crack (A), which, because of the single-sided repair, induces bending moments at the edges of the patch (B). As a result of the deformation, disbonds can occur at the crack location

6

(DC) or at the edge of the adhesive (DE). Qualitative plots of bond line peel stress (σ) and shear stress (τ) are presented above and below the schematic. Peel stresses are highest at the adhesive boundaries away from the free edges. The shear stresses peak at both boundaries of the adhesive layer, and an "elastic trough," or region of low shear stress, occurs away from these boundaries. The design conditions listed in the Figure are the key engineering quantities for bonded repair: ultimate and yield strengths of the patch and skin materials, damage due to low and high-cycle fatigue, and cure and service temperatures (temperature ranges).

Design quantities
A - adjoining structure
B - baseline at edge of patch
C - adhesive at crack
D - disbond
E - adhesive at edge
F - flaw growth
L - length of elastic trough
P - patch at crack

Design conditions
U - ultimate
Y - yield
LCF - low cycle fatigue
HCF - high cycle fatigue
T - thermal
 TC - cure
 TS - service, e.g., cruise
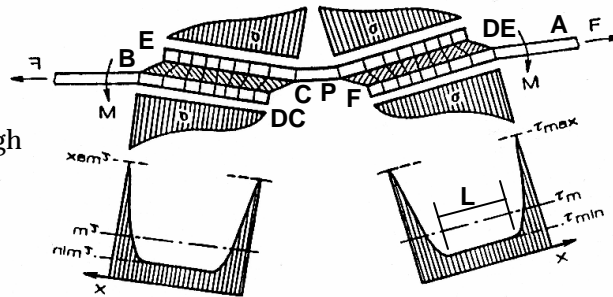
reference: *Adhesion and Adhesives: Science and Technology*, by A. J. Kinloch

Figure 4. Durability Patch Design Quantities and Conditions

Figure 5 illustrates a finite element model that was used for preliminary trade studies of damped patch configurations. The model is a clamped-clamped beam of unit width, representing a one-sided bonded repair with an integrated damping region. One clamped end is at the crack location and the other at the uncracked edge of the skin panel. All elements were 20-noded bricks. Note that mesh size is reduced for greater fidelity at the crack location, at the transition from viscoelastic material to structural adhesive, and at the edge of the Patch.

Patch configurations were evaluated by applying a static pressure load equivalent to the peak dynamic pressure that would result in high-cycle fatigue failure at 1,000,000 cycles. An oscillatory stress of 8.5 ksi in 2024 aluminum will result in a high cycle fatigue failure at 10^6 cycles, the threshold of sonic fatigue occurrence. Consistent with sonic fatigue methodology (reference 9), the numerical value for a static uniformly distributed pressure, P_o, was established that would result in a stress of 8.5 ksi at the crack location for a bare uncracked beam. The same value of pressure, P_o, was used as an out-of-plane loading for analysis of all patch configurations investigated. In-plane (membrane) loading was investigated for the same configurations by applying a remote 10-ksi stress to the finite element model (FEM) and calculating resulting stresses.
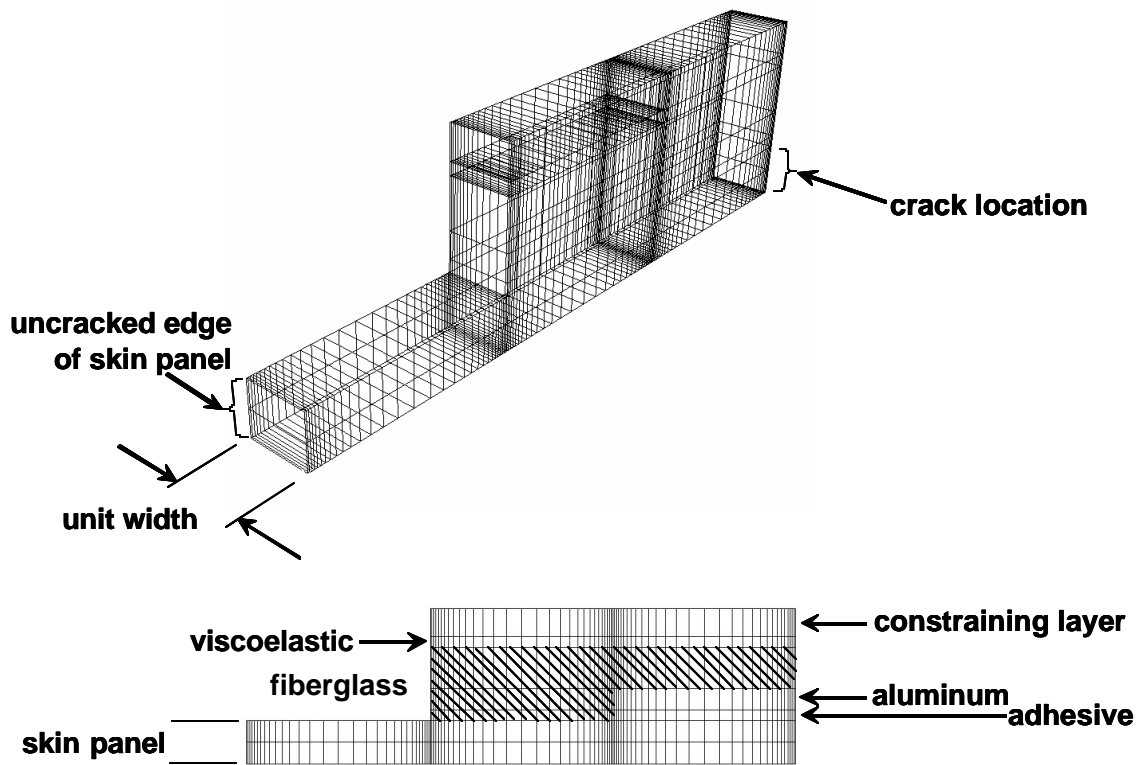
Figure 5. Beam Finite Element Model used for Configuration Trade Studies with Elements Expanded in Thickness for Clarity

Methodology. The recommended Durability Patch design methodology meets all of the requirements identified above, i.e., (1) restoration of static load capability, (2) life enhancement, (3) minimum quality assurance requirements, and (4) simplified installation procedure. These requirements are addressed here.

Restoration of static load capability. In-plane or membrane loads are transferred from the skin through the structural adhesive into the patch material, around the crack, and then back through the adhesive into the original skin. In-plane capability of the repaired structure may not approach that of uncracked virgin structure depending on how much the substructure stabilizes the skin; this is due to the eccentric load path of the one-sided repair, and is a potential limitation of one-sided repair. Of the patch configurations analyzed, there was as much as a seven times increase in stress levels relative to an applied remote stress. However, in-plane capability of the repaired structure is adequate in most cases due to the fact that loads ordinarily do not approach yield strength of the structure. It is assumed that the one-sided repair will adequately handle any in-plane loading without further analysis. Static out-of-plane loads have a more complicated path. The flexural stiffness of the combined fiberglass layers transfers a very significant fraction of the load into the perimeter substructure. The cracked original skin also participates with an enhanced flexural stiffness.

Life enhancement. Assuming that sonic fatigue cracks first occur at 100 flight hours, a Life Improvement Factor (LIF) of 600 would result in a service life of 60,000 hours, which is believed to be more than adequate. All configurations of the Durability Patch analyzed for high cycle fatigue life

8

exceeded a value of 600 for LIF; the configurations considered covered all practical design possibilities. This indicates that the repaired cracked structure HCF (high cycle fatigue) life exceeds that of virgin structure by a factor of 600 or more. This relates to the initiation of a new crack and covers the original skin, the patch material, and the adhesive. Regarding the rate of growth of the existing crack, the elastic repair region reduces the stress intensity factor, and the damping further reduces the stress intensity factor. It is estimated that the rate of repaired crack growth is slowed by a factor of 100 times that of the unrepaired crack. The scope of this program did not permit quantifying the remaining service life after repair of an existing crack.

Minimum quality assurance and inspection requirements. Established materials, processes, and personnel are utilized to install the Durability Patch. Coin tap and close visual inspection are appropriate at installation as the quality assurance. No scheduled inspections are necessary in service because the Durability Patch is applied to secondary structure.

Simplified installation procedure. Durability Patch acceptance in field applications will depend in part on the elapsed clock time required to install a patch. The present practice of riveted scab patches requires approximately two hours. The surface preparation available at present for the Durability Patch is Grit Blast/Silane, which requires a minimum of 8 hours. This disparity cannot be accommodated when there is schedule pressure to meet aircraft mission requirements and quick turnaround is mandatory. In other words, net cost savings is not a primary driver; turn-around time can preempt the situation. The scope of this effort did not permit establishment of alternative processes, some of which appear attractive. Since the Durability Patch is typically only applied to secondary structure, safety of flight considerations are generally not a concern.

Appendices D and E summarize a more detailed analysis of the recommended configuration as well as a variety of configurations, materials, and processes in an attempt to cover all practical designs. All critical locations in the original skin and in the patch were analyzed. All design conditions, including ultimate strength, yield strength, low cycle fatigue, high cycle fatigue, crack growth rate, and residual thermal stress were considered. Effects of residual stress, its relaxation, elastic repair, and damping on stress intensity and crack growth rates warrant further investigation.

Residual Thermal Stresses. Residual stresses can occur in aircraft structure due to thermal effects associated with bonded repair. The following factors should be considered for any bonded patch design for which residual stress at the crack location is significant:

1. coefficient of thermal expansion (CTE) of the original skin,
2. effective CTE of the original skin under local heating,
3. CTE of the patch material,
4. ambient temperature during cure,
5. cure temperature, and
6. minimum and maximum service temperatures.

The surrounding skin and substructure remain at ambient temperature during cure while the two bays of skin and the patch are exposed to curing temperature. As a result, there is an effective CTE (different

9

from the CTE as a material property) for the two bays of skin to be patched. Therefore, even if both the original skin and the patch are aluminum, there are residual stresses in the skin and patch. Upon exposure to service temperatures, the original skin and the surrounding structure are at the same temperature; for this condition the original patched skin and the surrounding structure have the same CTE. With some situations, the repaired crack tips can have a beneficial residual compressive stress before service loading is imposed. Alternatively, there could be a deleterious residual tensile stress. Also there could be thermally induced out of plane deformations at ambient and/or service temperatures.

For Durability Patch structures, the service temperature is typically ground-level ambient outside-air temperature (between 0 °F and 125 °F) because the high acoustic environment ordinarily occurs for the same conditions (although there are exceptions). One example of an exception is the C-130 flap well lower fairing application, described in Section 5.3, where engine exhaust heating is approximately 70 °C (126 °F) greater than ground-level outside-air temperature. This contrasts with high-altitude cruise temperatures for most bonded repair of primary structure as the relevant service temperature. The scope of this effort did not permit a detailed investigation of residual thermal stresses.

3.1.3 Detailed Patch Design Procedure

The detailed design of a Durability Patch for a specific application, described below, is straightforward. The materials for the Patch consist of structural adhesive film, viscoelastic material, and fiberglass. The recommended configuration of the Durability Patch is shown in Figure 3 and described in Section 3.1.2.

The following materials are recommended for the Durability Patch:

- The structural adhesive film may be either Dexter EA 9696, Cytec FM 73, or equivalent. The expectation is that any and all 250°F-amine-cure (not anhydride-cure) resins meeting Boeing BMS 8-79 would be compatible.
- The layer of viscoelastic material (VEM), which is a vibration damping polymer, is selected from the VEM database of this report (Appendix D), or any other reliable source, to provide damping at the service temperature and vibration frequency at which high cycle fatigue damage is accumulated. This is necessary because the dynamic mechanical properties of VEMs are strongly dependent on temperature and significantly dependent on frequency. Selection of the material is therefore based on Dosimeter data, for both temperature and frequency, as described below.
- Fiberite MXB-7701/7781 woven fiberglass prepreg (or equivalent) is utilized in multiple layers.

The following steps outline the Design Procedure for a specific Durability Patch based on dosimeter data:

1. Determine the vibration frequency at which high cycle fatigue damage occurs.

Examine Dosimeter Data from three or more flights for the vibration frequency at which the high cycle fatigue damage occurs. The frequency of the vibration is important because detailed design of a particular Durability Patch includes selection of a VEM, and VEM mechanical properties are frequency dependent. Third-octave-band distributions, strain PSDs, and/or normalized cumulative RMS plots should be analyzed to determine the design frequency or frequency range. Selection of a single frequency at which damage occurs is an approximation, but is usually reasonable for the purpose of Patch design. Figure 6 presents a typical normalized cumulative RMS plot. Based on the data in this plot, all significant strain for this measurement occurs below 300 Hz, with 80% of the cumulative RMS due to dynamics below 160 Hz.

Normlized Cumulative RMS
Flight 5, Strian Gage 1

RN = 25
Time, t = 35.8 sec
Location: Peak
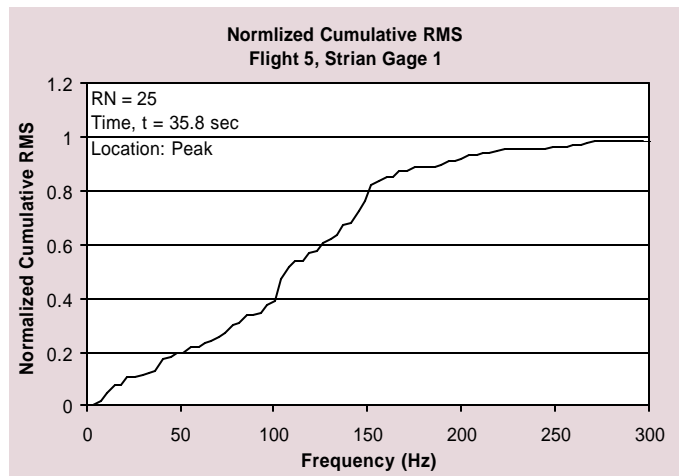
Figure 6. Sample Normalized Cumulative RMS Plot

2. Determine the temperature at which high cycle fatigue damage occurs.

Examine Dosimeter Data from three or more flights for the temperature at which the high cycle fatigue damage occurs. Strain versus temperature cross-plots and/or cumulative damage versus temperature should be analyzed for the temperature (range) at which damage occurs in service. Figure 7 shows a typical plot of temperature as a function of RMS strain level, where nearly all of the significant strains are observed between 22°C and 32°C.

Flight 6
Strain vs. Temperature Cross-Plot
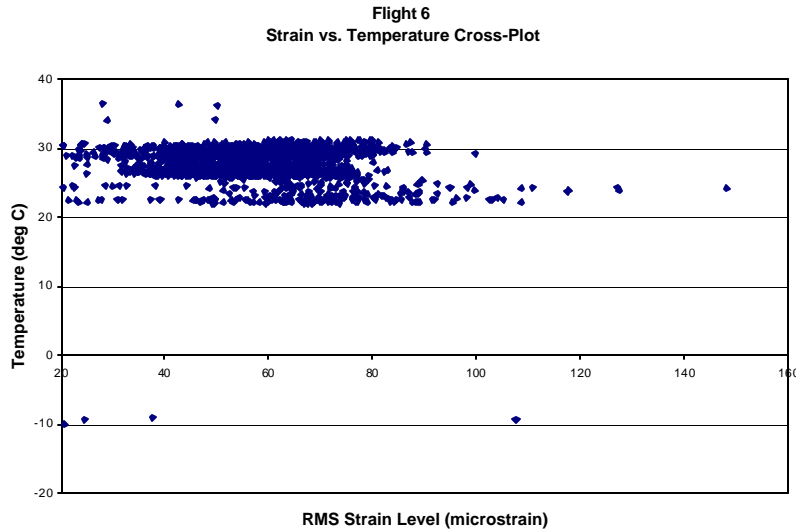
Figure 7. Cross Plot of Temperature as Function of RMS Strain Level

In analyzing the damage, it must be remembered that a factor of two in strain results in a factor of 50 on life (and, therefore, on damage). Cumulative Normalized Damage inherently takes this into consideration; furthermore, the temperature has been adjusted for the difference between ground level ambient for the particular service record and standard day temperature of 15 °C (59°F). See Sections 5.1 and 5.3 for examples.

3. Select a viscoelastic material (VEM).

VEM selection can be made once the design temperature and frequency have been established. Material selection is based on measured material properties. The VEM with the highest loss factor for the target temperature and frequency is the material that should be used. Finite element analysis (FEA), though not required, can be used for prediction of damping levels obtained in the patched structure. Sections 5.1 and 5.3 provide examples of VEM selection for specific applications.

Tabulated properties from the VEM Database (Appendix D) are shown in Table 1, including peak loss factor and temperature at which this loss factor occurs at 100 Hz. If damage occurs between approximately 20 and 300 Hz, the frequency effects can be ignored and the properties tabulated at 100 Hz used directly. The 100-Hz material properties are valid for design in this frequency range because VEM properties are less dependent on frequency than on temperature. For Durability Patch applications, the "cocured" data should be used. (The "not cocured" properties are given as a reference, for viscoelastic applications where the material is not subjected to temperature and pressure cure cycling.)

	temperature		peak		modulus (psi)			
	peak damping, 100 Hz		loss factor		at peak damping		thickness	
VEM	not cocured	cocured	not cocured	cocured	not cocured	cocured	inches	material
3M 9469	68°F	86°F	1.2	0.6	165	1500	0.005	acrylic
3M 468	68°F	91°F	1.2	0.7	150	750	0.005	acrylic
Dyad601	53°F	53°F	1.3	1.3	1100	420	0.020	polyurethane
Dyad606	98°F	97°F	1.2	1.2	1000	1100	0.020	polyurethane
Dyad609	136°F	135°F	1.0	1.1	1300	1800	0.020	polyurethane
Avery3099	92°F	83°F	2.5	2.3	120	190	0.022	rubber-based
Avery1125	53°F	na	2.0	na	420	na	0.005	acrylic
Avery1191	82°F	na	2.4	na	125	na	0.011	rubber-based
3M 9245	na	na	0.5	0.6	13000	7000	0.020	acrylic/epoxy
Densil2078	260°F	162°F	1.3	0.5	20	900	0.002	silicone

Table 1. Comparison of Cocured and Un-cocured for Candidate VEMs

Appendix D contains complete material property nomograms for the ten VEMs in Table 1. These nomograms provide measured complex modulus properties for the ten materials in both un-cocured and cocured conditions. If the damage occurs out of the frequency range of 20 to 300 Hz, temperatures of maximum material loss factors for the damaging vibration frequency can be read from these nomograms or other reliable sources. A sample nomogram from Appendix D is shown in Figure 8.

Shear modulus and loss factor for any combination of frequency and temperature are obtained from a nomogram as follows:
- Locate the target frequency (Hz) on the right-hand vertical axis.
- Locate the target temperature on the top horizontal axis.
- Follow a horizontal line across the chart from the target frequency value to its intersection with the line corresponding to the target temperature.
- From the intersection point of the target frequency and target temperature, draw a vertical line that intersects the curves for loss factor and real modulus. The values for loss factor and shear modulus can then be read on the left-hand vertical axis.
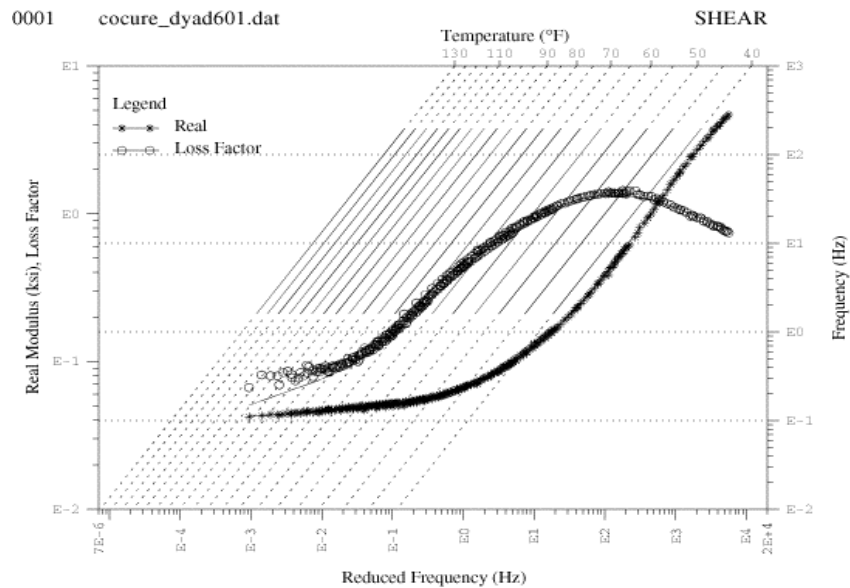
Figure 8. Temperature-frequency Nomogram for Cocured Soundcoat Dyad601

For prediction of damping levels in the patched structure, FEA can be used with the Modal Strain Energy method and real normal-mode eigenanalysis. Complex eigenanalysis can also be used. The VEM is modeled with solid (brick) elements, and the existing skin and patch can be represented with shell elements. The adhesive layer is not required to be included in the model, but if it is, solid elements are preferred for this layer also. Clamped boundary conditions are applied at the perimeter of the "figure 8" of fasteners (see Figure 3). Using the Modal Strain Energy method, modal damping of the Patch is approximated by the product of the loss factor of the VEM and the fraction of strain energy in the VEM for the target mode.[1] For complex analysis, the VEM material loss factor is included as a material property for the VEM elements, and the modal damping is computed directly.

4. Determine the crack location and substructure configuration.

Determine the location of the existing crack and the associated "figure 8" of fasteners. (If it is desired to reinforce the structure before a crack actually occurs, the same applies.) For example, if the skin crack is parallel to a frame on a fuselage, the "figure 8" will be the fasteners associated with:
- the cracked skin panel,
- the skin panel on the opposite side of the frame, and
- the three stringers associated with the two skin panels.
-

If there are no stringers, the dimension should be approximately three times the frame spacing (see Figure 5).

---

[1] Johnson, C. D., Kienholz, D. A., "Prediction of Damping in Structures with Viscoelastic Materials," MSC/NASTRAN User's Conference Proceedings, March, 1983.

5. Determine the fiberglass layup for the Patch.

Determine the original skin thickness and refer to Figure 9 to determine the total number of plies of fiberglass. Generally, the number of layers of fiberglass increases with skin thickness. The layers of fiberglass should be tapered, in "wedding cake" fashion, i.e., largest plies closest to the original skin. Corners should be as square as possible without interfering with fasteners.

No. Layers of Fiberglass


Thickness of Aluminum
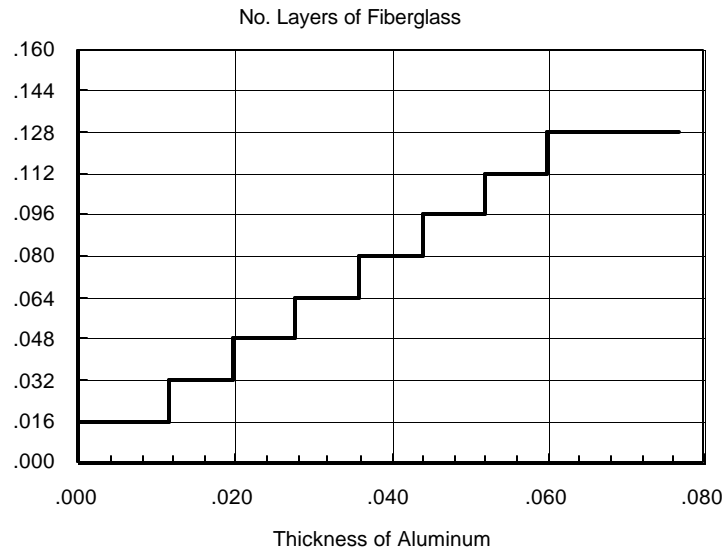
Figure 9. Fiberglass Thickness as Function of Aluminum Thickness

6. Determine the size of the VEM cutout.

The width of the cutout in the VEM layer should be approximately 1 inch greater than the length of the crack, or approximately one third the width of the Patch if no crack exists. The cutout may be elliptical, as shown in Figure 3, or octagonal.

3.2 DOSIMETER DEVELOPMENT

This section discusses the motivation and requirements for the Damage Dosimeter, along with an overview of the design and construction. The acceptance environment, software and operational modes will also be presented.

In order to design a repair with effective damping properties, the in-service structural strains and temperatures must be known, since damping material properties are a function of both frequency and temperature. An engineer must be able to easily instrument an in-service aircraft to obtain the structural characteristics necessary to properly select damping materials, and design a repair with optimum effectiveness. In addition to gathering the design information (structural strain and temperature) for the repair, the instrumentation can also be used to check the effectiveness of the repair after it is installed. In order to minimize the impact on an aircraft's normal operations, the data collection system should be a stand-alone device that does not require aircraft power or cooling. This greatly reduces the amount of modifications to the aircraft

At the outset of the durability patch program a survey of existing commercial data recorders (Ref. 21) did not yield a commercial off the shelf (COTS) product that could do the following:

1. Record three channels of strain data from 5 kilo-samples per second (ksps) to 15 ksps.
2. Meet our weight and size goals of 1.5 lb and 3 inches by 5 inches by 1 inch for the Damage Dosimeter (same goals for the battery).
3. Operate on battery power for at least a week.
4. Perform complicated data analysis. Multiple Discrete Fourier Transforms (DFT) are performed for each data processing cycle. A relatively fast digital signal processor (DSP) is needed to get the required performance.
5. Provide the necessary flexibility for differing applications.

The Durability Patch Program set out to develop its own data acquisition computer, and nicknamed it the Damage Dosimeter, since one of its outputs is a measure of cumulative structural damage.

Running off of battery power in an autonomous fashion the Damage Dosimeter measures three channels of strain at sample rates as high as 7500-samples per second and a single channel of temperature. The strain gages are configured in an Anderson loop with constant current excitation. These four channels of analog data are converted to digital data. The digital data is then processed by a DSP and stored in flash memory. Data download and program upload is accomplished via an RS-232 connection to a PC. A block diagram of the Damage Dosimeter functionality is shown in figure 10.
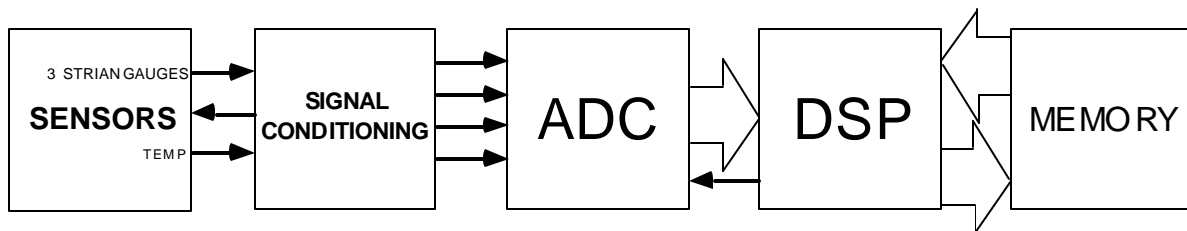
Figure 10.   Damage Dosimeter Functional Schematic

The United States Air Force often needs to measure structural strains and temperatures on in-service aircraft in order to diagnose difficult-to-analyze structural conditions, such as high cycle fatigue. The Damage Dosimeter developed on this program is a rugged, small, and lightweight data acquisition unit that can be used to perform these functions. The Damage Dosimeter was designed to fill a void in commercially available data recorders. It merges both analog signal conditioning and a digital single board computer on a single 3.5 by 5-inch card. The entire unit (without battery) weighs less than 1.5 lbs (kg). A dosimeter is shown in figure 11.
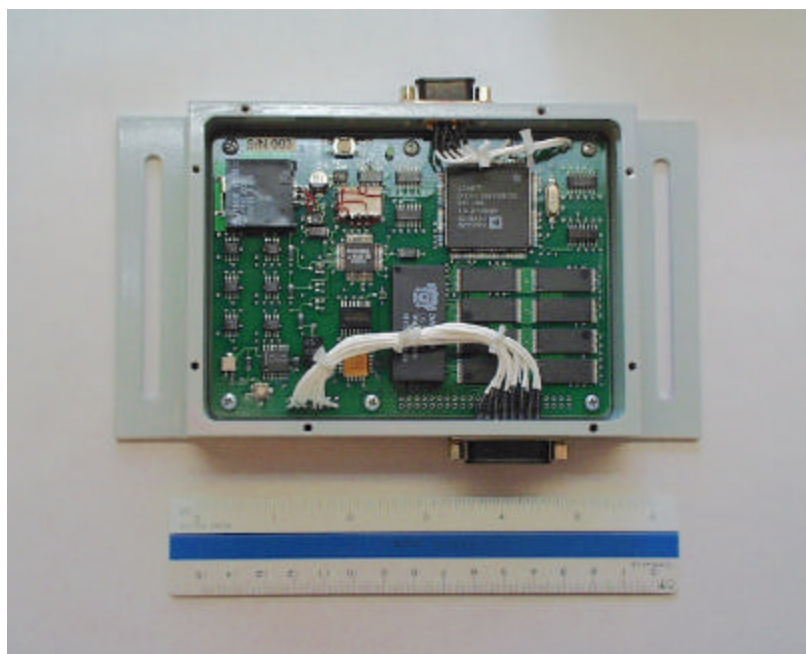
Figure 11.   Damage Dosimeter

The single board computer allows the dosimeter to operate autonomously, again a measure designed to reduce interference with the aircraft and its crew once the Damage Dosimeter is installed. Once installed, the Damage Dosimeter checks the sensors at a preprogrammed interval to determine if data acquisition is necessary. The raw data are low frequency structural temperature (approximately 1 Hz) and high frequency (approximately up to 3.5 kHz) structural strains. Data can be processed by the dosimeter using software specifically written for it. As an example in this report, data can be processed to produce 42 strain time histories and RMS values in 18 predefined 1/3-octave frequencyfor up to

29,544 records.. Data time is limited by the quantity of memory. The standby time is limited by battery capacity. Data is stored in non-volatile memory. A laptop computer can download the collected data. Data is then given to the Durability Patch design engineer for use in selecting the best viscoelastic damping material properties and designing the optimum overall repair.

Optionally, the Damage Dosimeter can be left on the aircraft, or re-installed after the aircraft has been repaired to verify that the repair does achieve its objectives. The repair effectiveness can be demonstrated by either comparing the before and after strain magnitudes in certain one-third octave bands, or by computing structural damping from the raw time histories and comparing the before and after structural damping properties.

3.2.1 Requirements

In addition to the usual operational requirements such as sample rates and pass-band frequencies, the dosimeter was designed with an additional set of user requirements. These requirements do not directly improve the performance of the dosimeter. Rather, they help ensure that the dosimeter will actually be used in the future by making the dosimeters use as easy and efficient as possible. The most significant obstacle for flight instrumentation schemes, is making modifications to the aircraft electronics, even to draw power. Requiring that the dosimeter run off battery power eliminates the concerns associated with integrating new electronics on an existing aircraft. Additional requirements on dosimeter, battery size and weight help ensure that the dosimeter can be used on as many different aircraft as possible. Lastly, requiring that the dosimeter operate with up to 50 feet of strain gage lead wire length and 100 feet of battery power cable offers the end user plenty of flexibility in finding suitable mounting locations for both the dosimeter and battery.

3.2.1-1 Operational Requirements.

The Damage Dosimeter must gather strain data from three strain gages. This data must have 5 μ-strain resolution, sampled at 7.5 samples per second (sps), over the frequency range of 50 Hz to 3.5 KHz. The temperature data must be +/- 2 ^{o}C, sampled at 1sps. The data shall be time stamped (Date, Hour, Minute, Second). The Damage Dosimeter data shall be a once –per-1.3-second representation of the frequency, amplitude, temperature and time stamp of the instrumented area. The Damage Dosimeter shall store a sample time history data for ?strain for each channel, peak RMS strain for each channel and minimum temperature in a Time History format (storage of all raw data for that sample). The Damage Dosimeter shall operate in the *industrial* temperature range (-40 to +85 ^{o}C). The Damage Dosimeter shall be able to operate in a standby mode for 10 days, and be able to collect 10 hours worth of data anywhere in those 10 days. The Damage Dosimeter data shall be capable of communicating with a laptop PC, including data download. The operational software (embedded) shall be written in the C-language, and compiled on and uploaded from a laptop PC through an RS-232 interface.

3.2.2   Dosimeter Hardware Design

3.2.2-1   Data Acquisition

The signal conditioning utilizes the Anderson Constant Current Loop (ref. 18) conditioning, shown in figure 12, to interface three strain gages to the analog-to-digital converter (ADC). The current proportional output of the temperature sensor is measured across a series resister.
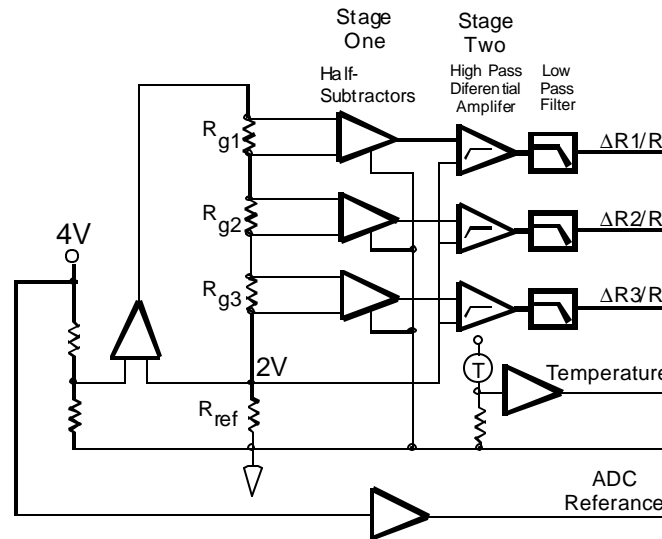

Figure 12.   Anderson Constant Current Loop Block Diagram

3.2.2-2 Strain Measurements

The Damage Dosimeter strain gages are resistive strain gages. The change in resistance in the gages is proportional to the physical change of the length of the gage. The gage is intimately bonded to the aircraft structure such that the change in the length of the gage is the change in the material. The strain is equal to:

$$\text{Strain} = (\Delta R/R_g)/GF$$

Where ΔR is the change in the gage, R_g is the nominal resistance of the gage, and GF is the gage factor (provided by the manufacture). It is the $\Delta R/R_g$ change in resistance that the Damage Dosimeter measures.

The three strain gages and a reference resistor are connected in series with a current source (fig. 9). The current in the loop is calibrated to give a voltage drop across the 350Ω reference resistor of 2 volts, this is equal to one-half the ADC reference voltage. The voltage drop across each gage passes though an RFI filter to two amplifier stages (ref. 19). The first stage accomplishes active subtraction by replicating the voltage drop across the strain gage at a point where it can be observed in series

19

opposition across the reference resistor. The second stage amplifies the difference between the gage voltage and the reference voltage with an amplifier having a high pass response. The reference voltage of the second stage is as follows:

$[(1/2)ADC_{ref}$ – the gage DC offset].

The scale is set by the gain in the second stage. The gain of the second stage is adjustable by a single component change (feedback resistor). The Damage Dosimeter at present has a full-scale measurement of +/- 3000 μ-strains. The Anderson loop was used for its low power requirement and the measurement's independence upon lead wire length. The installation of the Damage Dosimeter will be different with each application. Thus, usage is simplified if the lead wire length does not affect measurement sensitivity.

3.2.2-3 Temperature Measurement
The temperature sensor is a two-terminal integrated circuit temperature transducer that produces an output current proportional to absolute temperature. For supply voltages between +4 V and +30 V the device acts as a high impedance, constant current regulator passing 1 mA/°K (ref. 20). One terminal of the temperature sensor is connected to the +12V supply. The other terminal is connected to analog common through a 1 KΩ series resistor. The voltage drop across the 1 KΩ resistor is amplified with an instrumentation amplifier with a gain of ten. This is done to scale the measurement and to produce buffered input for the ADC.

3.2.2-4 Digital Conversion
A single ADC converts the outputs of the signal conditioning to 12-bit data. The multiplexing and sample rate of the ADC is controllable by the DSP. The inputs to the ADC are low pass filtered with an anti-aliasing single pole passive filter. The present design's –3 db point is set to 5 kHz. The filter is a simple resistor/capacitor (RC) network, so making a single component change can modify the corner frequency. The reference for the ADC is generated by the same voltage reference that is used to regulate the loop current. This is done to achieve a high pass zero corrected ratiometric measurement and to automatically adjust average strain gage output to mid-scale of the ADC.

The voltage of interest is as follows:

$$V_0 = V_g - V_{ref}$$

$$V_0 = I (\Delta R + R_g) - I (R_{ref})$$

When the reference resistor is equal to the nominal gage resistance,

$$V_0 = I (\Delta R).$$

The output of the ADC is the ratio of the voltage at the input (V_0) divided by the reference voltage for the ADC (V_{REF}) as follows:

$$DATA = V_0/V_{ADC\text{-}ref} \ .$$

Since the same reference voltage source is used for the ADC reference and to determine the set point for the current loop:

$$DATA = I\ (\Delta R + R_g) - I(R_{ref})/I\ (R_{ADC\text{-}ref}).$$

yielding $DATA = \Delta R/R_g$ as the data point.

3.2.2-5   Data Processing

All data processing functions are performed on the Analog Devices ADSP-2181 chip. The ADSP-2181 is a fixed-point processor that runs at 33 Mhz and consumes a minimal amount of power for a DSP. The DSP contains 16 k words of program memory on board the chip, allowing the processor to boot its program from flash memory and load the program, in its entirety, into RAM.

The data processing portions of the dosimeter programs are written in the C-language. Analog Devices sells a development kit that includes a C compiler, assembler, linker, and prom-splitter. With these tools, the dosimeter programs have been developed on an Intel PC. Dosimeter programs were kept under the 16 k-word size limit so that program paging and memory allocation could be avoided. This effort involved using a shorter length DFT and manually performing the decimation in time operation. Keeping the 16 k size limited saved 2048 words of array space by reusing the complex portion (which is all zeros) of the input to the high speed DFT subroutines supplied by Analog Devices.

The remaining operations are a mixture of mostly integer and some floating point (Floating point operations are performed in software). The fundamental operation is the computation of the power spectral density (PSD), also known as the signal Autospectrum. The PSD is by definition positive and real valued as shown in the following:

$$\tilde{G}_{xx}(f_x) = \frac{2}{N\Delta t}|X(f_k)|^2 \ , k = 0,1,2,...\frac{N}{2}$$

where

$$X[k] = \sum_{n=0}^{n=N-1} x[n]e^{-j(2p/N)kn}, k = 0,1,2,...N-1$$

is the definition of the DFT. Once the PSD has been calculated, the 1/3-octave band RMS values can be calculated with a simple integration scheme. The dosimeter uses the trapezoidal rule for this purpose.

The ADSP-2181 has 16 k words of data RAM (in addition to the program RAM) allowing all calculations to be performed in RAM. At the conclusion of the data processing cycle, the output is written to nonvolatile flash memory.

3.2.2-6 Power Supply – Battery

The Damage Dosimeter requires +/- 12 direct current voltage (VDC). The analog front end uses +/- 12 V and the digital back end runs on +5 V. The +5 V is derived from the +12 V by a switching regulator on the Damage Dosimeter board. Efficient operation, or low power draw, was a primary consideration during the design of the dosimeter. As a result power consumption during data gathering operations is less than two watts. In spite of the low power draw the need to operate the dosimeter in temperatures as low as –40 ^{o}C drives the need for specialized batteries. Lithium battery chemistries offer the highest energy densities in primary (nonrechargeable) cells. After running several cold temperature tests the Li-MnO$_2$ battery chemistry was chosen. After further testing, the Duracell D2/3A cells were chosen, primarily for their ability to withstand the large (2-ampere) in-rush currents. The batteries are not rechargeable but are readily available and inexpensive (about 3 to 4 dollars per cell). Fifteen cells are required to power the dosimeter through a typical mission. After each mission, the positive side battery pack (10 cells) must be replaced. The negative side pack (5 cells) can last up to seven missions. Figure 13 shows both the negative (in the rear) and the positive (in the middle) packs. In the forefront is a single Duracell cell. If the missions are shorter in duration, or moderate temperatures are experienced, the battery could last significantly longer. The battery is housed in a COTS die-cast aluminum box lined with polyethylene foam for vibration isolation.

Figure 13.   Damage Dosimeter Battery Cells

22

3.2.3   DOSIMETER ENVIRONMENTS AND ACCEPTANCE TESTING

The Damage Dosimeter was tested under various environmental conditions to prove its flight worthiness. These tests included vibration, thermal, and EMI environments. Dosimeter operation was verified after each test. This section provides descriptions of each test and presents the test results.

3.2.3-1   Random Vibration Environment

The Dosimeter was tested in the laboratory under the random vibration environment envelopes shown in figure 14. The baseline environment represents the vibration levels for the B-52 bomb bay body frame (BS900, WL156) during takeoff. This is the aircraft and location for the first scheduled Dosimeter application. The energy level for this profile is 5.1 Grm. Also included in this figure are two higher level envelopes with energy levels of 6.1 Grm and 7.2 Grm.

B-52 Random Vibration Environment
**Bomb bay body frame (BS900, WL156) during takeoff.**
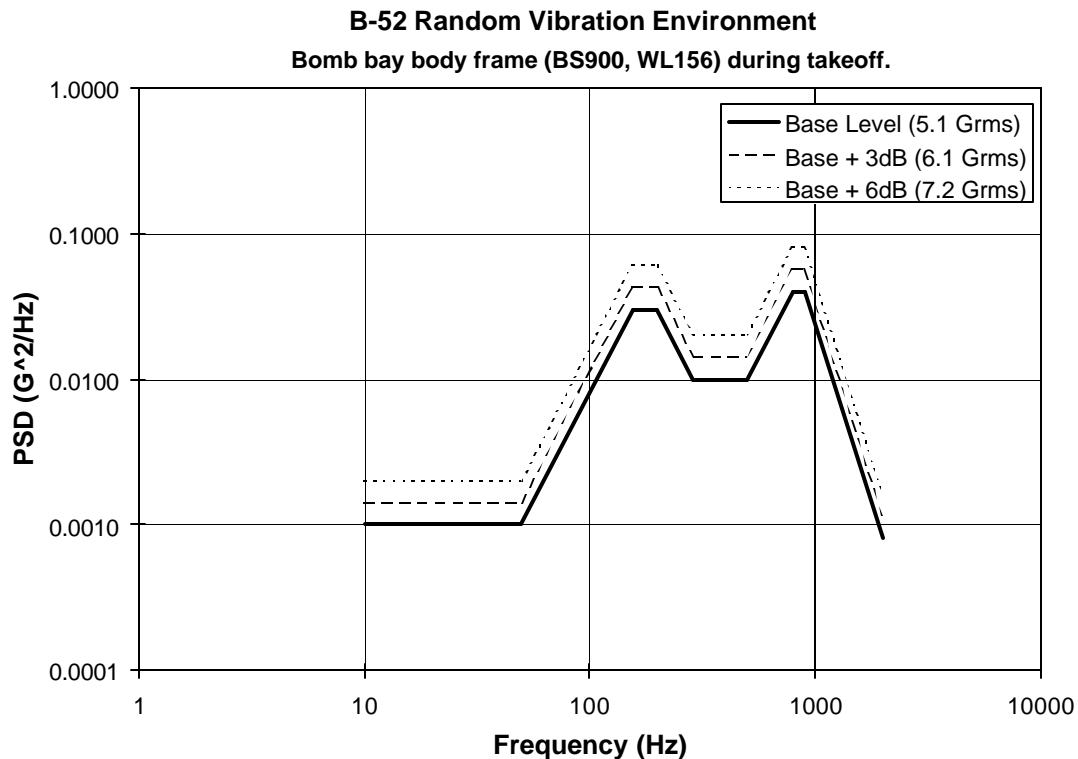
Figure 14.   Vibration Test Environment Envelopes.

The Dosimeter was subjected to the baseline vibration level for one hour per axis. Dosimeter operation was verified during and after each test. The Dosimeter was then subjected to the 6.1 Grm level for 2 minutes per axis and the 7.2 Grm level for 2 minutes per axis. Again, Dosimeter operation was verified during and after each test.

Results of the tests showed that the Dosimeter electronics and battery enclosures both survived all vibration testing without failure. Testing of the dosimeter operation during and after each vibration test showed normal results in every case.

3.2.3-2 Temperature Environment

The Dosimeter and battery were tested for the temperature environment envelope shown in figure 15. This environment represents the "industrial" temperature range (-40 °C to 85 °C).

**Dosimeter Temperature Cycling**
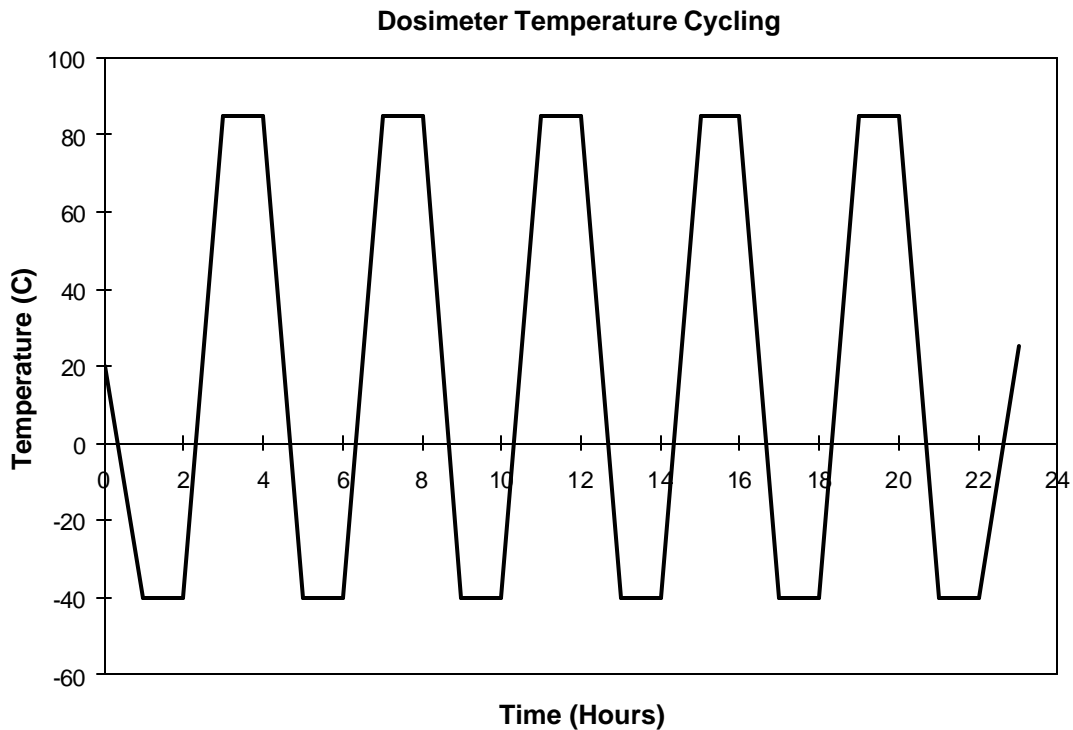
Figure 15.   Temperature Test Profile.

The Dosimeter was subjected to each extreme of the temperature range for 1 hour. Dosimeter operation was verified during and after each plateau. The Dosimeter was tested in two states: power on during transitions and power off during transitions. Additional tests that were run include:

- Cold soak:
  Soak at –40 °C for 8 hours power off and then power on and run for 1 hour at –40 °C.

- Heat soak:
  Soak at 85 °C for 8 hours power off and then power up and run for 1 hour at 85 °C.

- Warm environment takeoff to altitude:
  Soak at 85 °C for 8 hours and then transition to –40 °C in less than 2 minutes, power up at –40 °C.

- Cold duration test:
  Soak at –40 °C for 8 hours power off. Power on and gather data for 8 hours.

Results of the tests showed that the Dosimeter electronics and battery both operated over the industrial temperature range without anomalies. Testing of the Dosimeter operation during and after each temperature test showed normal results in every case.

3.2.3-3 Electromagnetic Interference (EMI) Environment

The dosimeter was tested for radio frequency radiated emissions. The tests were conducted in accordance with EMI Control Requirement (ref. 23) for installation of electronic equipment on Boeing commercial transport aircraft. Two measurement bandwidths, narrow band and broadband, were used in the tests. Results from the two tests are plotted in figures 16 and 17, respectively. The curves representing the maximum allowable emission level are also included in the figures. The figures show that the emission levels from the Dosimeter were within allowable levels.

Also included in figure 16 is the maximum allowable radiated emissions of electronic equipment in military aircraft applications (RE102, MIL-STD-461D) (ref. 24). The curve defining this requirement for Navy and Air Force applications is reproduced in figure 16. The Dosimeter met the radiated emission requirements in the range tested. Note however, that Dosimeter testing was performed through a maximum frequency of only 6 GHz (in accordance with ref. 23). The full range of the RE102 requirement is from 2 MHz to 18 GHz.
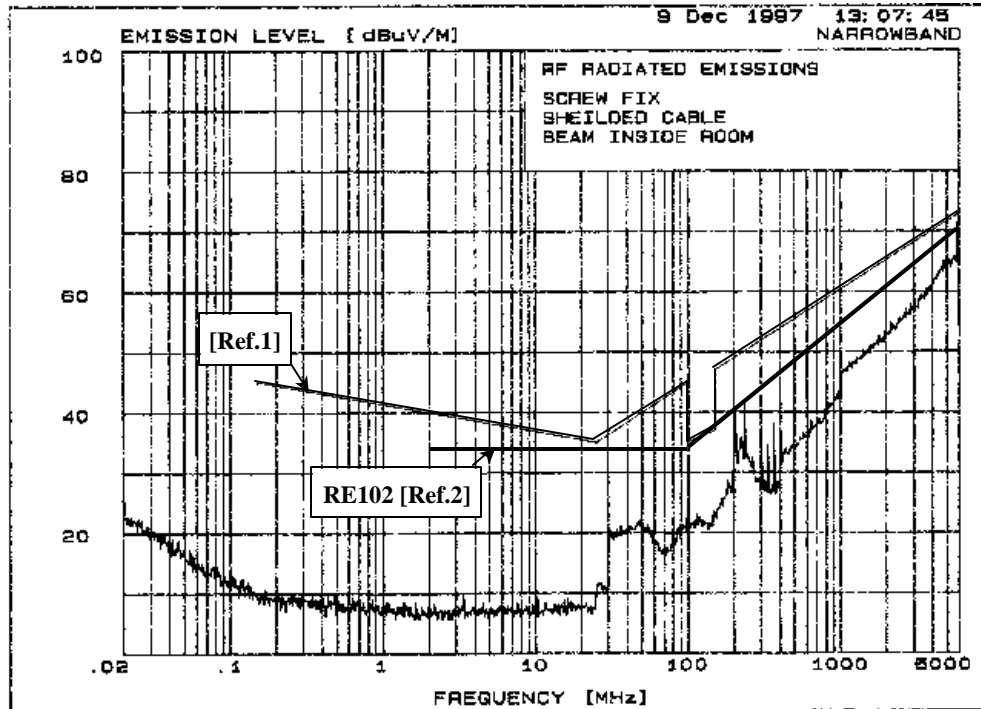

Figure 16.   Narrow Band RF Radiated Emissions Test Requirement and Results.
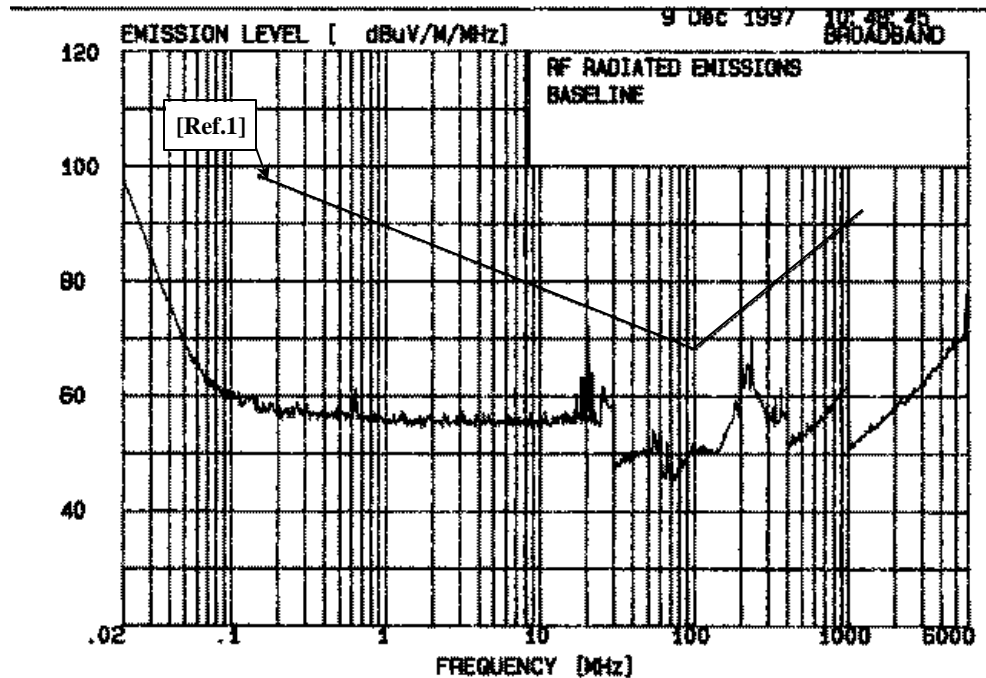
Figure 17. Broadband RF Radiated Emissions Test Requirement and Results

3.2.3-4 Explosive Atmosphere Assessment

An assessment of the dosimeter and battery for operation in an explosive atmosphere on the B-52 was performed by Steven R. Hopper, Boeing-Wichita. A review of the unit and installation drawings, schematics and test report was conducted. Based on the following the dosimeter and battery were deemed acceptable for temporary installation on the B-52:

1. The dosimeter has mostly digital components and does not provide a method of arcing or sparking.
2. The printed circuit boards are conformally coated making them resistant to fluids.
3. The connectors are potted to prevent fluids from being induced into the connectors.
4. During operation, the temperature of the internal components does not reach the auto ignition temperature of JP-4 or JP-8 fuel (435 °F).
5. The location of the dosimeter and battery in the B-52 (bomb bay) allows the units to be well ventilated. Therefore, the possibility of igniting a fuel vapor in this area is extremely improbable.

3.2.4 Dosimeter Software Design and Description

The damage dosimeter operational software program governs dosimeter operation and data processing. The program was written in C programming language, which allows for easy maintenance and modification. C-callable low-level device drivers for the DSP were written in assembly code, which offers efficiency and reusability. Several program variables can be easily modified which allows the program to be adapted to different data processing requirements seen in differing applications. This section describes the basic flow and capabilities of the software. It also identifies the key program variables and explains how those variables can be set to achieve desired operation and data processing characteristics.

3.2.4-1 Program Flow
The flowchart shown in figure 18 illustrates the dosimeter operational program flow. Each section of the flowchart is described below.
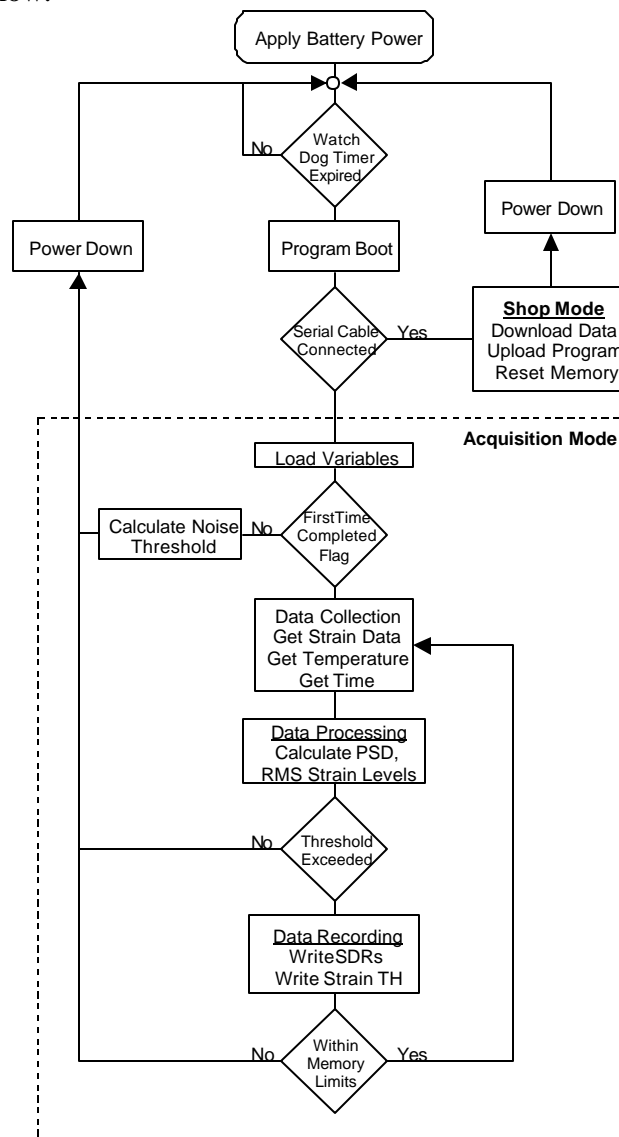

Figure 18.   Flow Chart for Dosimeter Operational Program.

Watchdog Timer.   Upon application of power, the Watchdog Timer (WDT) governs the Dosimeter power up activity (see section 3.2.5 Dosimeter Operation). The WDT is a device that continuously performs a timer countdown. The period of countdown time is called the idle time. The idle time is a program variable, which can be set to anything between 10.00 and 99.99 seconds.

As the WDT counts down to zero and expires for the first time, the Dosimeter will boot up. Once booted, the Dosimeter checks for the presence of a specialized RS-232 serial cable. The presence of this cable will force the Dosimeter to enter Shop Mode, which is used for interfacing with an external computer (see section 3.2.5 Dosimeter Operation). With no cable present, the Dosimeter will enter Acquisition Mode, in which sensor data will be collected, processed and recorded.

Load State Variables. Each time the Dosimeter enters Acquisition Mode, the program will load an array of external state variables, which are stored in memory outside of the operational program memory. Those variables, which include current date and time, memory write locations, and program flags, are stored in the active memory of the Dosimeter outside of the operational program. This allows their values to be retained even when the Dosimeter operational program is not being executed (powered down state). By loading these variables, the Dosimeter program remembers its status from the last time it was powered up.

FirstTime Calculation.   After loading external variables, the program runs through the FirstTime subroutine, which is responsible for calculation of the background noise level and subsequent assignment of an appropriate Noise Threshold. Below this threshold, the data will be regarded as noise and will not be recorded. Multiplying the measured background noise level sets the Noise Threshold by a programmable factor.

The FirstTime subroutine is executed while the aircraft is standing idle. Establishing the appropriate Noise Threshold will ensure that the Dosimeter does not collect low-level strain data caused by electrical noise, wind, or other low-level activity not relevant to the strain behavior under investigation. Once the Noise Threshold is calculated, it is stored as a state variable and a program flag is set, which prevents this subroutine from being executed again until the Dosimeter memory has been reset. Having completed the FirstTime subroutine, the Dosimeter powers down and remains in that state until the WDT counts down the Idle Time and expires again.

Data Collection. When the WDT expires again, the Dosimeter will boot, enter Acquisition Mode (assuming no serial cable connection), bypass the FirstTime subroutine, and begin collecting data. Strain and temperature data are collected from the sensors in sample sets. One sample set consists of a single temperature measurement and 2048 samples at each of the three strain gages. In addition, a time stamp is collected from the real-time clock and added to the sample set.

Data Processing. The raw strain data for each of the three gages is immediately processed through a Fast Fourier Transform (FFT) to generate a PSD. The PSD is then integrated over 18 discrete frequency bands to obtain a course representation of the vibration environment (see section 3.2.5 Dosimeter Operation). The frequency bands are defined within the software, and can be modified to

meet specific application requirements. Typically these bands are defined to be 1/3-octave bands. This provides a 1/3-octave band distribution of strain activity across the specified frequency range.

Threshold Comparison. Before the processed data is stored to flash memory, the Dosimeter checks to determine whether the average strain level exceeds the Noise Threshold calculated in the FirstTime subroutine. The RMS of the 18 discrete frequency bands is calculated for each of the three gages, and then averaged to determine the average RMS strain level for that sample set. This strain level is measured and averaged over a specified number of sample sets to determine the average level of strain activity over a nominal period of time (a program variable usually set to three sample sets). The average RMS strain level from those sample sets is compared to the Noise Threshold. If the current RMS strain activity is below the Noise Threshold, then the Dosimeter will power down and remain in that state until the WDT expires again. If the current RMS strain activity is above the Noise Threshold, the Dosimeter will begin recording data.

Data Recording. Processed data sets are recorded by writing to non-volatile flash memory. Two types of data records are written: Standard Data Records (SDRs) and Strain Time-Histories. One SDR and one Strain Time-History are written for each sample set.

The SDRs primarily consist of the RMS strain levels for each of the 18 frequency bands for each gage. These data sets provide a characterization of the strain environment in the frequency spectrum. In addition, the temperature, time stamp, and maximum strain for each gage are recorded with each SDR. The Strain Time-Histories contain the raw strain data for each of the three strain gages from one sample set. In addition, the temperature and time stamp for that sample set are recorded for each data set.

Continuous Threshold Comparison. As the Dosimeter records data, the Noise Threshold comparison is continuously made for each sample set. If the strain activity falls below the Noise Threshold for a specified number of consecutive sample sets, the Dosimeter will stop recording data and power down. The actual number of consecutive sample sets below the threshold needed to trigger power-down is a program variable called Count Down. This feature prevents data collection and battery drain during periods of low strain activity flight such as cruise.

Memory Limits. Data recording will cease when the nonvolatile flash memory is filled. The SDRs and Strain Time-Histories have separate memory allocations. Thus, when memory is filled for one type of data record, the other type may still be recorded until its allocation is filled. When both memory allocations are filled, the Dosimeter will power down. It is worth pointing out that the Strain Time-History data records are approximately 100 times larger than the SDRs. (For a detailed list of data elements and sizes, see section 3.2.5 Dosimeter Operation.) Therefore, the Strain Time-History memory allocation will typically fill up long before the SDR memory allocation, depending on relative allocation sizes. The actual allocation sizes are program variables, which can be modified to meet specific application requirements.

3.2.4-2 Program Variables

Some of the key program variables are listed below along with descriptions of how those variables can be set to achieve desired operation and data processing characteristics.

1. Idle Time – Sets the countdown time period used by the WDT. This governs how long the Dosimeter will sit idle before powering up to sample data. A value of 99.99 seconds was used during service confirmation activities.
2. Count Down – Sets the number of consecutive sample sets with strain levels below the Noise Threshold required to trigger a power down due to strain inactivity. A value of 10 was used during service confirmation activities.
3. Noise Threshold Factor – The factor by which the measured background noise is multiplied to obtain the Noise Threshold. A value of 3 was used during service confirmation activities.
4. Band Frequency Ranges – Define the frequency ranges for each of the 18 discrete frequency bands. During service confirmation activities, continuous 1/3-octave bands were defined. The starting point for those bands varied depending on application.
5. First memory write location for Standard Data Records – The memory address for the beginning of the SDR memory allocation. During service confirmation activities, this address was set such that approximately 3.6 MB of memory were allocated for SDRs.
6. First memory write location for Strain Time-Histories – The memory address for the beginning of the Strain Time-History memory allocation. During service confirmation activities, this address was set such that approximately 500 KB of memory were allocated for Strain Time-Histories.

3.2.4-3 Program Size Limitations

The compiled operational program resides in the program memory onboard the ADSP-2181 chip (see section 3.2.2). The operational program size is limited to 16 k words. Program execution must work within a 16 KB RAM limit. Total nonvolatile memory for storing data records is currently limited to approximately 4.1 MB.

3.2.5 Dosimeter Operation

The Damage Dosimeter has two modes of operation: Acquisition Mode and Shop Mode. Acquisition Mode refers to the mode in which the Dosimeter gathers, processes, and stores strain and temperature data. Shop Mode refers to the mode in which a computer can communicate with the Dosimeter, either downloading data, or uploading new programs. When using Shop Mode, a specialized serial communications cable is used to connect the Dosimeter to computer. The presence of this serial cable will automatically instruct the Dosimeter to enter Shop Mode during the next powerup cycle. A program named *DPD_Loader*, which runs on DOS, Windows-95, or Windows NT, provides a user interface to the Dosimeter when in Shop Mode. The two operational modes and the interface software are described in more detail below.

3.2.5-1 Acquisition Mode

When the Dosimeter boots up without a serial cable in place, the Dosimeter enters Acquisition Mode. In this mode, the Dosimeter accomplishes two tasks. The first task is to establish the background noise threshold for the strain gages. The second task is to collect strain and temperature data during flight. A brief description of these two tasks is given below. Additional details are provided in Appendix C.

The objective of the first task is to measure the strain activity during nominal conditions to establish a background noise level. The Dosimeter performs this measurement upon initial powerup after the Dosimeter memory has been reset. During this measurement, the Dosimeter collects approximately 20 seconds of data, and uses that data to calculate a background noise level. The RMS background noise level is then multiplied by a programmable factor to establish the noise threshold that is used to distinguish real strain activity from background noise. Once the noise threshold is established the Dosimeter is ready to collect data. The threshold determination is performed only on the first powerup cycle after Dosimeter memory has been reset. The operation is not performed again until after the Dosimeter memory has been reset again.

The second task performed in Acquisition Mode is data collection. The Dosimeter collects strain and temperature data, processes that data, and stores the processed data in flash memory. (A description of the data collection and recording is contained in Appendix C.) In general, only strain levels, which exceed the previously determined noise threshold, are recorded. This avoids filling the limited memory with low-level strain data. In addition, when the Dosimeter detects sustained low-level strain activity, it will power down to conserve its battery. After power down, the Dosimeter waits for a specified period of time before powering up again to measure the level of strain activity. On powerup, if the strain activity exceeds the noise threshold then data collection resumes. The Dosimeter continues to collect data until either the memory is full or the gage activity level falls back below the noise threshold.

The automatic powerup and power down capability is partially governed by a WDT. The WDT is a device that continuously performs a timer countdown. The Dosimeter uses this device to monitor idle time. When the Dosimeter is idle for a certain period of time, called the *IdleTime*, the WDT triggers the Dosimeter to power down. When the Dosimeter has been powered down for a period of time equal to

the IdleTime, the WDT triggers the Dosimeter to power up. The IdleTime is a program variable, which can be set to anything between 10.00 and 99.99 seconds.

The ability to power down during sustained periods of inactivity give the Dosimeter added functionality. This allows the Dosimeter to be setup in the aircraft several days or even weeks prior to flight. During this time the Dosimeter will power up, check strain activity, and power down about once every 99 seconds (or whatever the IdleTime variable has been set to). No data will be recorded during that time as long as strain levels are below the threshold (which they will be for nonflight conditions).

The power-down capability is also used in flight. Once data collection has begun, a period of sustained low-level strain activity will cause the Dosimeter to power down. The period of time necessary to cause power down is set as a program variable called *CountDown* in the Dosimeter software. A period of at least ten seconds is typically assigned to CountDown so that a brief period of gage inactivity does not cause the Dosimeter to power down. After power down, the Dosimeter will wait through the IdleTime period before powering up again to measure the strain activity. Again, this feature prevents data collection and battery drain during periods of low strain activity flight such as cruise.

3.2.5-2 Shop Mode

When the Dosimeter boots up with the specialized RS-232 serial cable in place, the Dosimeter enters Shop Mode. While in Shop Mode, the Dosimeter can communicate to a laptop or desktop computer through the serial cable. The software application *DPD_Loader* provides a simple menu-driven user interface to support the Dosimeter communication functions. The *DPD_Loader* program is written in C programming language and can be run in DOS, Windows-95, or Windows NT. A brief description of Shop Mode operation through the use of *DPD_Loader* is given below. Additional details are provided in Appendix C.

   Three main tasks are accomplished in Shop Mode:
1. Downloading data from Dosimeter data memory.
2. Resetting Dosimeter data memory.
3. Uploading new software to Dosimeter program memory to modify Dosimeter operation.

The first two tasks are usually performed routinely on a once-per-flight or once-per-several-flights basis. The user can download the SDRs and strain time-history data in binary format to the computer. Also, program variables stored in volatile RAM can be downloaded and checked for validity. The Dosimeter real-time clock can also be checked using the download function. The procedure for accomplishing these tasks is outlined in Appendix C.

Once the data has been downloaded, the Dosimeter data memory (approximately 4 Mbytes of nonvolatile RAM) must be reset. This is easily accomplished through *DPD_Loader*. Again, the procedure for accomplishing this task is outlined in Appendix C.

Occasionally, it is necessary to upload new Dosimeter software. There is a substantial amount of flexibility built in to the Dosimeter software architecture, which allows its performance to be tailored to the application at hand. The most common reason for modifying the Dosimeter software is to adjust the

frequency range over which data is recorded. New software can be easily uploaded through *DPD_Loader*.

4 FLIGHT LINE INSTALLATION PROCEDURES

4.1 STRAIN AND TEMPERATURE GAGE INSTALLATION PROCEDURE

The Dosimeter is designed to support three strain gages and one temperature sensor. The temperature sensor is a two-terminal integrated circuit temperature transducer. The three strain gages must be 350-ohm resistive gages. The strain gages must be wired in a constant current loop (fig. 19). The dosimeter will not operate if the gages are wired in a conventional bridge. Only constant current loop wiring will allow proper dosimeter operation. The 350-ohm resistance level is necessary to match the 350-ohm reference resister internal to the Dosimeter, which is part of the constant current loop.
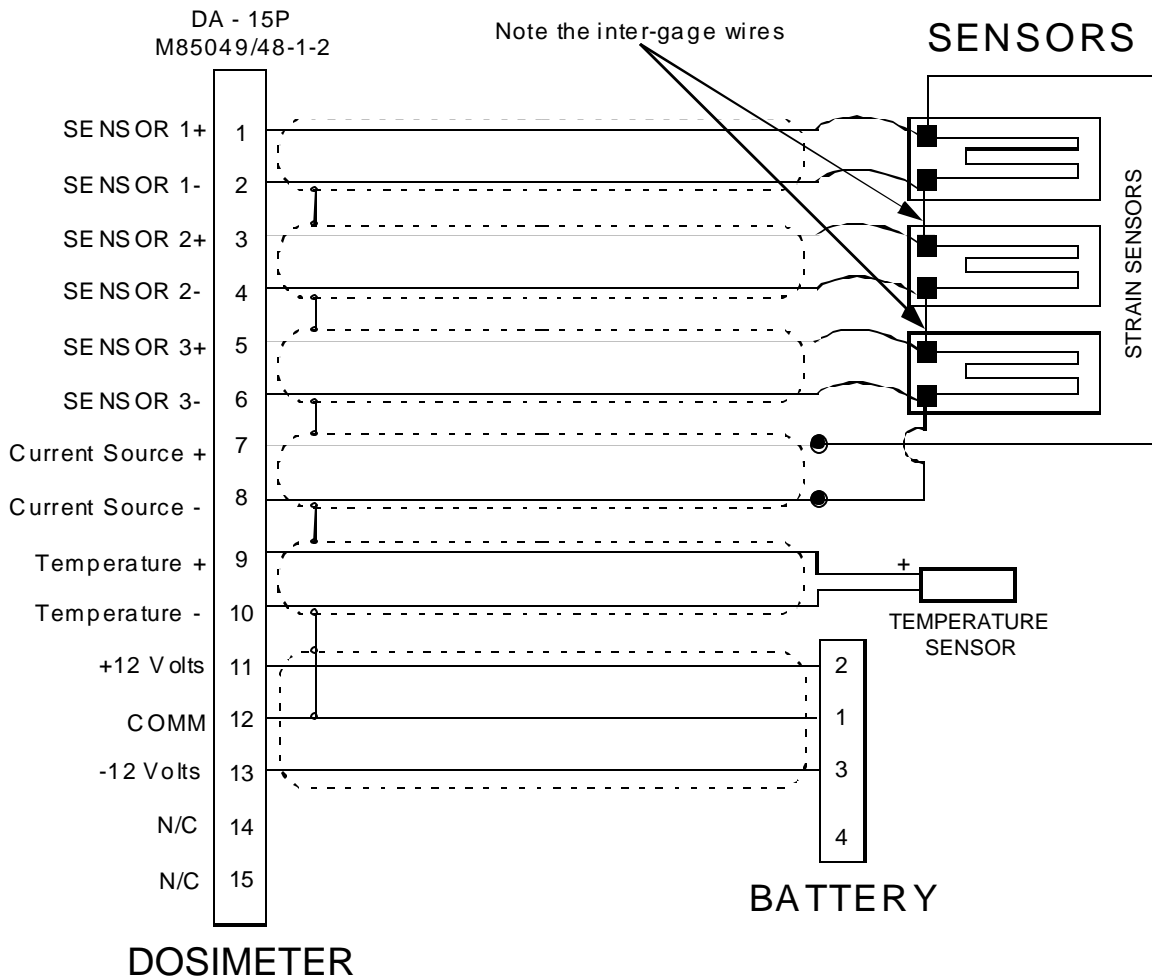
Figure 19.   Constant Current Loop Wiring Diagram

An outline of the general steps involved for the strain and temperature gage installation for the dosimeter is given below. Detailed installation procedures are provided in Appendices A (strain) and B (temperature). The procedures for strain gage installation and temperature gage installation are very similar. Many of the steps are identical and can be performed at one time for both sensor types.
Strain Gage Installation

34

1. Strain gage layout
2. Strain gage preparation
3. Surface preparation
   - Degreasing
   - Removal of paint and coatings
   - Finish abrasion and cleaning
   - Conditioner and neutralizer application
5. Strain gage application
   - Gage positioning
   - Adhesive application
6. Cure
   - Pressure application
   - Controlled heat application (if necessary)
7. Removal of cure apparatus
8. Verification testing for individual gages
9. Leadwire installation
10. Wiring of constant current loop
11. Verification testing for wired assembly
12. Weatherproofing

Temperature Gage Installation
1. Surface preparation
   - Degreasing
   - Removal of paint and coatings
   - Finish abrasion and cleaning
   - Conditioner and neutralizer application
2. Temperature gage application
3. Cure
   - Pressure application
   - Controlled heat application (if necessary)
4. Removal of cure apparatus
5. Leadwire installation
6. Weatherproofing

There are several important items to note regarding the gage installation process:

1. Proper surface preparation is essential to a successful installation. The purpose of surface preparation is to provide a surface that is chemically clean and has an acceptable surface finish. The detailed strain gage installation procedure in Appendix A describes the steps necessary to ensure a satisfactory bonding surface. Care must be exercised with each of the operations for consistent success with the installations.

2. In preparation for strain gage installation the surface should be abraded to remove adherents such as scale, rust, paint, coatings, oxides, etc. Baked enamel, anodizing, alclad, and electroplating may

give the appearance of providing a satisfactory surface but their presence can cause undesirable characteristics. Surface finishes should be removed unless drawings for the strain gage installations state otherwise.

3. Time is an important factor between the surface finishing step and the adhesive application. Materials such as aluminum begin to oxidize rapidly after the surface has been abraded. Therefore:
    - It is good general practice to install the gages as soon as practical after surface preparation is complete.
    - Before beginning surface preparation, all materials for bonding, and equipment for pressure application and for curing should be ready for use so that the bonding procedure can progress without time interruption.
    - When working outside, even greater precautions should be taken to prevent contamination of materials and surfaces between the time of surface preparation and bonding.

4. CAUTION: Many of the solutions specified in the strain gage installation procedure in Appendix A are considered hazardous materials and should be treated accordingly.

4.2 DOSIMETER FLIGHTLINE OPERATION INSTRUCTIONS

The Dosimeter is intended to be readily operated by aircraft maintenance personnel without the need for technical support from Boeing. There are two main procedures typically carried out in the field once the Dosimeter has been installed. The first is data collection and the second is software upgrade. Both procedures are outlined in this section.

4.2-1 Operation Procedure for Typical Data Collection Cycle

Once the Dosimeter has been installed on an aircraft, the basic operating procedure consists of downloading data at regular intervals, resetting Dosimeter memory after downloads to allow further data collection, and refreshing batteries at regular intervals. Depending on the situation, the Dosimeter may need to be removed from the aircraft to perform these operations. For a full dosimeter data download may take up to 90 minutes. The procedure below outlines the steps required for Dosimeter operation through a typical data collection cycle. The procedure is written for the case where the Dosimeter must be removed from the aircraft to perform the data download. Caution: Windows software screen saver should be disabled.

Step 1: Reset Dosimeter and Battery Installation on Aircraft
- Make sure that Dosimeter memory has been reset since last data download (see Step 8 for memory reset).
- If Dosimeter was removed from aircraft, reattach Dosimeter to aircraft mounting brackets.
- If battery box was removed from aircraft, reattach battery box to aircraft mounting brackets.
- Connect strain gage wiring harness to Dosimeter.

Step 2: Connect Battery
- Attach connector from wiring harness to battery terminal.
- Dosimeter will power up automatically within 100 seconds. (Actual time of powerup will vary between 1 and 100 seconds depending on status of internal timer.)
- Battery should be connected no more than 2 weeks prior to the next expected flight date. The battery can support idle-mode operation for approximately 2 weeks before beginning to consume the power necessary to support full data collection.
- Once the battery is connected, the dosimeter will flash twice if it is in acquisition mode and 3 times if it is in shop mode (this is the mode where the PC is connected). If the dosimeter does not flash at all there is a problem with the connection, dosimeter circuitry, or the battery is not functioning.

Step 3: Collect Data
- Upon powerup, Dosimeter will begin automatic operation until battery is disconnected. Normal Dosimeter operation consists of the following steps:
  - Noise Threshold measurement - Measurement of background RMS strain levels. Performed only once, upon initial powerup of new data collection cycle.
- Data sampling - RMS strain levels are measured and compared to Noise Threshold to determine if current strain activity is worthy of recording. Sampling performed every 100 seconds.

- Data collection - If measured RMS strain levels exceed Noise Threshold, data collection begins. Data is recorded continuously until measured RMS strain levels fall below Noise Threshold.
- Completion of data collection - Data collection will automatically cease and Dosimeter will powerdown under any of the following conditions:
    - Measured RMS strain level below Noise Threshold
    - Dosimeter memory full (occurs after approximately 11 hours of data collection)
    - Battery runs out of power
    - Battery is disconnected
    - Strain gage wiring harness is disconnected

Step 4: Remove Dosimeter and Battery from Aircraft
- Disconnect battery.
- Disconnect strain gage wiring harness.
- Remove Dosimeter from aircraft mounting bracket.
- Remove battery from aircraft mounting bracket.

Step 5: Connect Dosimeter to Download Computer
- Connect RS-232 cable to serial ports on Dosimeter and computer to be used for download.
- Connect a dummy strain gage load to the Dosimeter. The Dosimeter should not be powered up without an appropriate strain gage load in place.
- Connect a fresh battery pack to dummy strain gage terminals.
- Dosimeter will power up automatically within 100 seconds. (Actual time of powerup will vary between 1 and 100 seconds depending on status of internal timer.)

Step 6: Download Standard Data Records (SDRs)
- Launch DPD_Loader application on computer to be used for download. (Program name floader)
- While running DPD_Loader perform the following steps:
    - Execute CONNECT command by typing "C" or using arrow keys. Dosimeter must be powered up for connection to be established.
    - On computer a warning will appear: Hardware configuration table is not valid. Invalid HW ID= Ø. Select OK
    - Execute READ MEMORY command by typing "M" or using arrow keys.
    - A dialog box will appear requesting addresses for memory read. Enter the following numbers for the start address and finish address for memory read:

Start address: 010000 Hex
Finish address: 400200 Hex

    - After entering the memory read addresses, a new dialog box will appear asking where to write the data. Use the arrow keys to select BINARY DUMP TO FILE. Dosimeter data records will then be automatically written to binary file named "dunp.lru".
    - Exit DPD_Loader by typing "X".
- Rename file "dunp.lru" to the dated filename taking the form: SDR_dd_month_yy.dat (e.g., SDR_31_Dec_98).
- Resulting file size should be approximately 4.0 MB.

Step 7: Download Status Summary Data

- Re-launch DPD_Loader application on computer to be used for download.
- While running DPD_Loader perform the following steps:
  - Execute CONNECT command by typing "C" or using arrow keys. Dosimeter must be powered up for connection to be established.
  - Execute READ MEMORY command by typing "M" or using arrow keys.
  - Enter the following numbers for the start address and finish address for memory read:

Start address: 400201 Hex
Finish address: 400230 Hex

  - Use the arrow keys to select BINARY DUMP TO FILE. Dosimeter data records will then be automatically written to binary file named "dunp.lru".
  - Exit DPD_Loader by typing "X".
- Rename file "dunp.lru" to "eeprom.dat".
- Resulting file size should be exactly 48 bytes.

Step 8: Reset Dosimeter Memory
- Re-launch DPD_Loader application.
- While running DPD_Loader perform the following steps:
  - Execute CONNECT command by typing "C" or using up and down arrows. Dosimeter must be powered up for connection to be established.
  - Execute RESET MEMORY command by typing "R" or using arrow keys. Memory reset will take approximately 3 minutes.
  - Exit DPD_Loader by typing "X".

Step 9: Disconnect Dosimeter from Download Computer
- Disconnect battery.
- Disconnect strain gage dummy load.
- Disconnect RS-232 cable.

Step 10: Transfer Data Files
- E-mail data files to Boeing Point of Contact for post processing and analysis.

Step 11: Refresh Battery Box
- The battery box contains two battery packs: a ten pack and a five pack. Under typical operating conditions, the ten pack is expected to last for approximately 12 hours of continuous data collection. The five pack is expected to last for approximately 24 hours of continuous data collection. Actual battery life is dependent on operating temperature.
- Data collection hours on each battery should be tracked, and batteries should be replaced accordingly to avoid losing data.
- If it is of the highest priority to collect all data for every flight, it is recommended that the ten-pack batteries be replaced once every flight, and the five-pack batteries be replaced once every two flights.
- If the risk of occasionally losing data is acceptable, the battery change intervals can be based on tracked data collection hours or battery voltages after each flight. Voltages for each pack should be around 14 V. A lower voltage may indicate a failing battery.

4.2-2 Operation Procedure for Upgrading Dosimeter Software

Dosimeter software may need to be modified or upgraded after initial installation. Modifications are typically used to adjust key program variables which tune Dosimeter function and operation for a specific application. The dosimeter software contains several programmable variables including frequency range, idle period, and type of data to be recorded, which give it the flexibility required to support a variety of applications. The procedure below outlines the steps required to upload modified software onto the Dosimeter. The procedure is written for the case in which the Dosimeter has been removed from the aircraft to perform the software upload.

Step 1: Connect Dosimeter to Upload Computer
- Connect RS-232 cable to serial ports on Dosimeter and computer containing new software.
- Connect a dummy strain gage load to the Dosimeter. The Dosimeter should not be powered up without an appropriate strain gage load in place.
- Connect a fresh battery pack to dummy strain gage terminals.
- Dosimeter will power up automatically within 100 seconds. (Actual time of powerup will vary between 1 and 100 seconds depending on status of internal timer.)

Step 2: Upload New Software
- Launch DPD_Loader application on and computer containing new software.
- While running DPD_Loader perform the following steps:
  - Execute CONNECT command by typing "C" or using arrow keys. Dosimeter must be powered up for connection to be established.
  - Execute LOAD PROGRAM command by typing "L" or using arrow keys.
  - In the dialog box that appears, enter the full path and filename of the new software.
  - After upload, a new dialog box will appear indicating upload complete.
  - Exit DPD_Loader by typing "X".

Step3: Reboot Dosimeter
- Disconnect the RS-232 cable from the Dosimeter and allow the Dosimeter to turn itself off.
- Once the Dosimeter has powered down, reconnect the RS-232 cable and allow the Dosimeter to turn itself on.

Step 4: Reset Dosimeter Memory
- Re-launch DPD_Loader application.
- While running DPD_Loader perform the following steps:
  - Execute CONNECT command by typing "C" or using up and down arrows. Dosimeter must be powered up for connection to be established.
  - Execute RESET MEMORY command by typing "R" or using arrow keys. Memory reset will take approximately 3 minutes.
-      Exit DPD_Loader by typing "X".

4.3 DURABILITY PATCH INSTALLATION PROCEDURE

A brief outline of the general steps involved for the installation of a Durability Patch on an aircraft is presented below according to the procedure outlined at Wright-Patterson Air Force Base. The steps are very similar to conventional hot bonded structural repair. A detailed procedure is found in Appendix E.

1. Cut structural adhesive film to final size, one or two peel ply(ies) in place.
2. Cut outer perimeter of VEM layer, release liner in place.
3. Cut VEM and release liner for cutout.
4. Install a release liner on VEM on other side from existing release liner.
5. Cut outer perimeter of new release liner.
6. Cut all fiberglass prepreg layers (template may be useful).
7. Lay smallest fiberglass layer onto transparent peel ply.
8. Lay second ply, de-bulk.
9. Lay and debulk remaining fiberglass layers.
10. Make vacuum bag, thermal blanket ready.
11. Perform surface prep, primer.
12. Seal cracks for vacuum as necessary.
13. Lay structural adhesive on skin to be repaired/reinforced.
14. Remove peel ply.
15. Lay VEM onto structural adhesive.
16. Remove release liner.
17. Lay stack of fiberglass layers down.
18. Remove peel ply.
19. Install thermal blanket.
20. Install vacuum bag.
21. Perform cure cycle.
22. Inspect visually and with coin tap.

5. SERVICE APPLICATIONS

The purpose of the three service applications were to assess the damage dosimeter and durability patch design process. The first application, discussed in section 5.1, was to evaluate a high cycle fatigue application on the B-52 aircraft. It was initially believed that this application would require a durability patch attached to the exterior surface of the fuselage skin. After using the damage dosimeter and discussions with the B-52 SPO, it is likely that a damping treatment installed on the interior skin surface of the airplane will be the preferred concept.

The second application (section 5.2) was to evaluate the dynamic characteristics for an F-15 access panel on the underside of the airplane. This location had been previously evaluated and a durability patch had been installed. Additionally this application will evaluate the use of the dosimeter in a relatively severe fighter environment.

The third application (section 5.3) was on the edge of the flap well of a C-130 aircraft. Turbulent airflow from the prop-wash causes HCF in this region. It is expected that this evaluation will be a durability patch.

5.1   B-52 DURABILITY PATCH DEMONSTRATION

The B-52 fleet is experiencing cracking in the fuselage skin at the location of the deployed flaps apparently due to sonic fatigue damage. A damage dosimeter gathered service data to accurately determine conditions at which damage occurs. The dosimeter data showed that cumulative damage occurs for vibratory response frequencies between approximately 20 to 200 Hz and at or near ambient ground temperature. This corresponds to a flaps deployed condition. An add-on vibration damping treatment was designed and tested in the laboratory for this service condition. The damping design consists of an aluminum angle with a layer of damping polymer/pressure sensitive adhesive (PSA) between one leg of the angle and the skin. For the installation on the interior surface of the fuselage skin, the paint is mildly abraded and wiped clean with solvent. Then, a protective liner is peeled from the PSA and the angle is pressed against the skin. Several angles are used. A vibratory SIF greater than 2 has been preliminarily derived from measurements made in the laboratory with a portion of actual aircraft structure. The dynamic characteristics of the structure were measured prior to and after application of the damping treatment. A HCF LIF) of approximately 50 is associated with a SIF of 2. The LIF would be applied to the residual fatigue life existing at the time of installation of the damping. For example, if the damping were installed at 40,000 flight hours, and if the existing untreated residual life was one hour, the treated residual life would be 50 hours and failure would occur at 40,050 instead of 40,001 hours. The incremental residual life is extended. HCF analysis establishes that damping would dramatically reduce the number of failures occurring in the remaining operational life of the fleet. A second ground experimental investigation was performed on a retired B-52 aircraft stored outdoors; in this case the constraining layer was a square pultruded fiberglass tube.

Several aircraft in the B-52 fleet are experiencing cracking the in side-of-body fuselage skin at the location of the deployed flaps as shown in figure 20. This cracking is considered premature with respect to the design life of the fuselage structure. It is believed that oscillatory airflow

associated with deployed flaps excites the vibration of the skin panels. The skin at the fastener row attaching the substructure is subjected to vibratory out of plane bending. This creates HCF loading in the substructure to skin fastener row and leads to premature cracks emanating from the fasteners as illustrated in figure 21. The structure of interest is 12 bays of skin between two major frames fore and aft, and between a longeron at the bottom and a skin splice at the top. The substructure defining the 12 bays is composed of Z-section frames members oriented vertically at 9-inch spacing. The skin is approximately 0.090 inch thick. It is understood that the cracking most often occurs in the six bays of skin forward of the aft major frame.
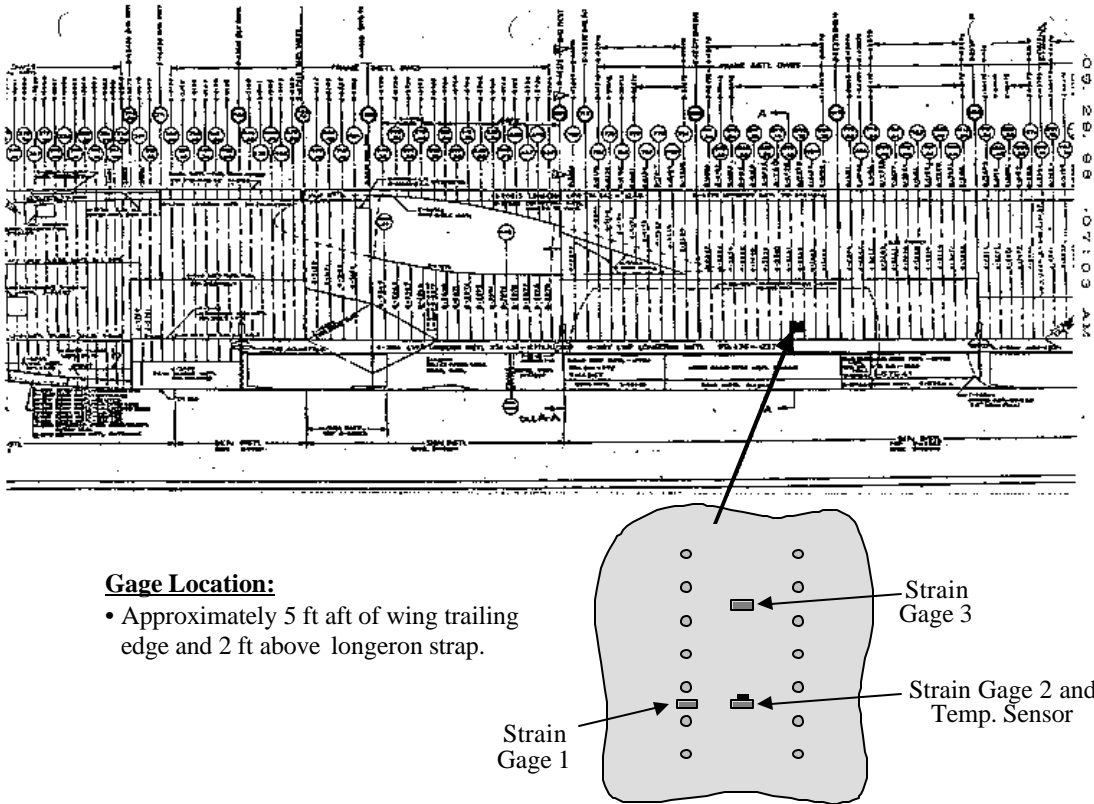
Gage Location:
• Approximately 5 ft aft of wing trailing edge and 2 ft above longeron strap.

Strain Gage 3

Strain Gage 2 and Temp. Sensor

Strain Gage 1

Figure 20.   Location of Interest on Fuselage Body.

The disturbed air flow associated with the deployed flaps excites cumulative resonant HCF damage, commonly known as acoustic or sonic fatigue. The excitation is nearly periodic, which results in high modal density. The structure carries inplane static stresses, imparted by fuselage vertical bending shear loads, which vary depending on ground, flight, and transient loading conditions. The effect of the in-plane loading is to vary the natural frequencies of the skin panels.
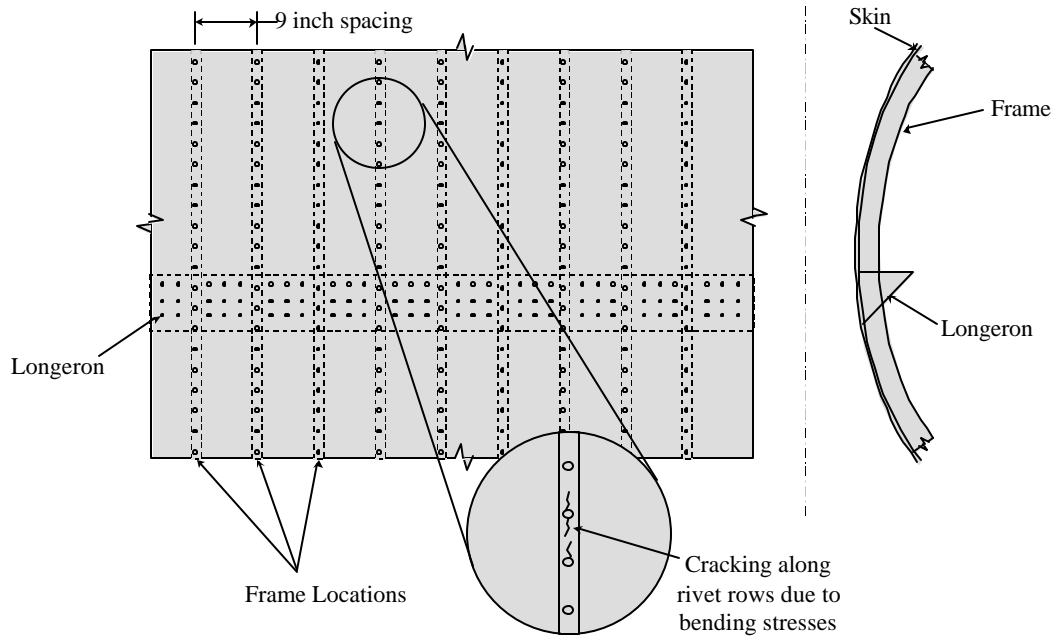
Figure 21. Sketch of B-52H Side-of-Body Panel with Cracking Along Rivet Rows
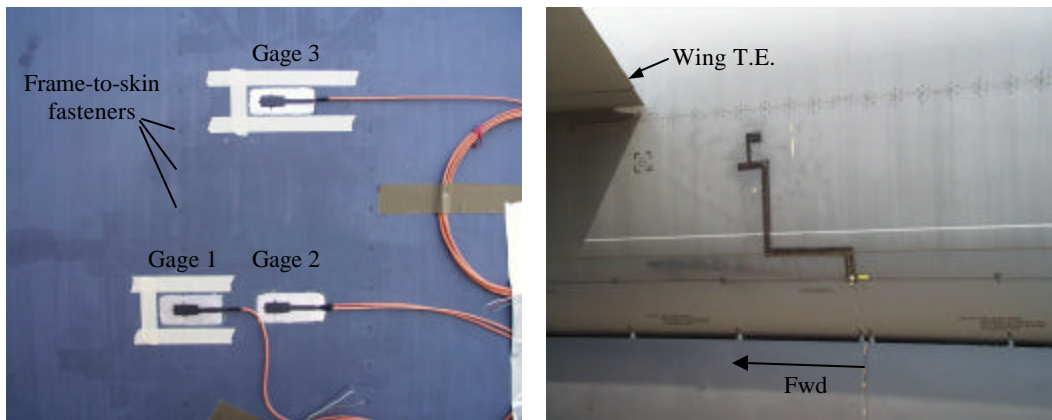
Figure 22. Strain and Temperature Sensors Mounted to Fuselage (left), Sensors and Cable Run Covered in Black Sealant. Note Position Aft of Wing (right).

5.1-1   Service Data Collection using the Damage Dosimeter

Dynamic strain gages were installed on typical structure in the region of cracking as indicated previously in figure 20. The gage installation is shown in figure 22. The temperature sensor was also installed in the same area near gage 2. The Dosimeter and battery were installed as shown in figure 23.
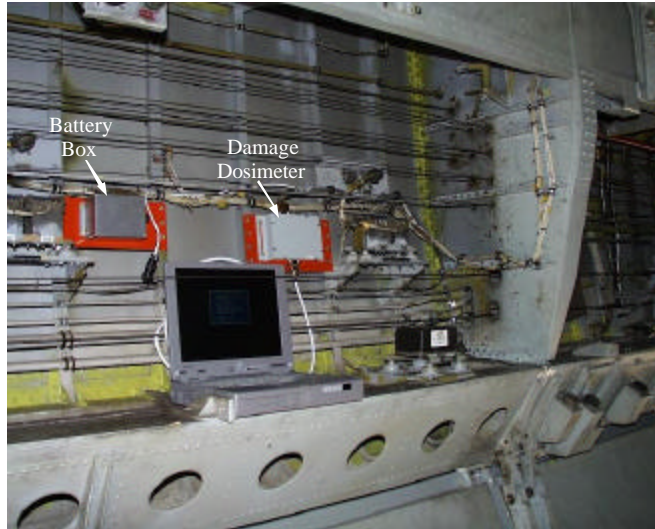
Figure 23. Damage Dosimeter and Battery Box Mounted Inside B-52 Weapons Bay

Data collected from several flights show that the highest RMS strains occur during takeoff roll and climbout and possibly during landing approach. A typical takeoff RMS strain versus time plot is shown in figure 24. It was collected during flight number 6. Ground operation has a level of activity less than 10 $\mu\varepsilon$ RMS. With takeoff roll, liftoff, and climb out, activity ramps up to approximately 80 $\mu\varepsilon$ RMS. There is then a plateau of approximately 70-90 $\mu\varepsilon$ RMS followed by a peak as high as 140 $\mu\varepsilon$ RMS lasting approximately 15 seconds. This is then followed by a decrease to less than 10 $\mu\varepsilon$ RMS with flaps retracted. The peak occurs during flap retraction/deployment; for flap retraction, it initially translates forward, then rotates up until it is tucked against the wing trailing edge structure. The translation causes greater discontinuities in the wing/flap air flow. The RMS strain and the temperature are shown for the entire flight in figure 25 and 26. The takeoff shown in figure 24 is in a very compressed region near the origin of figure 25. Multiple touch and go's are included in figure 25 and 26. Figure 27 is a cross-plot of those strain levels which exceed 20 $\mu\varepsilon$ RMS and their associated temperature for one entire flight.
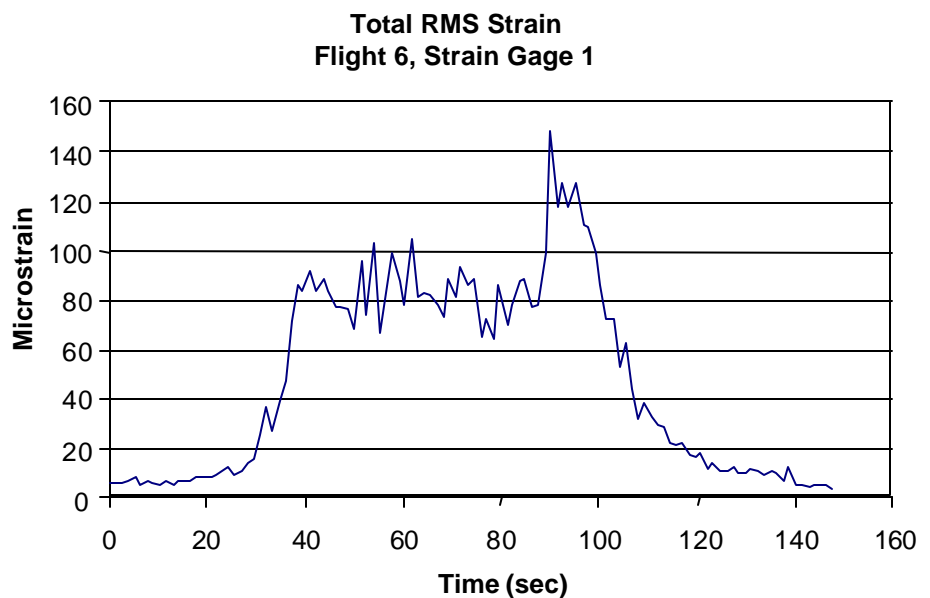
Figure 24. Total RMS Strain Time History During Take-Off (Flight 6)

Flight 6
RMS Strain Levels for Full Flight
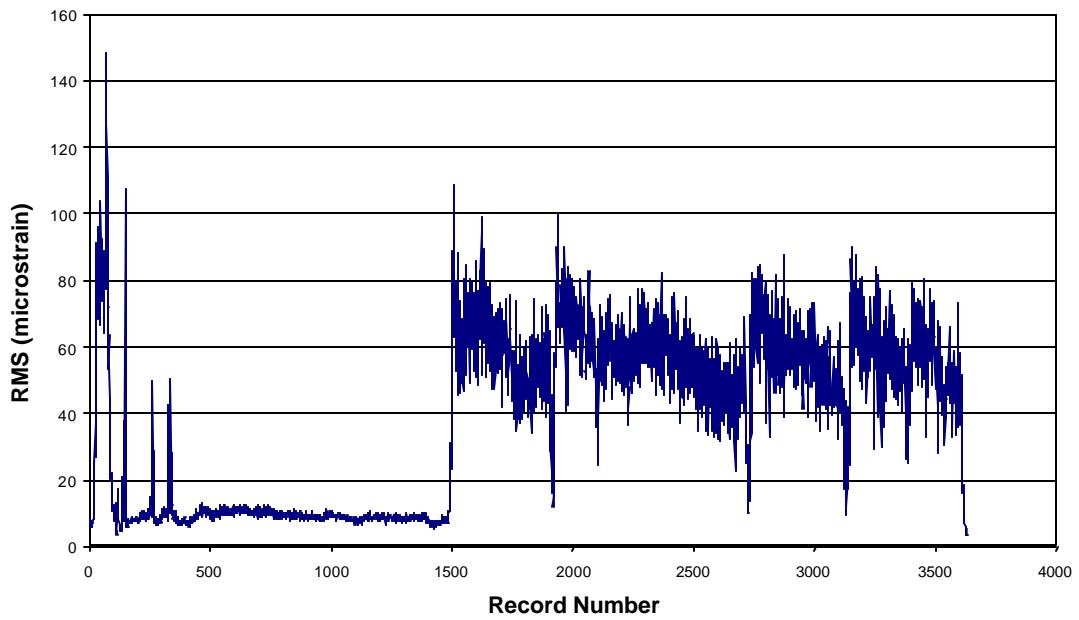
Figure 25.   RMS Strain Time History for Entire Flight (Flight 6)

Flight 6
Temperature for Full Flight
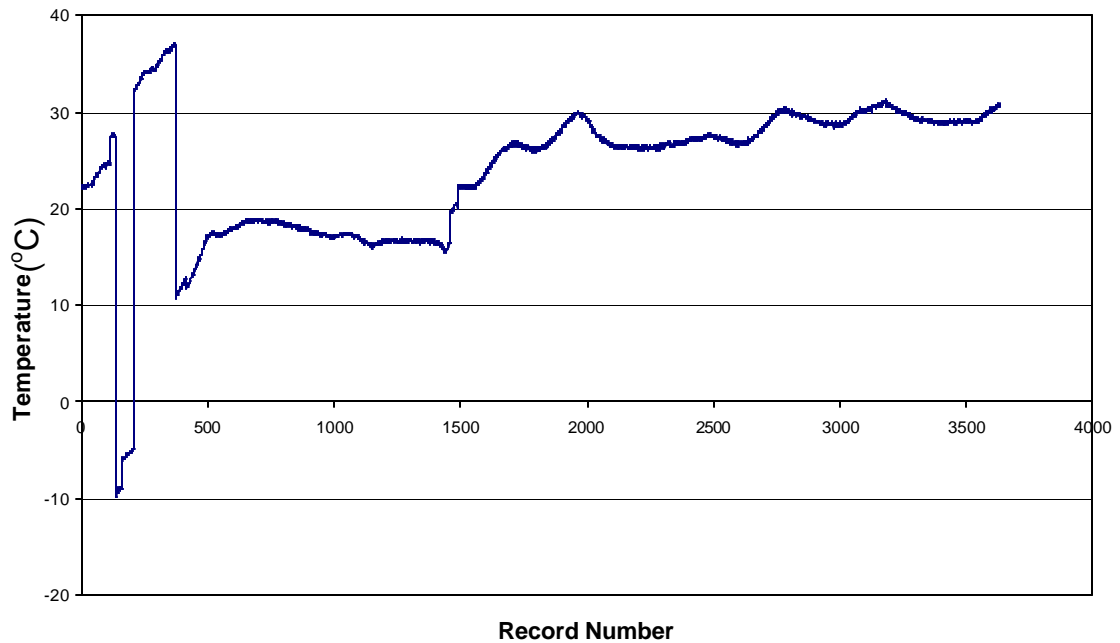
Figure 26.   Temperature Time History for Entire Flight (Flight 6)

46

Flight 6
Strain vs. Temperature Cross-Plot
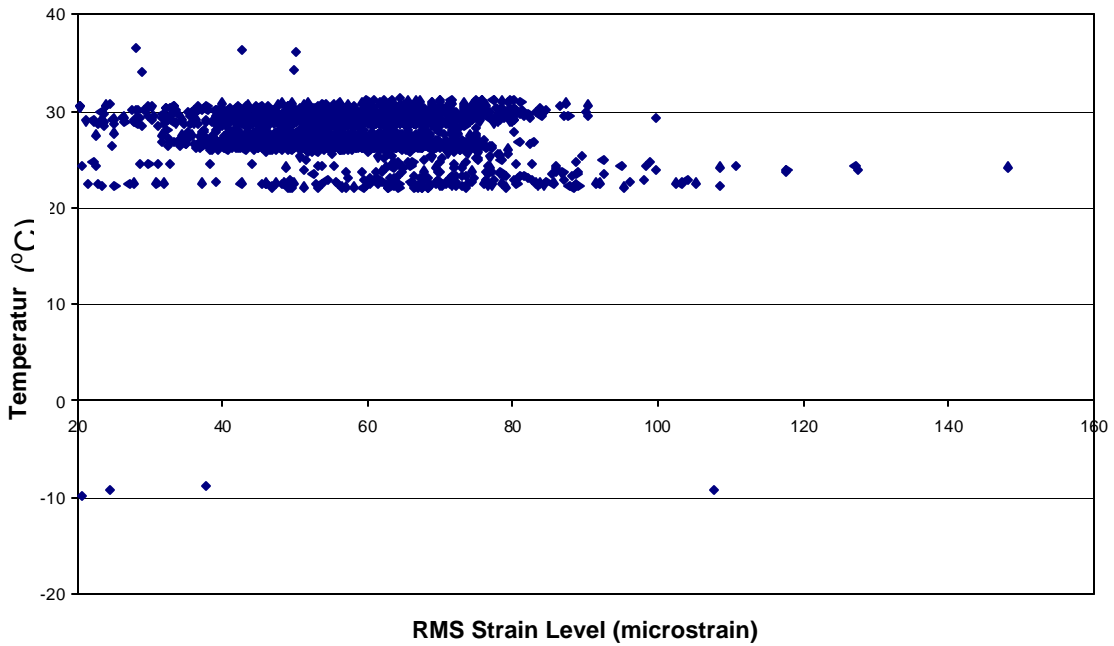
Figure 27.   Cross Plot of Temperature Versus RMS Strain for Entire Flight (Flight 6)

Figure 28 presents RMS strain versus time for that portion of the takeoff captured during data flight number 5. It includes some plateau, plus the peak.   Further analysis was performed for the record numbers (RNs) 1, 15, 23, 25 and 27.   RNs correlate to time. Figures 29 and 30 shows strain and temperature for the entire flight.   Figures 31, 33, 35, 37 and 39 are PSD's for the various RN's. Figures 32, 34, 36, 38 and 40 are the associated normalized cumulative RMS microstrains. These indicate that vibratory response is broadband with the exception that figure 29 indicates that 50 percent of the response is in a mode or modes near 50 Hz in frequency. On occasion, PSDs have peaks at approximately 55 and 110 Hz. It is therefore concluded that the character of the vibration is broadband with approximately 95 percent of the response between 20 and 200 Hz. Figure 41 is similar to figure 27.   Together they indicate that high levels of strain are associated with service temperature near ambient ground temperature. This is consistent with flaps only being deployed for landing and take off operations.

47
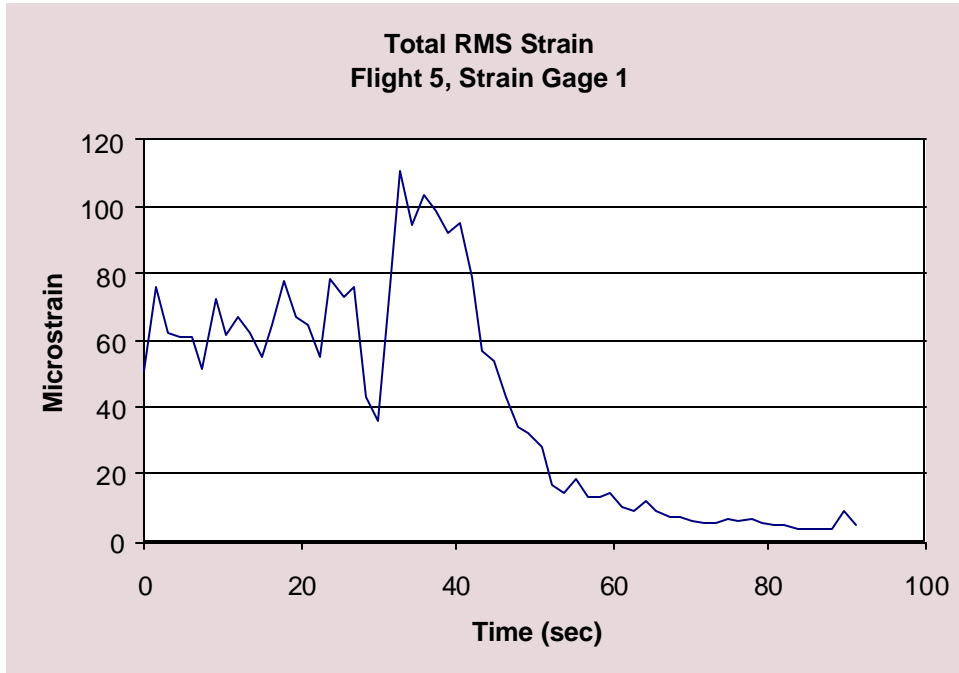
Figure 28.   Total RMS Strain versus Time During Takeoff (Flight 5)
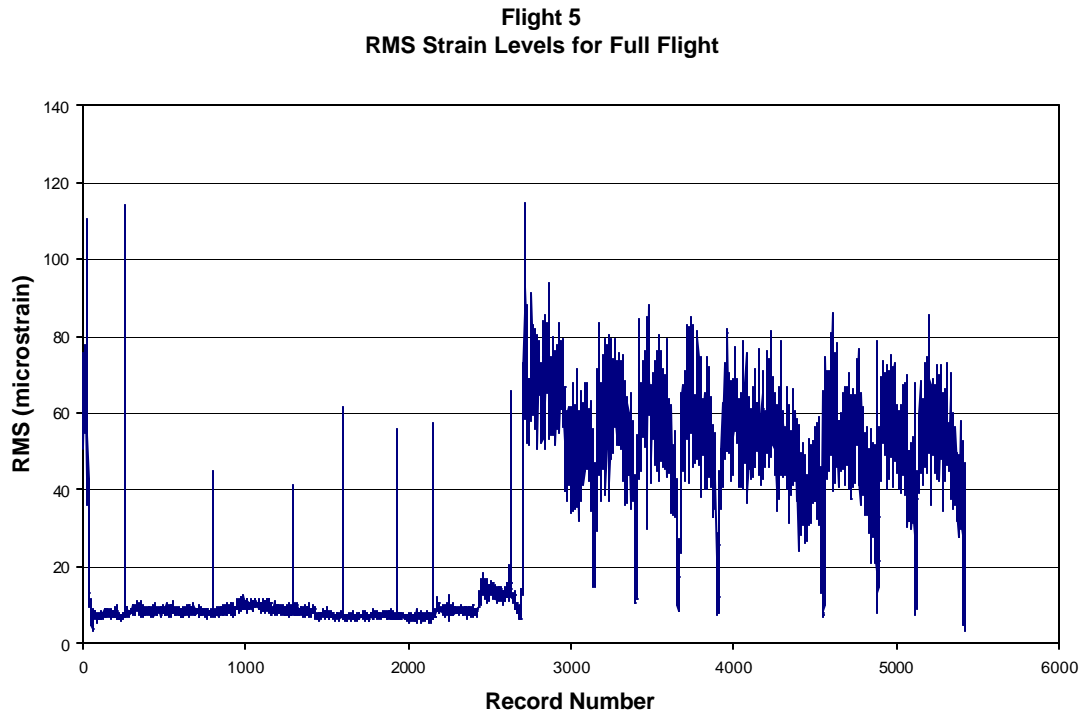
*Figure 29. RMS Strain Time History for Entire Flight (Flight 5)*

48

Flight 5
Temperature for Full Flight
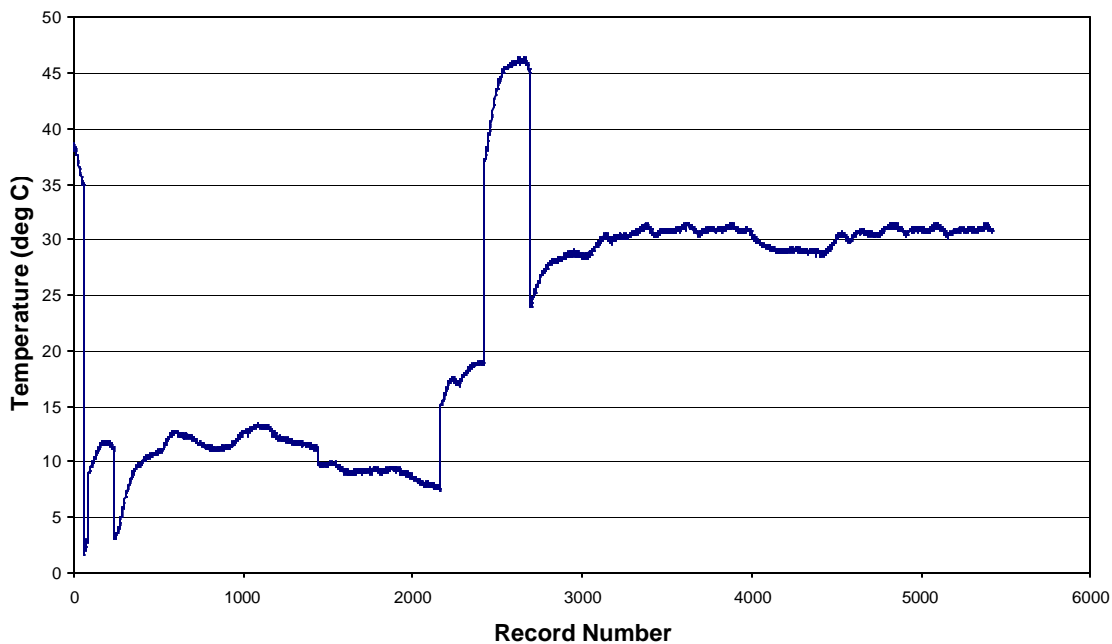
Figure 30.   Temperature Time History for Entire Flight (Flight 5)

Strain PSD
Flight 5, Strain Gage 1

RN = 1
Time, t = 0.0 sec
Location: Plateau
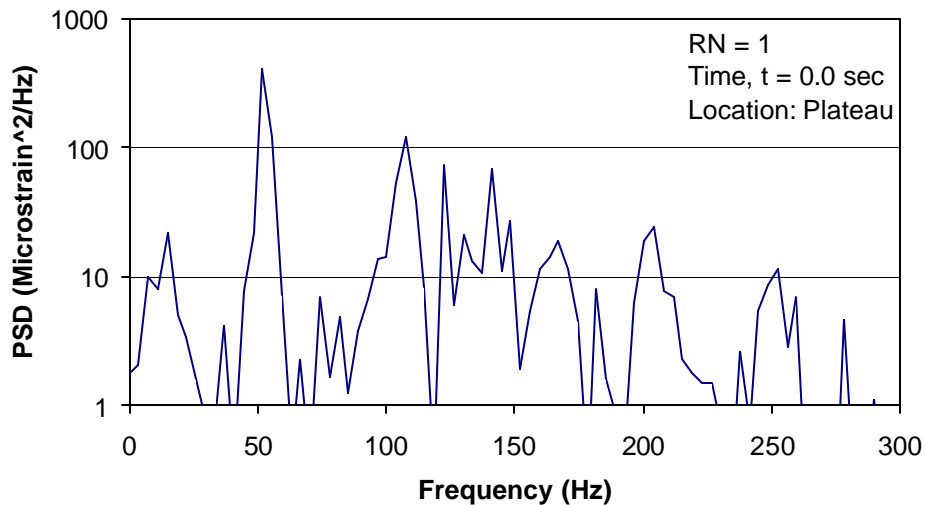
Figure 31.   Strain PSD for RN 1 (Flight 5)

49
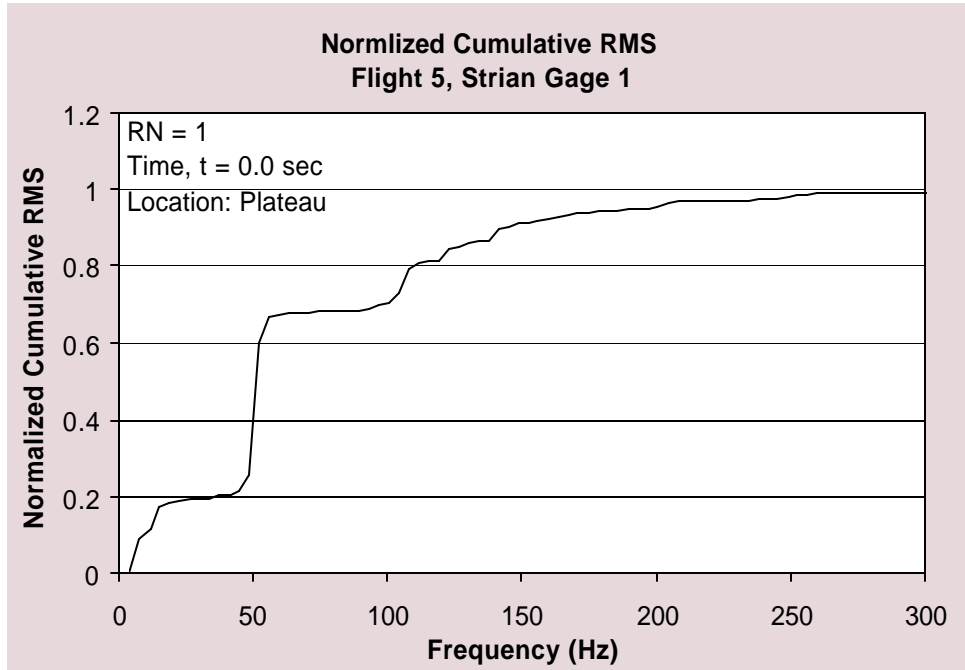
Figure 32. Cumulative RMS Strain Versus Frequency for RN1 (Flight 5)
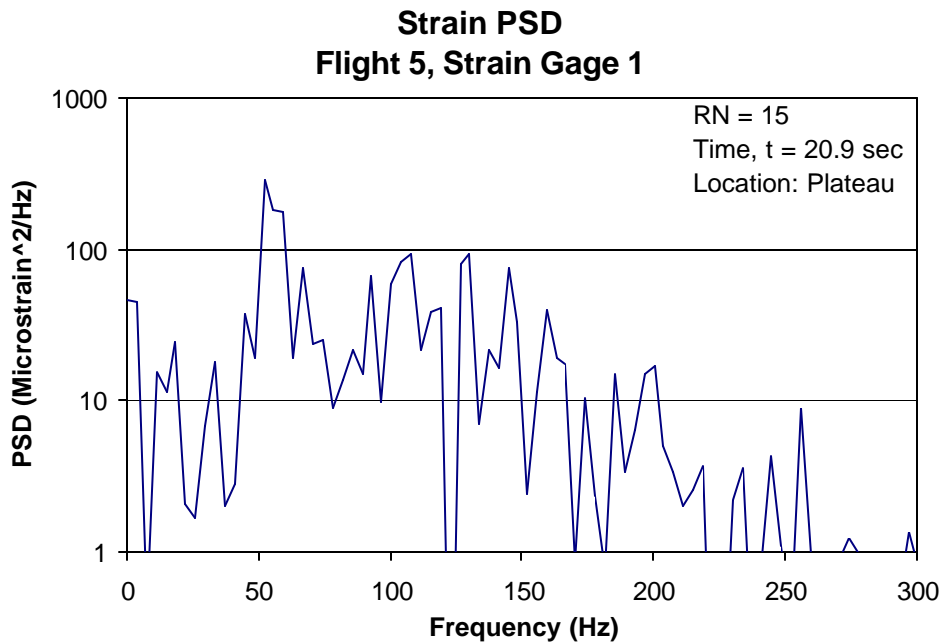
Figure 33. Strain PSD for RN15 (Flight 5)

Normalized Cumulative RMS
Flight 5, Strain Gage 1
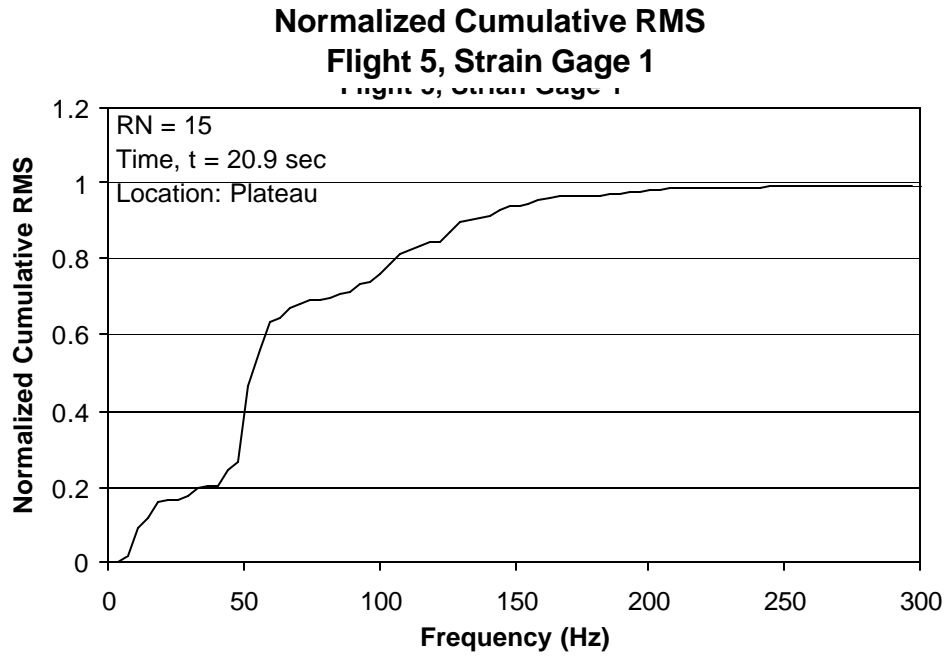
Figure 34. Cumulative RMS Strain Versus Frequency for RN 15 (Flight 5)

Strain PSD
Flight 5, Strain Gage 1
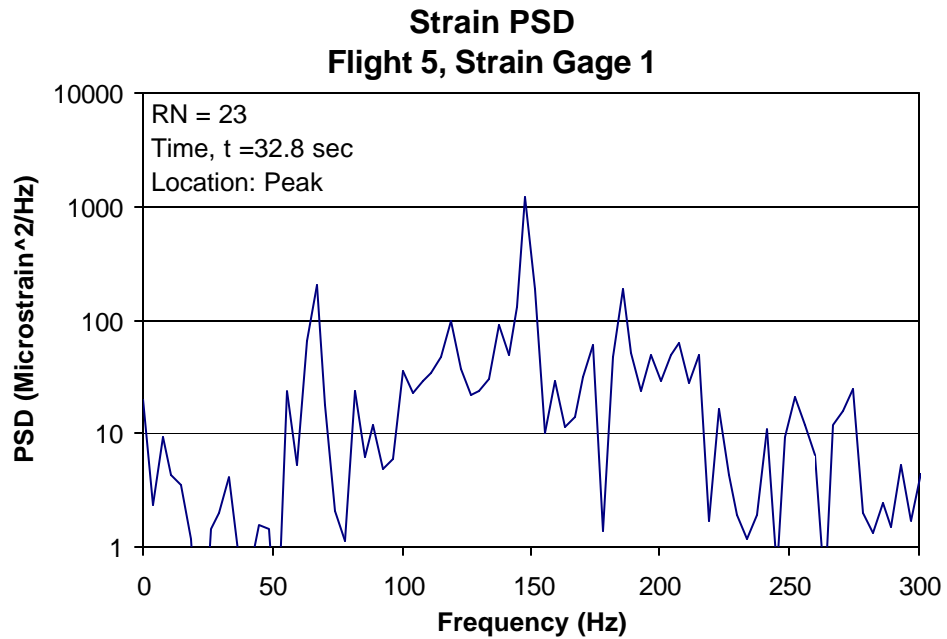

Figure 35. Strain PSD for RN 23 (Flight 5)

51

Normalized Cumulative RMS
Flight 5, Strain Gage 1
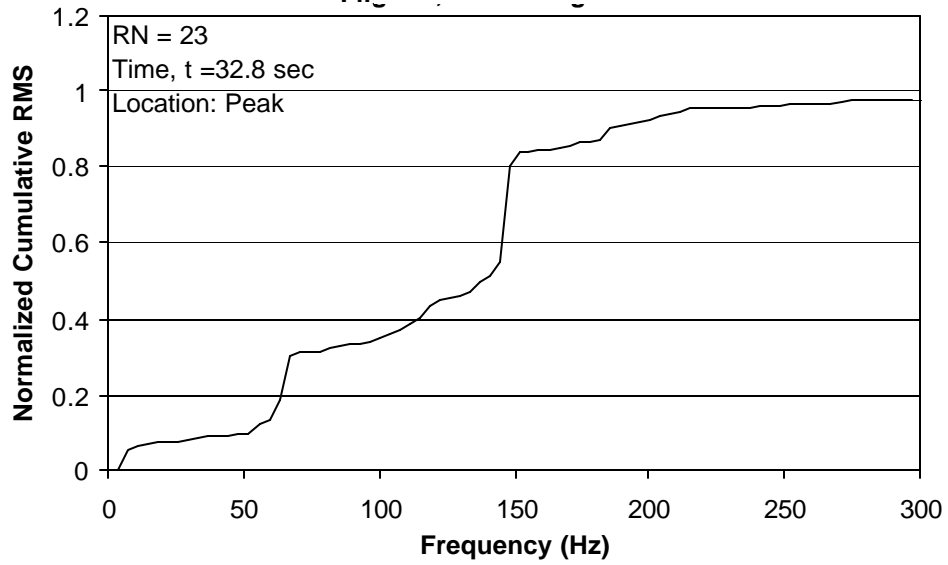
Figure 36.   Cumulative RMS Strain Versus Frequency for RN 23 (Flight 5)

Strain PSD
Flight 5, Strain Gage 1
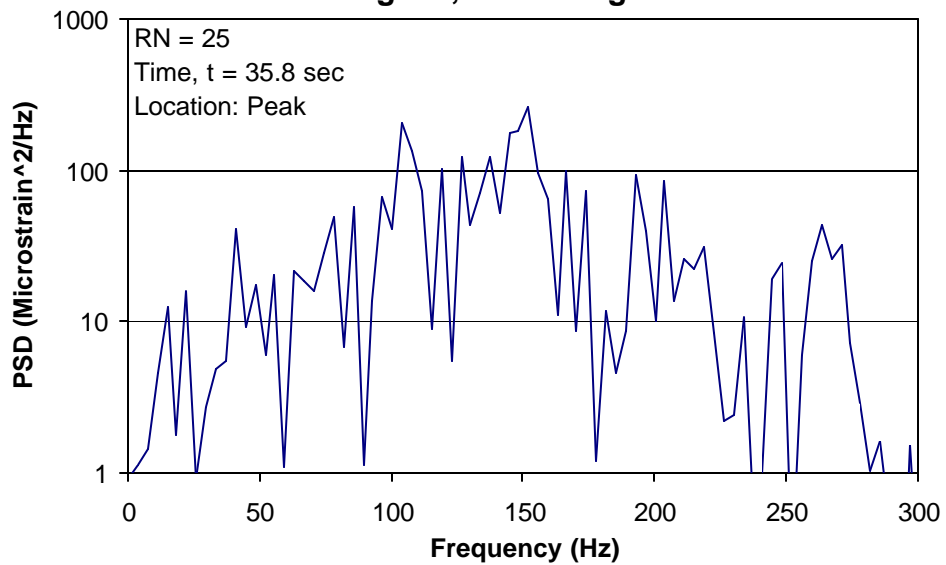
Figure 37.   Strain PSD for RN 23 (Flight 5)

52

Normalized Cumulative RMS
Flight 5, Strain Gage 1

RN = 25
Time, t = 35.8 sec
Location: Peak
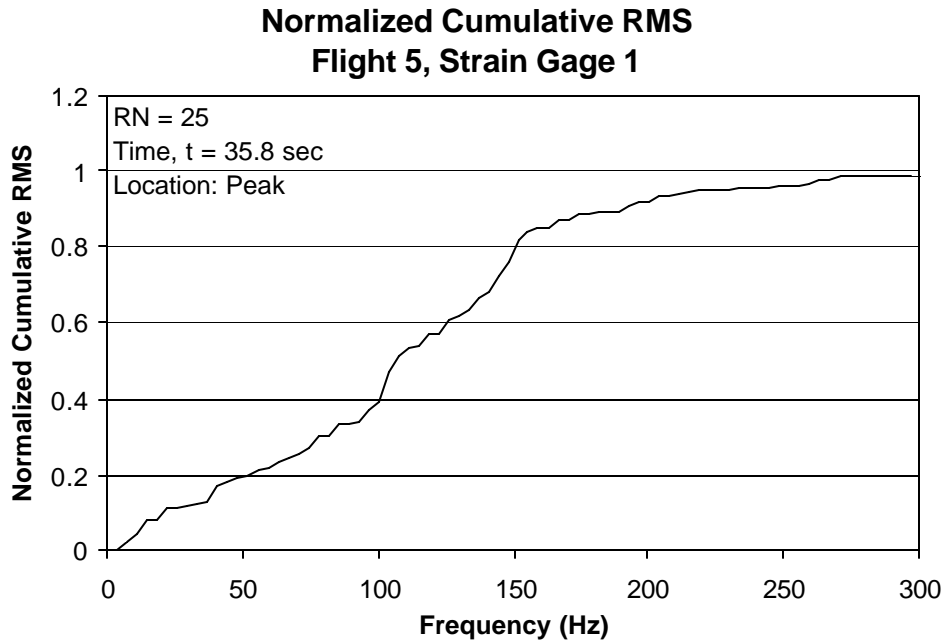
Figure 38.   Cumulative RMS Strain Versus Frequency for RM 25 (Flight 5)

Strain PSD
Flight 5, Strain Gage 1

RN = 27
Time, t = 38.8 sec
Location: Peak
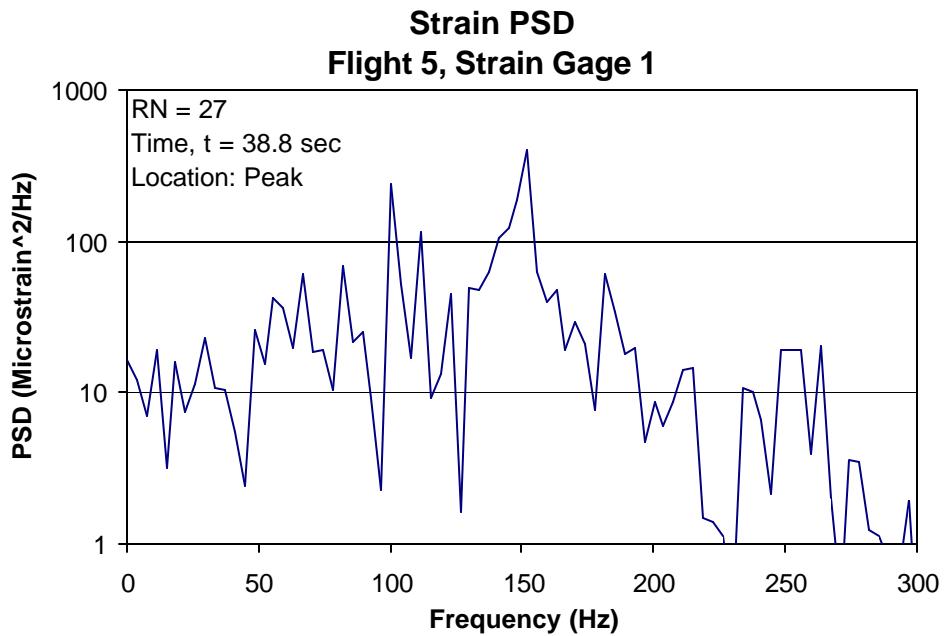
Figure 39.   Strain PSD for RN 27 (Flight 5)

Normalized Cumulative RMS
Flight 5, Strain Gage 1

RN = 27
Time, t = 38.8 sec
Location: Peak
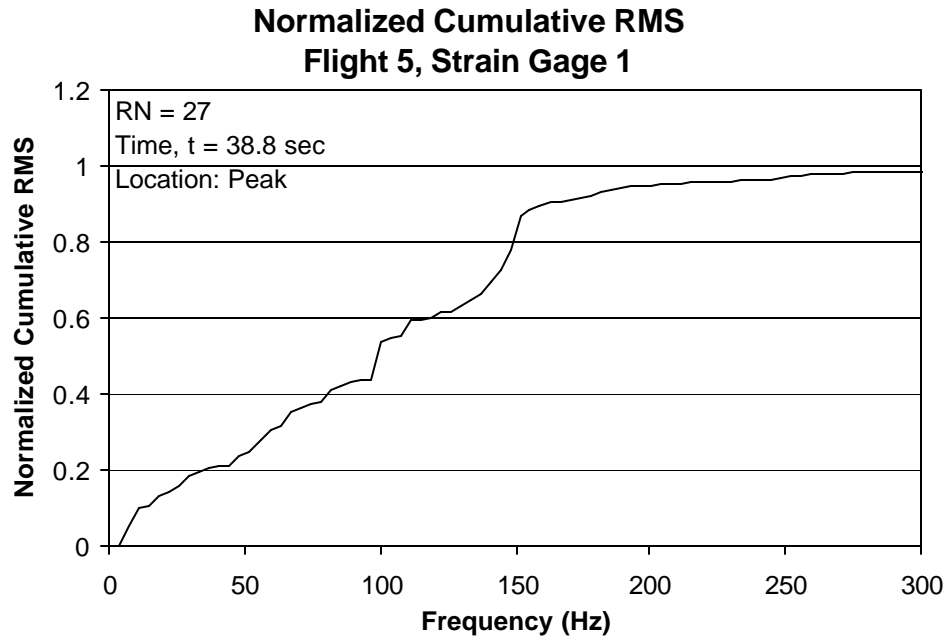
Figure 40.   Cumulative RMS Strain Versus Frequency for RN 27 (Flight 5)

Flight 5
**Strain vs. Temperature Cross-Plot**
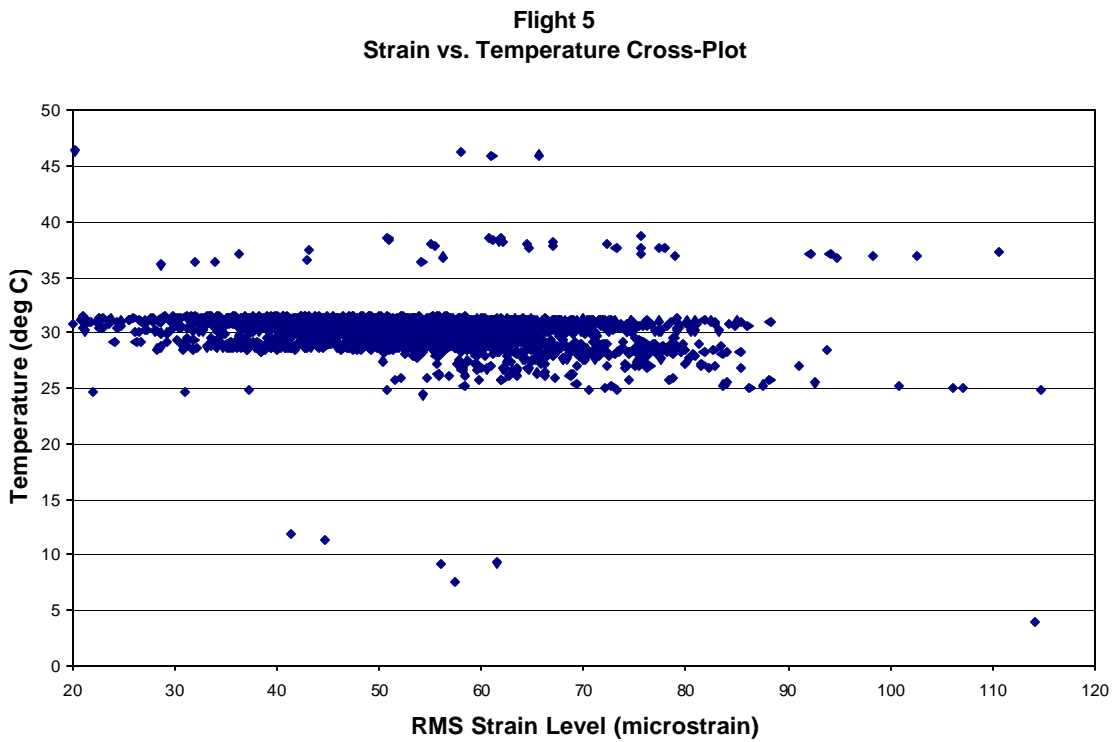
Figure 41.   Cross Plot of Temperature Versus RMS Strain for Entire Flight (Flight 5)

5.1-2. Excitation in Service

The excitation in service was measured using the damage dosimeter. Figure 42 shows the applications of the strain gages and temperature sensor to the B-52 side of body panel. Flight test data acquired by the dosimeter showed the panel excitation to be a broadband vibration response due to the aerodynamics associated with the deployed flaps during take-off. The measured peak vibration frequencies were correlated with the panel vibration modes predicted by the FEA model as described in section 5.1-5. This enabled the design of a viscoelastic constrained layer damping that properly attenuated the in-flight vibration response of the panels. Anticipated vibration attenuation eliminates further crack initiation, therefore eliminating the need to design a strength component into the repair.
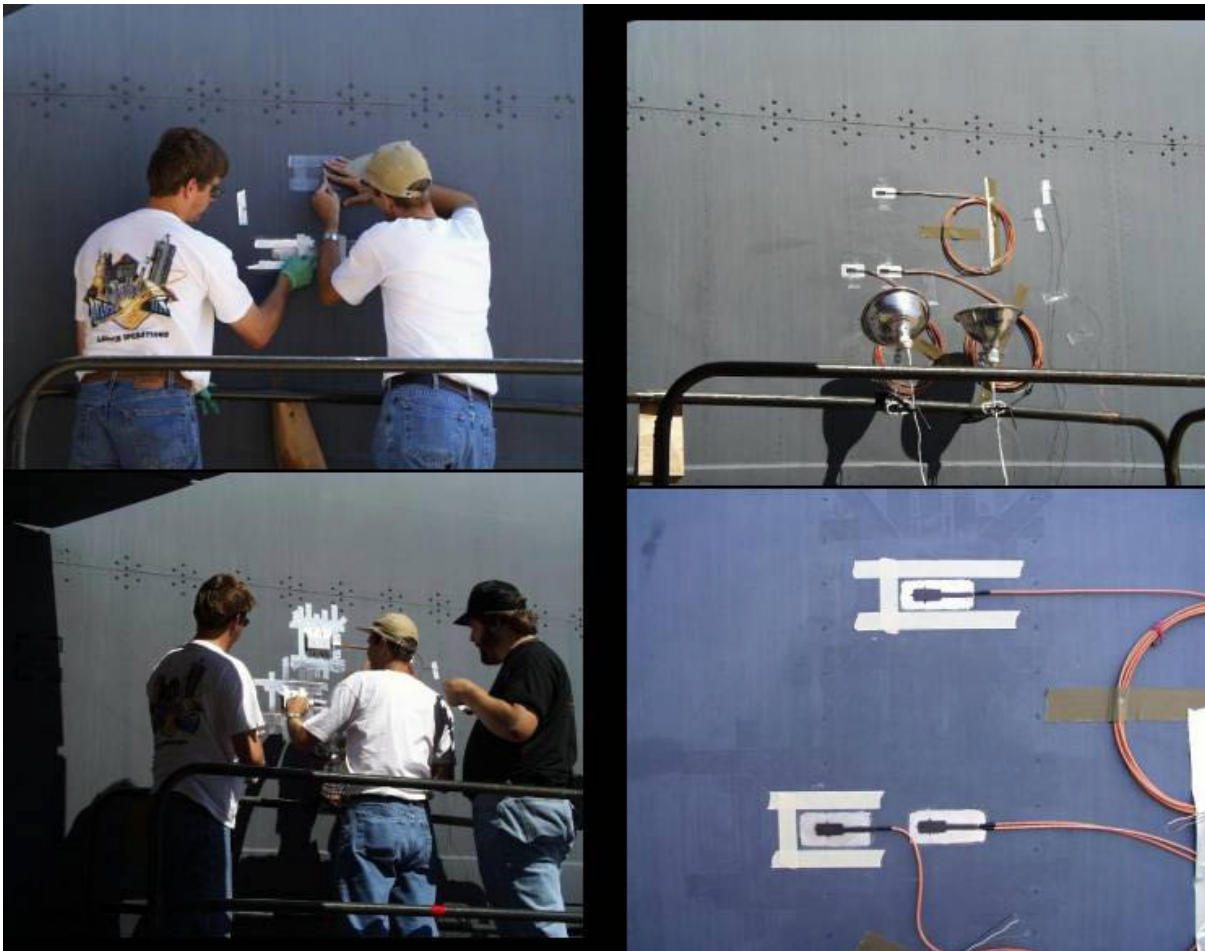
Figure 42. Dosimeter Instrumentation Installation on B-52 Side of Body Panel

5.1-3. Laboratory Test Article

A portion of the B-52 fuselage sidewall at the location of the deployed flap was obtained by Boeing Seattle to be used as a laboratory test article. It is approximately 40 inches high and 100 inches long. It has a large fore and aft longeron at the bottom and there were 11 Z-frames oriented vertically and attached to the longeron. There are 10 skin bays between the Z-frames and the skin extended approximately 6 inches both fore and aft beyond the end Z-frames. The skin in some locations was

permanently bent out of plane. The spacing of the Z-frames fastener row is approximately 9 inches; the flat portion of skin on the inside between the Z-frames was approximately 8 3/16 inches. There was a small amount of curvature. At the top, the skin and the Z-frames had been cut parallel to and below the longeron. For testing, it was suspended on a cord attached to the top of two Z-frames such that it would minimize the effect on the higher vibration modes. Because of the size (and associated inertia) of the longeron, the test condition lay somewhere between having all 4 edges free (FFFF) and having the edge at the longeron clamped with 3 edges free (CFFF). Although the test article is from an actual airplane, the vibration modes are affected by the boundary conditions and by in-plane loading. As a consequence, allowances must be made to interpret laboratory test article results for ground and flight conditions on the aircraft.

5.1-4. Finite Element Analysis (FEA)

A finite element model (FEM) having eleven Z-frames, ten skin bays and no skin beyond the end Z-frames, was developed. It was run with two sets of BCs: 1) no translation and no rotation at any boundary (FFFF), and 2) no translation and no rotation at bottom; both end Z's free; top skin and Z's free. (CFFF).

The FEA model analysis was run and 91 vibration modes were found in the specified range between 50 and 120 Hz (on occasion there are peaks at near 55 and 110 Hz).

The structure with 10 skin bays identical except for the fixed ends is a very nearly periodic structure, especially since the Z-frames are stiff in torsion. The vibration modes occur in family groups. Figure 43 lists mode number, frequency in Hz, percent strain energy in the skin, and a brief description of the skin panel mode shape.   Figures 44 through 47 present 1) displacement mode shape, 2) strain energy, 3) longitudinal stress and 4) the profile section view respectively for mode 73 at 106.12 Hz. This mode is a 1x2 mode with stringer bending (not rotating). Mode 1 at 52.868 Hz is a 1x1 skin panel mode. The 1x1 family has from 91 to 95 percent of modal strain energy in the skin whereas the 1x2 family has from 57 to 61 percent (which may indicate more difficulty in damping this mode with skin treatment). All other modes have a very large fraction of modal strain energy in the skin. The stress indicates strain and curvature of the skin surface, and therefore, a high stress indicates a desirable location for effectiveness and efficiency of add-on damping.

In the various modes within a family group, different individual skin panels may have the maximum amplitude and the other skin panels have some fraction. Of the 1x1 family, mode 1 is the most nearly spatially sinusoidal in the longitudinal direction and was selected for illustration. A section of the mode shape 73 (fig. 47) indicates that between the Z-frames the skin deforms as a sine wave plus a straight line. Mode 73 is also approximately spatially sinusoidal in the longitudinal direction, as was mode 1. Note that there is significant "Z" substructure bending (not rotating) is this mode.

Mode Number	Frequency Hz	% Strain Energy In Skin	Type Mode
1	52.86	91.46	1x1
2	52.92	91.68	1x1
3	53.01	92.02	1x1
4	53.14	92.47	1x1
5	53.28	92.99	1x1
6	53.44	93.53	1x1
7	53.6	94.06	1x1
8	53.76	94.54	1x1
9	53.91	94.92	1x1
10	54.09	95.22	1x1

Mode Number	Frequency Hz	% Strain Energy In Skin	Type Mode
11	54.82	97.27	2x1
12	54.89	97.39	2x1
13	55.02	97.68	2x1
14	55.19	98.06	2x1
15	55.37	98.40	2x1
16	55.53	98.62	2x1
17	55.65	98.74	2x1
18	55.73	98.78	2x1
19	55.79	98.79	2x1
20	55.82	98.79	2x1

Mode Number	Frequency Hz	% Strain Energy In Skin	Type Mode
21	58.08	99.54	3x1
22	58.11	99.54	3x1
23	58.14	99.60	3x1
24	58.17	99.54	3x1
25	58.28	99.56	3x1
26	58.41	99.59	3x1
27	58.55	99.63	3x1
28	58.67	99.65	3x1
29	58.77	99.67	3x1
30	58.88	99.68	3x1

Mode Number	Frequency Hz	% Strain Energy In Skin	Type Mode
31	63.762	99.39	4x1
32	63.765	99.41	4x1
33	63.79	99.47	4x1
34	63.83	99.57	4x1
35	63.89	99.66	4x1
36	63.95	99.73	4x1
37	64.01	99.79	4x1
38	64.07	99.83	4x1
39	64.12	99.87	4x1
40	64.16	99.88	4x1

Mode Number	Frequency Hz	% Strain Energy In Skin	Type Mode
41	72.15	99.78	5x1
42	72.16	99.81	5x1
43	72.24	99.87	5x1
44	72.25	99.87	5x1
45	72.26	99.87	5x1

Mode Number	Frequency Hz	% Strain Energy In Skin	Type Mode
46	72.27	99.89	5x1
47	72.30	99.91	5x1
48	72.33	99.92	5x1
49	72.36	99.94	5x1
50	72.38	99.95	5x1

Mode Number	Frequency Hz	% Strain Energy In Skin	Type Mode
51	83.604	99.88	6x1
52	83.606	99.88	6x1
53	83.6686	99.97	6x1
54	83.6688	99.97	6x1
55	83.669	99.96	6x1
56	83.671	99.94	6x1
57	83.675	99.91	6x1
58	83.68	99.89	6x1
59	83.685	99.86	6x1
60	83.688	99.83	6x1

Mode Number	Frequency Hz	% Strain Energy In Skin	Type Mode
61	97.07	81.99	7x1
62	97.42	89.60	7x1
63	98.024	99.76	7x1
64	98.027	99.77	7x1
65	98.028	99.78	7x1
66	98.034	99.85	7x1
67	98.037	99.78	7x1
68	98.041	99.91	7x1
69	98.047	99.97	7x1
70	98.055	99.81	7x1

Mode Number	Frequency Hz	% Strain Energy In Skin	Type Mode
71	98.77	84.14	Transition
72	99.50	71.82	Transition

Mode Number	Frequency Hz	% Strain Energy In Skin	Type Mode
73	106.11	60.88	1x2
74	106.41	60.97	1x2
75	106.93	61.08	1x2
76	107.70	61.14	1x2
77	108.75	61.05	1x2
78	110.13	60.69	1x2
79	111.82	59.91	1x2
80	113.66	58.67	1x2
81	115.26	57.46	1x2

Mode Number	Frequency Hz	% Strain Energy In Skin	Type Mode
82	115.51	99.97	8x1
83	115.52	99.97	8x1
84	115.541	99.98	8x1
85	115.548	99.98	8x1
86	115.55	99.98	8x1
87	115.57	99.97	8x1
88	115.58	99.97	8x1
89	115.59	99.96	8x1
90	115.60	99.95	8x1
91	115.61	99.94	8x1

Figure 43.   B-52 Skin Strain Energy Density Study

57

The same FEM with BCs CFFF was run; it was determined that there were 294 modes between 120 - 300 Hz, the lowest of which was 129.66 Hz in frequency. Many of these are high order in the fore and aft direction because of the skin free edge. The results of a tap test performed on the laboratory test article indicated that the actual modes of the structure more closely matched the fully clamped boundary conditions.

5.1-5 Damping Treatment Design

The objective is to provide internal add-on vibration damping for all skin modes including the 1x1 and the 1x2 modes. These modes are targeted because of the occasional peaks in the frequency response peaks from the dosimeter data. They are plotted in figures 44 through 47. Note that there is very little stringer rotation in these modes. Modal strain energy in the skin is 91 and 61 percent, respectively. Add-on damping to the stringer bending part of the modal strain energy would be very challenging, and is dropped from consideration. The recommended solution is to develop damping for the skin. Out-of-plane flexible motion as a function of longitudinal distance down the centerline of the skin panels indicate that the skin curvature is similar to the first and second modes of a clamped-clamped beam. As a consequence, the damping design is an adaptation of a constrained layer approach.
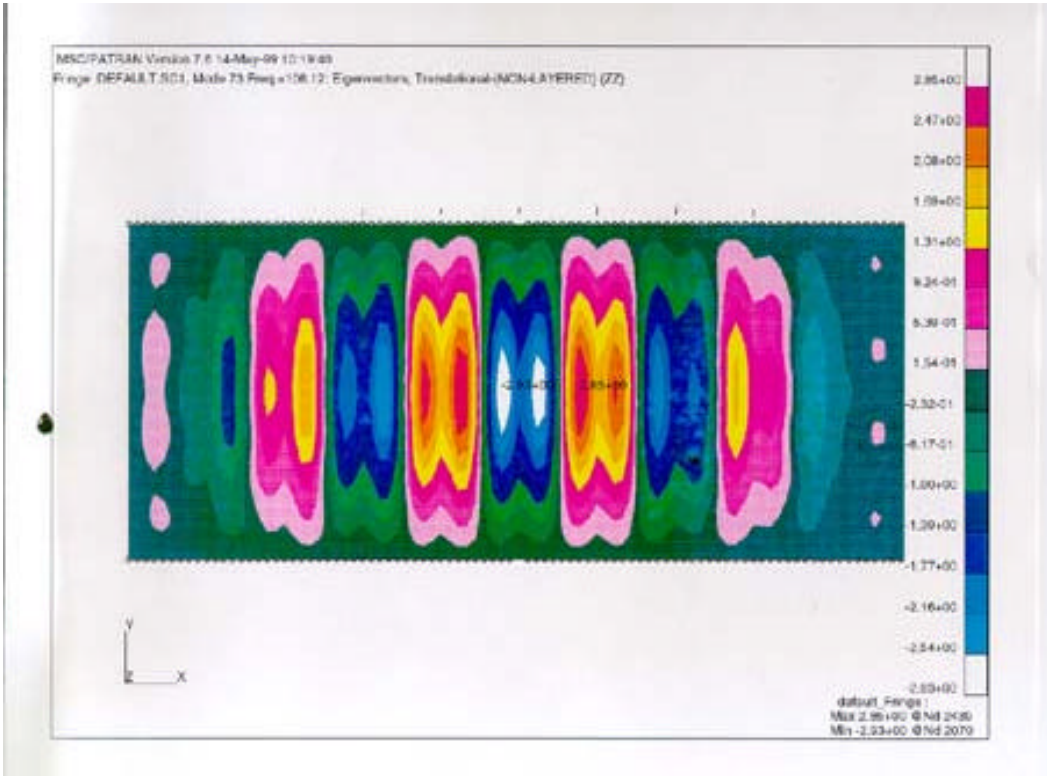
Figure 44.   Modal Displacement Distribution for Mode 73
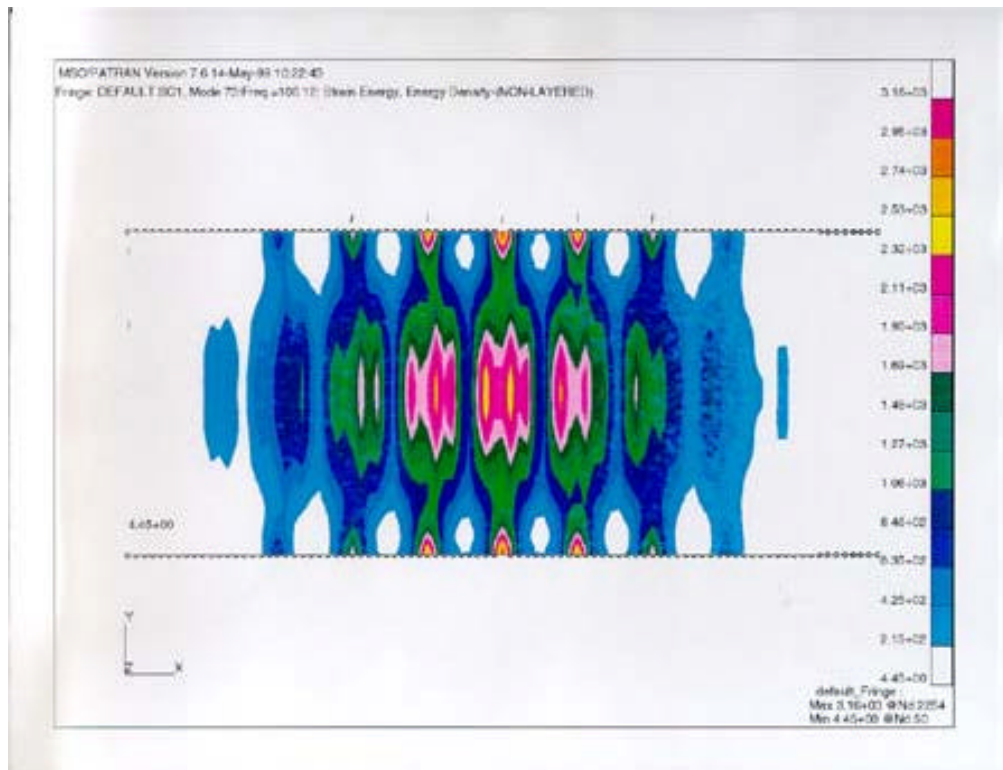
Figure 45. Modal Strain Energy Distribution for Mode 73
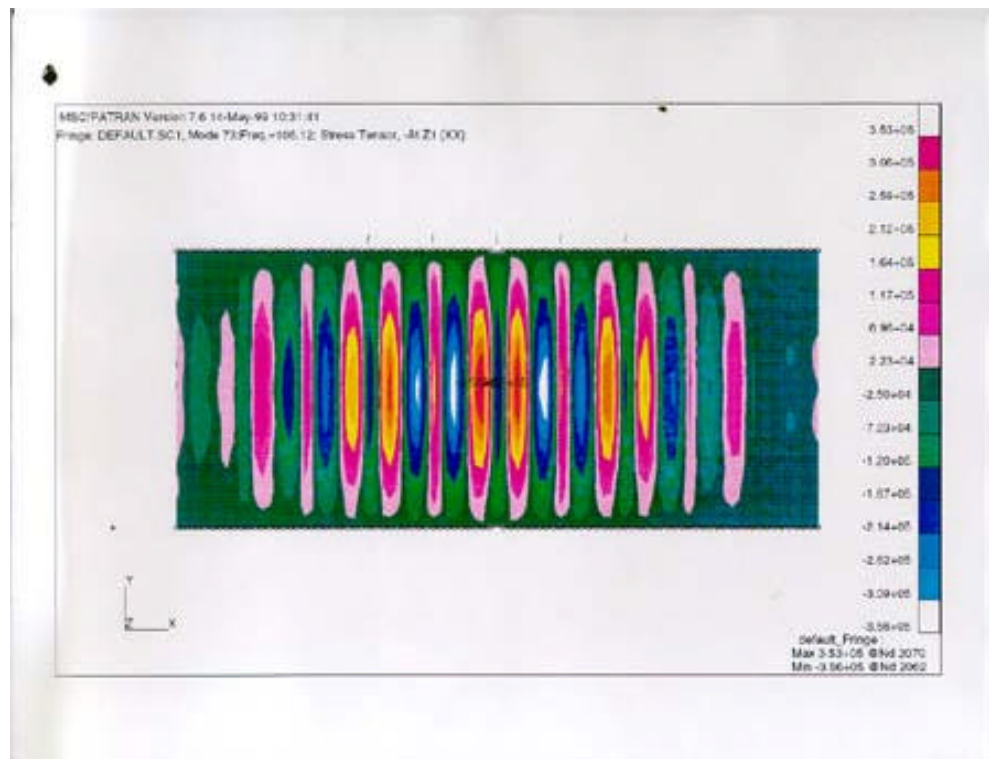
Figure 46. Modal Longitudinal Stress Distribution for Mode 73
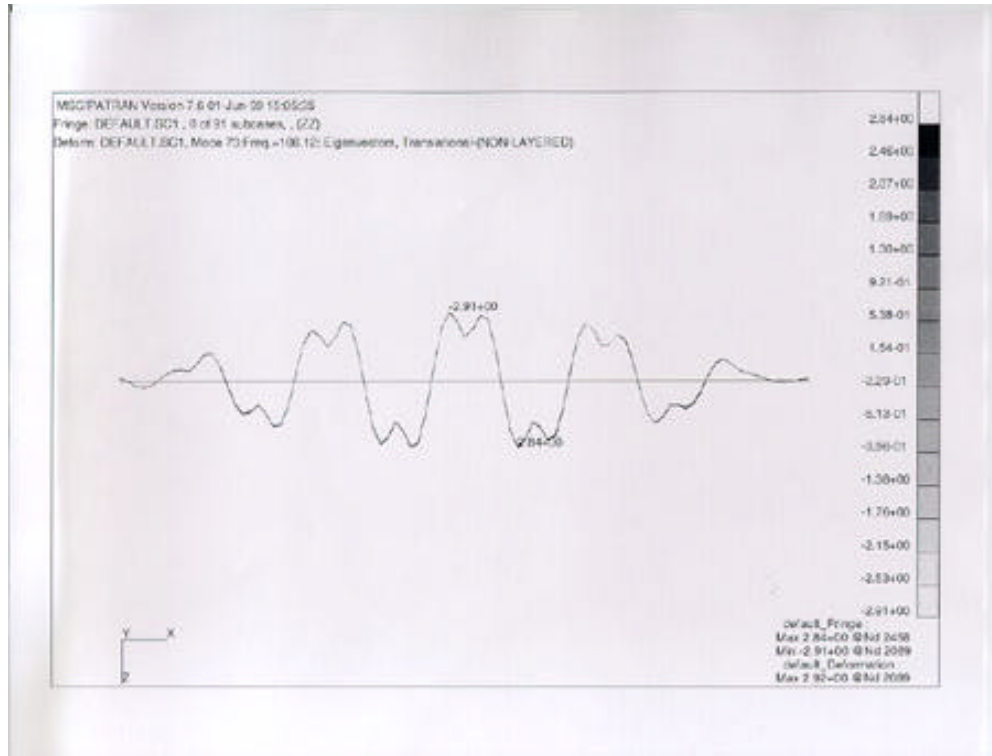
Figure 47. Modal Displacement Profile for Mode 73

The recommended internal fuselage add-on damping treatment consists of 1/16 by 2 by 2 inch aluminum angle cut into 8-inch lengths. The leg next to the skin is 2 by 8 inches. Each end of the upstanding leg is cut at a 45-degree angle for ease of installation. A layer of VEM or damping polymer, which is also a PSA, is between the angle and the skin (see figure 48). The angle is placed longitudinally (aligned with airflow) in the middle of the skin panel. This damping treatment was evaluated using the B-52 test panel. Measurements were taken in the laboratory over a range of temperatures and number of treatments as covered below. The skin surface was abraded with Scotch Bride Red, which removed a significant quantity of dirt and dust; however, there was significant roughness remaining in the paint. The paint was smoothed/removed with very coarse emery/sand paper. The skin was then wiped with alcohol. After installation of the angles, the contact between the skin and the angle was investigated by sliding a piece of release liner between them. It was possible to do this in several locations, thereby indicating that the skin was not flat.
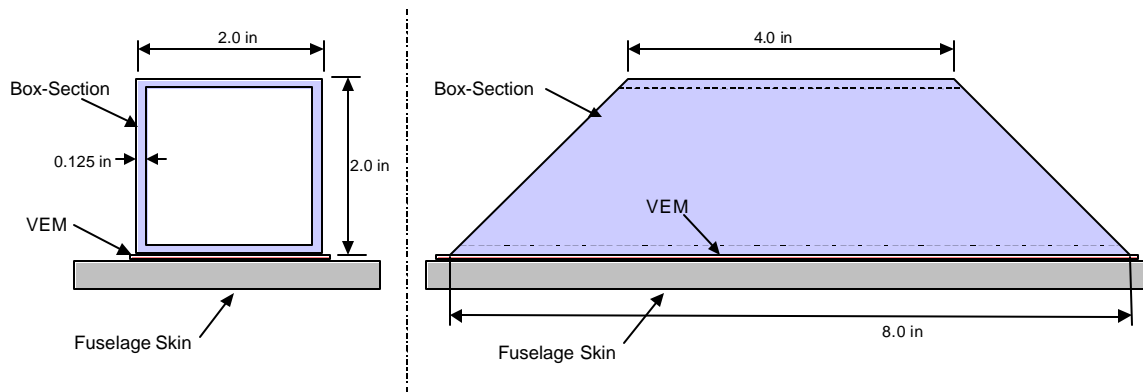
Figure 48. Damping Treatment Design.

5.1-6 B-52 Ground Test

The effectiveness of the damping treatment was tested by measuring the frequency response of an actual B-52 panel before and after application of the damping treatment. The Dosimeter was used to gather the frequency response data.

Before beginning the test, an excitation method was selected. The panel was excited by rapid, repeated striking with a metal object. Three metal objects of varying weight were tested in combination with two strike locations (see figure 49). Data was collected using the Dosimeter for each combination. The resulting frequency response plots are shown in Figure 50. Based on these results, Excitation Method 3 (mid-spar bolt striking middle of bay) was selected. However, the strike point for the remainder of the tests was moved up toward the middle of the strain gage pattern to ensure higher amplitude excitation of Strain Gage 3. Excitation Method 4 (mid-spar bolt striking frame) was used as a backup in the later stages of the test.
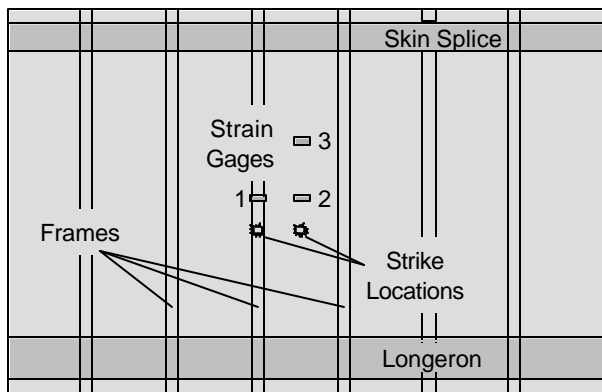
Excitation Methods

Excitation Method	Metal Object	Strike Location
1	Small Bolt	Bay
2	Small Bolt	Frame
3	Mid-Spar Bolt	Bay
4	Mid-Spar Bolt	Frame
5	Link	Frame

Figure 49. Selection of Panel Excitation Method

The main test was conducted in four stages, where dampers were added at each stage. The damper configurations for each stage are illustrated in Figure 51. Stage 1 established a baseline data set with no dampers in place. Stage 4 had all 20 dampers in place. Data was collected using the Dosimeter for each stage.

61

Results of the test are summarized in Figures 52 and 53. Figure 52 shows a comparison of the frequency response plots for Stages 1 and 4 using Excitation Method 3. The results show no consistent change in either amplitude or frequency content. Figure 53 shows the same comparison using Excitation Method 4. In this case, there is a clear reduction in response amplitude in the frequency band of 150 to 187 Hz. In addition, for the gage located on the frame centerline, there is a substantial reduction in the frequency bands of 187 to 240 Hz and 240 to 300 Hz. Also note the Stage 3 results which show intermediate levels of reduction for the response amplitude. (No data was collected in Stage 2 for Excitation Method 4.)

Note: Each frequency response curve in Figures 52 and 53 represents average values taken over five consecutive standard data records. A frequency response curve for each standard data record is automatically generated by the Dosimeter. These frequency response values were then averaged by frequency band to derive the curves shown here.
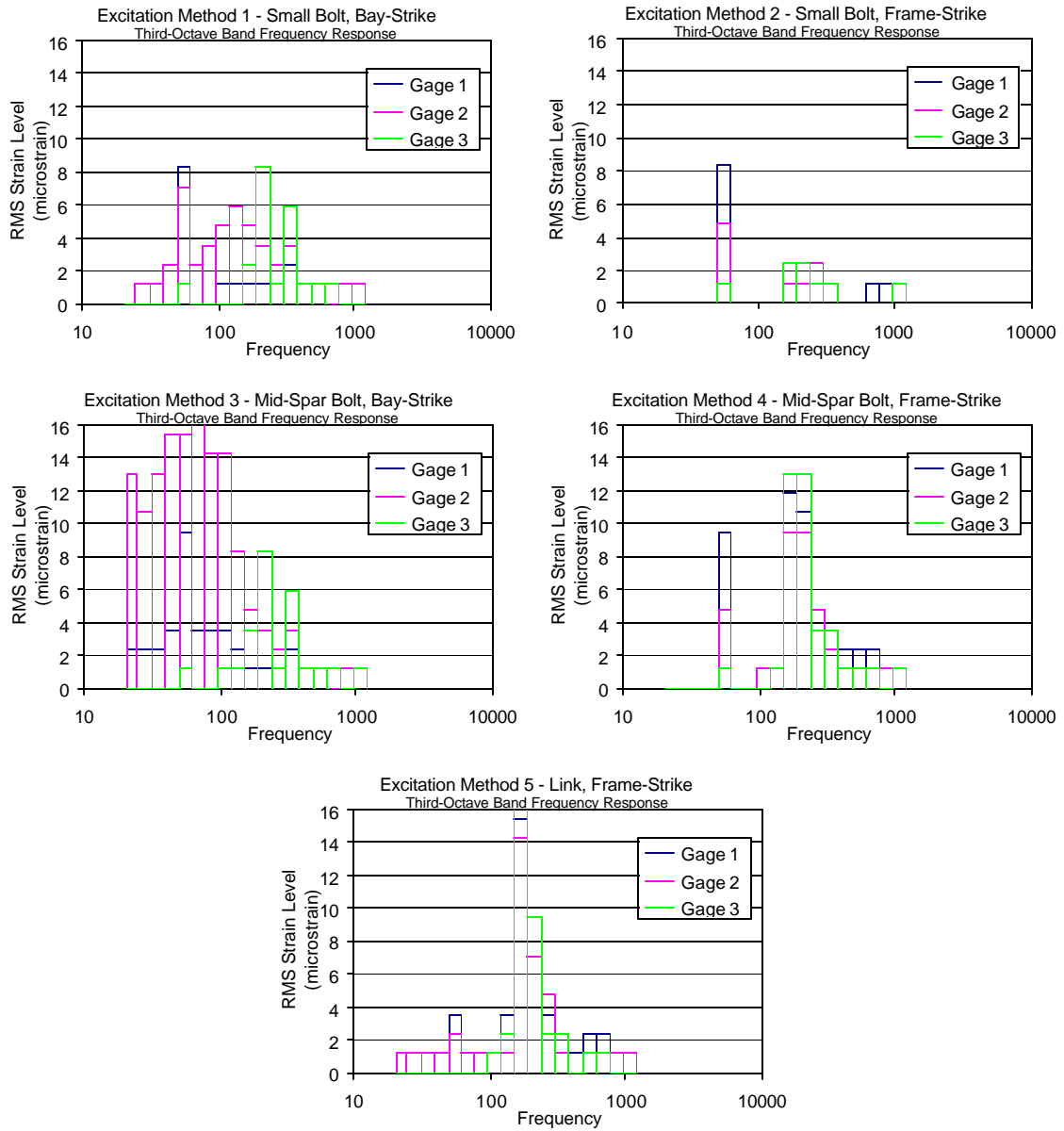
Figure 50. Frequency Response Plots for Various Panel Excitation Methods
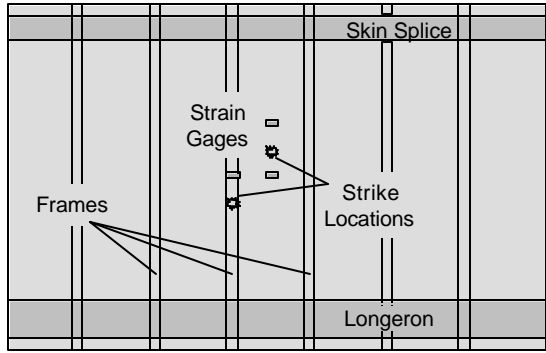
Stage 1 - Baseline
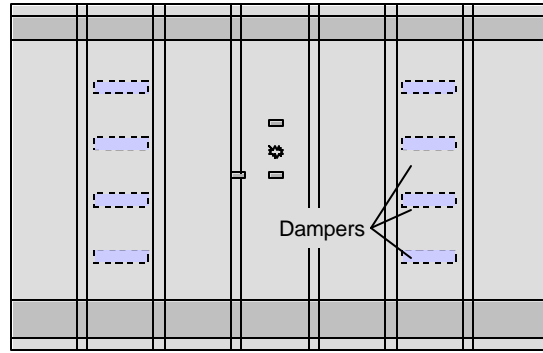
Stage 2
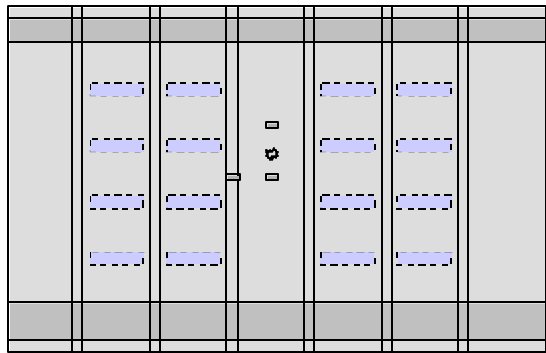
Stage 3
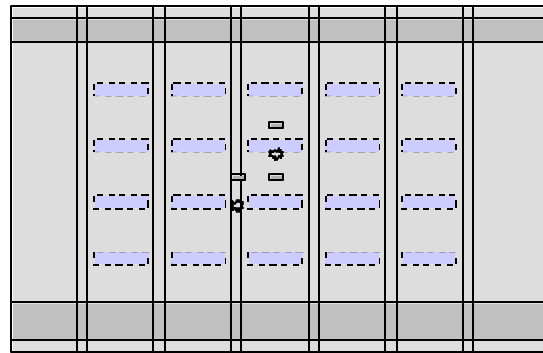
Stage 4

*Figure 51. Damper Configuration for Each Test Stage*
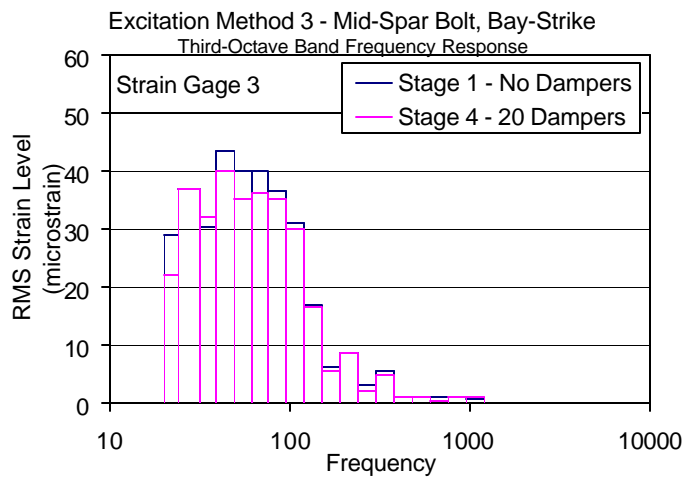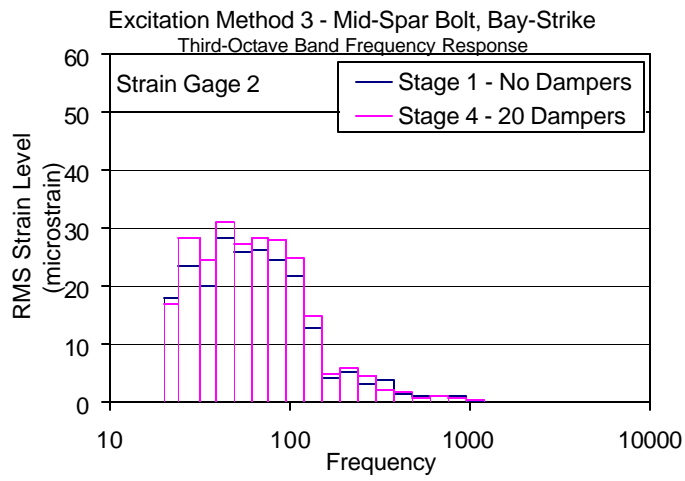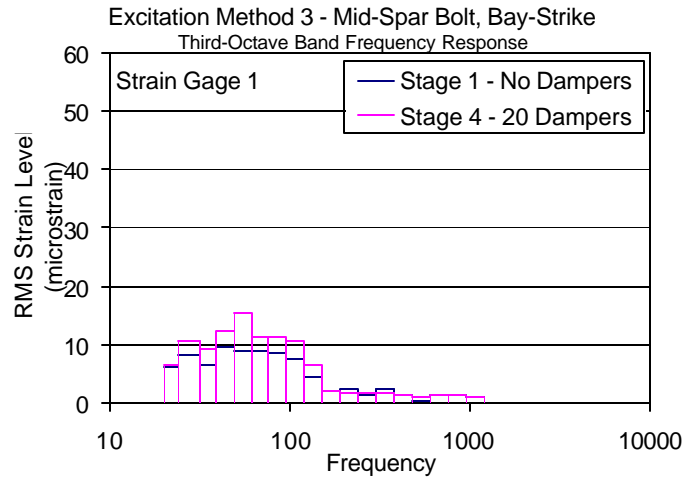
Figure 52. Comparison of Frequency Response Before and After Damper Application Using Excitation Method 3
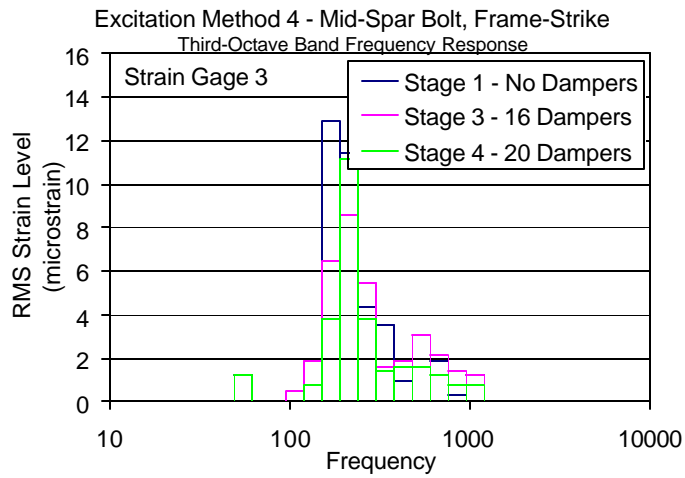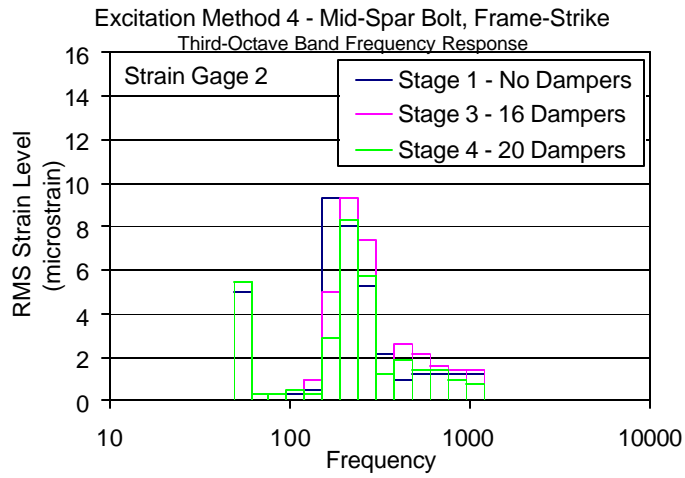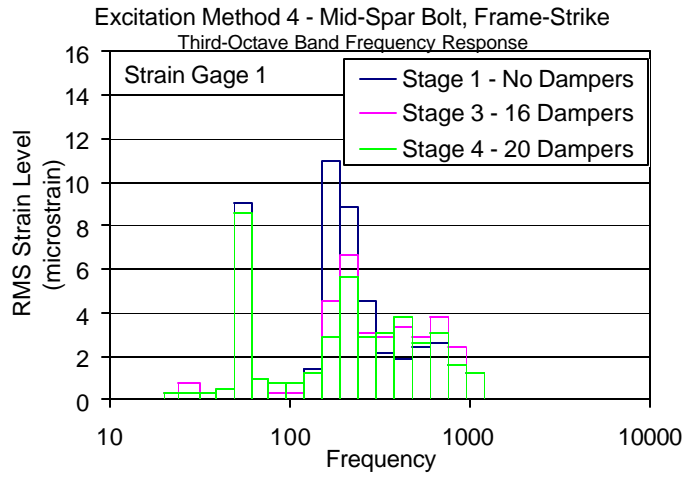
Figure 53. Comparison of Frequency Response Before and After Damper Application Using Excitation Method 4

5.1-7 Conclusions

The B-52 fleet is experiencing sonic fatigue damage in the fuselage skin at the location of the deployed flaps. Damage is induced during takeoff roll and climbout as well as landing approaches. The fuselage sidewall consists of several bays of skin with Z-frame substructure. A FEA indicated that this structure possesses very high modal density. Several sets of Dosimeter service data were gathered and analyzed. Typically, the overall rms strain level monotonically increases with speed/dynamic pressure during takeoff roll. Its value remains on a plateau for a while, then attains a peak which is associated with the flap translating forward (without rotating) during the initial phase of retraction before it rotates up against the lower surface of the wing. Damage is also accumulated during touch and go's and final full stop landing approach. The sets of Dosimeter data were also analyzed for frequency content of the strain responses; it was established that response was broadband between 20 and 200 Hz consistent with FEA high modal density and the broad band nature of flap noise. It was also established that the service damaging temperature is ground level ambient consistent with engineering judgment. A section of fuselage sidewall approximately 40 by 100 inch was used to install candidate designs for a Durability Patch in the laboratory. Another section was used to install vibration dampers which consisted of an aluminum angle and PSA on the interior surface of the fuselage skin. The effects of this damping were measured in the laboratory as a function of temperature. Similar dampers but with a square fiberglass tube instead of an aluminum angle were installed on a complete retired aircraft structure; measurements at ambient temperature before and after the damping were inconclusive in and of itself. The measurements of the effects of damping as a function of temperature in the laboratory, together with the other investigations in this program, are convincing evidence that adding damping to the interior surface of the fuselage skin would result in a dramatic life extension and consequent cost avoidance savings.

5.2 F-15 DURABILITY PATCH DEMONSTRATION

As part of the Durability Patch Program, aircraft F-15 E-1 was selected for a study to use a Damage Dosimeter for monitoring and recording structural strains during flight testing. A dosimeter was installed with three strain gages and a temperature sensor on the inside of the aircraft. This aircraft was selected because it has existing flight test data recording capability. The existing data system was used to show parameters not recorded by the dosimeter and as a check of dosimeter data. The success criteria was to demonstrate operational usage of the damage dosimeter under that flight environment and verify its operation by checking with data from the standard data recording system.

5.2-1 Background

On high performance aircraft, such as the F-15, dynamic loads have been a fatigue-limiting factor. The earlier F-15E experienced fatigue cracking at several locations on the lower fuselage surface, which were due to the high dynamic pressures and long dwell times during high-speed air-to-ground operations at low altitudes. The high acoustic loading was due to the formation of highly turbulent shocks behind LANTRIN pods and conformal carriage stores during terrain following missions.

5.2-2 Test Aircraft

F-15E-1 (see figure 54) served as the test aircraft. The lower fuselage environment was measured with – 4 CFTS, centerline pylon and external fuel tank, LANTRIN pods, and (12) MK-82s on the conformal fuel tank (CFT) stations left/right conformal tank (LCT/RCT) 1 through 6.


Door 47 and
Panel-1082

Figure 54. F-15E Critical Location, Dosimeter Installation

### 5.2-3 Description of Test Item and Installation

The Damage Dosimeter was installed in the door 47R in the lower center fuselage. The objective of the test program was to monitor strains on an adjacent external skin panel. This panel was part of the lower nacelle skin assembly and experiences high dynamic response during low altitude and high-speed maneuvers. The panel is made of 2024-T3 Aluminum. It is 0.071 inch thick with chem-milled pockets

to 0.060 inch and 0.044 inch, and has experienced cracks in the former and in the panel chem-mill boundary.   On operational F-15 Es, this location is just aft of the LANTIRN Pod (fig. 54).   The Dosimeter and battery pack were installed by hard mounting to an existing flight test equipment shelf.

The Damage Dosimeter was mounted under the F-15 internally on an existing flight test equipment rack Door 155R. The dosimeter actually replaces some existing equipment (fig. 55). Minimal modifications were made to the existing shelf for insertion of the Damage Dosimeter (fig. 56).

Figure 55. Internal Dosimeter Installation – looking at Door 47R location in the Lower Center Fuselage

Figure 56. Dosimeter Installation Inside Existing Equipment

There is also an existing instrumentation panel with gages. This location is panel-1082 FS481-494 (Door 47R). The new instrumentation on E-1 panel-1082 will be three strain gages and thermal couple instrumentation. The new gages were mounted as close to the existing gages as possible, TA-01, TA-02, and TA-06 (fig. 57).   Other instrumentation was also present on the panel, but was recorded by the Aircraft Test Instrumentation System (ATIS) data recorder.
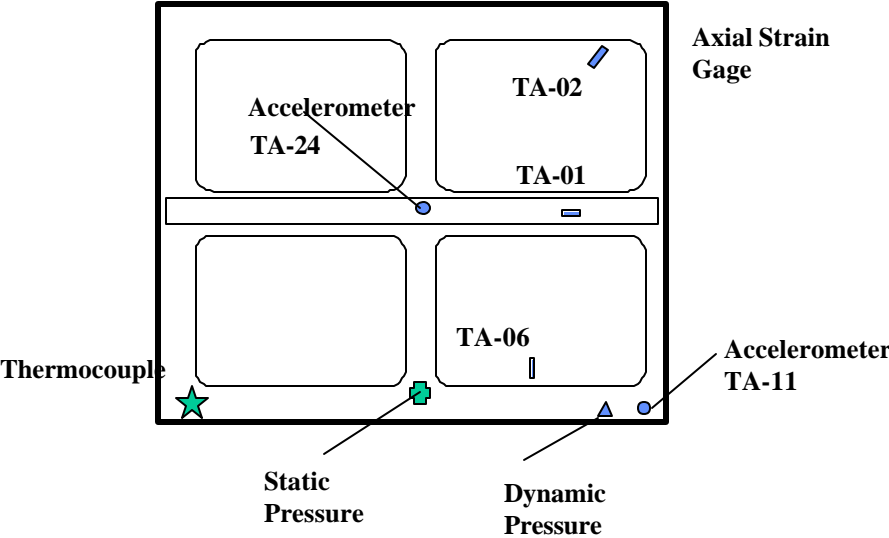

Figure 57. Instrumentation Location on Panel-1082

5.2-4   Test Approach/Procedure

All flight testing was performed as tag-along flight missions. The Damage Dosimeter was activated prior to each flight mission. After each flight, the data was downloaded and the memory cleared.

5.2-5   Data and Usage Assessment

The damage dosimeter was in operation on F-15 E-1 during the time period July 1999 – March 2001. The first four flight tests were unsuccessful due to problems with the system.   The main problems were either related to hardware or software glitches (fig. 58). The automatic triggering threshold never seemed to work on earlier tests. Hence, the automatic triggering software was replaced with software that sampled and stored continuously as long as the battery was connected. On the very last flight, data was recorded on the ATIS data system, in parallel with dosimeter.

Hardware Problems:	
Cause/Problem	**Solution**
A bad external battery pack	Battery pack was replaced
A faulty temperature sensor	New temperature sensor installed
A bad clock battery in the dosimeter	Dosimeter unit was replaced

Figure 58. Data Acquisition Problems

70

5.2-6 Data Processing

The Damage Dosimeter provides the data required for Durability Patch design, i.e., the vibration frequency at which damage occurs in service, and the temperature at which damage occurs in service. Third-octave-band distributions, strain PSDs, and/or normalized cumulative RMS plots should be analyzed as appropriate to determine the vibration frequency at which high cycle fatigue damage accumulates.

Damage Dosimeter data is summarized below for a typical recorded flight of the F-15 at St. Louis. All data looked reasonable. The strain data is summarized in the figures 59 through 63. Figure 59 shows the total RMS strain readings for the duration of the data collection cycle with temperature data overlaid. The temperature profile appears to follow the flight log.
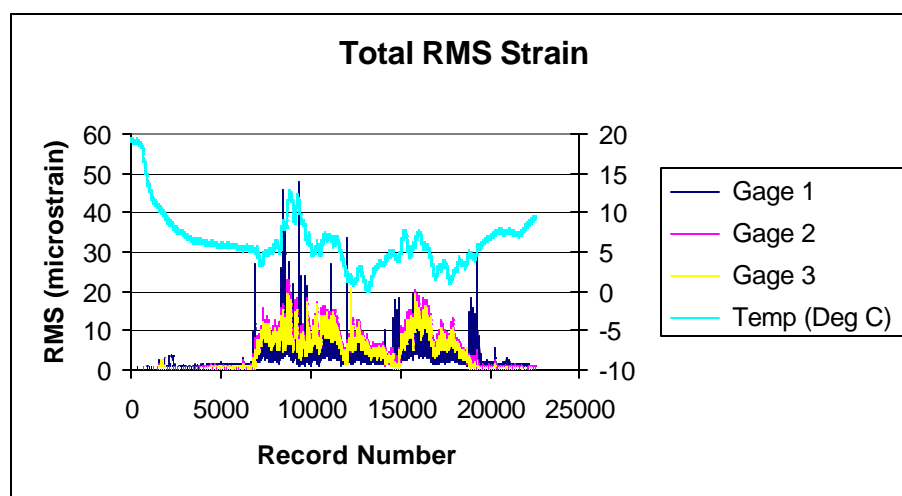
Figure 59. Total RMS as a Function of Record Number

A more detailed picture of the frequency content for an individual record can be seen by plotting the third-octave band distributions. Figures 60 through 63 are detailed pictures showing the third-octave band distributions for data records 6908, 8481, 9382 and 11967 where there were spikes in the RMS data.

71
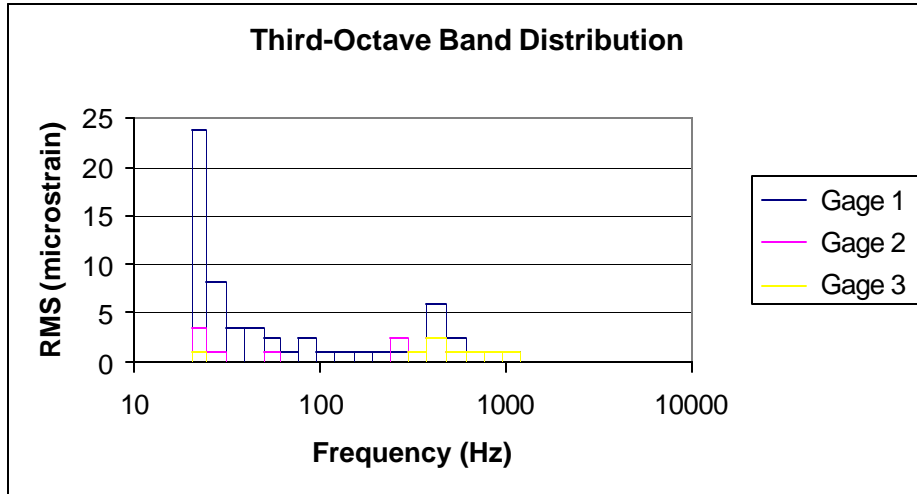
Figure 60. RMS Third-Octave Band Distribution for Record Number 6908
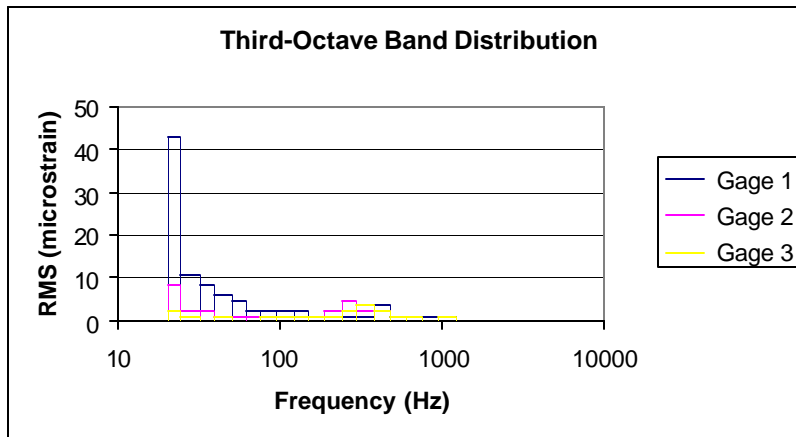
Figure 61. RMS Third-Octave Band Distribution for Record Number 8481
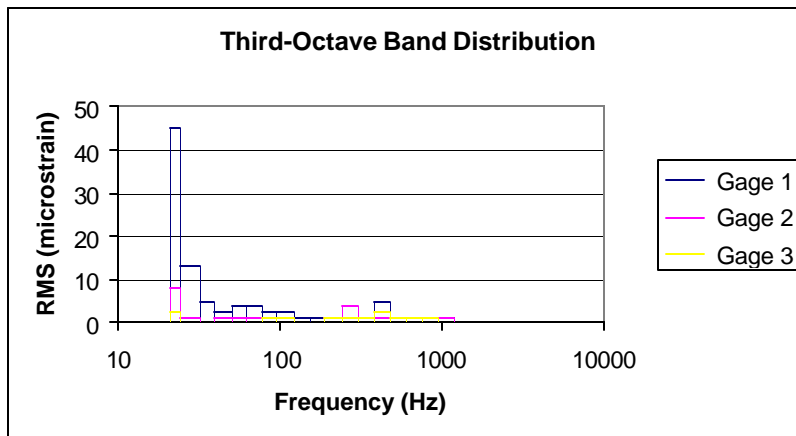
Figure 62. RMS Third-Octave Band Distribution for Record Number 9382

72
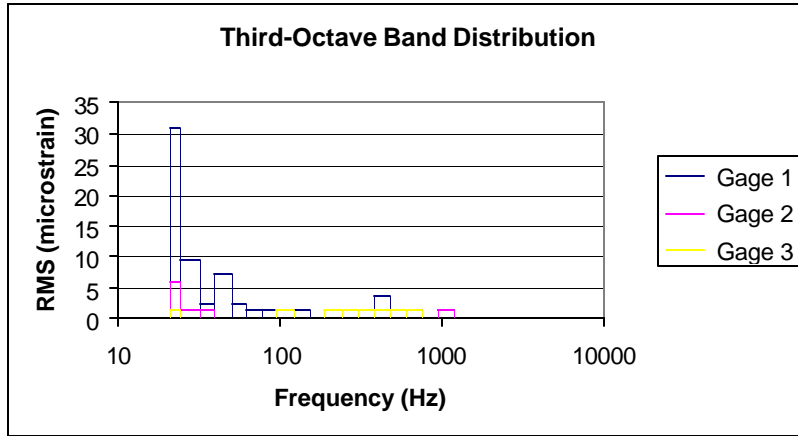
*Figure 63. RMS Third-Octave Band Distribution for Record Number 11967*
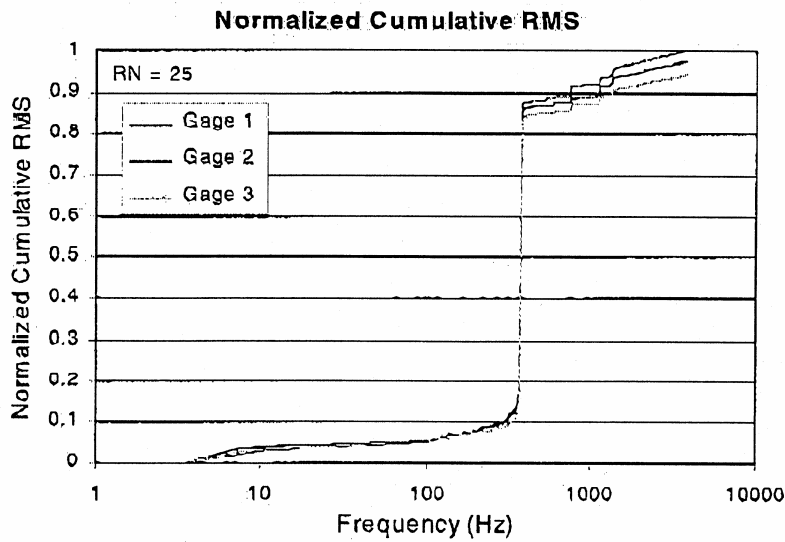
Figure 64. Normalized Cumulative RMS Strain for Record Number 25

5.2-7   List Future Recommendations

Several recommendations were noted during the F-15 service confirmation:

- Replace plastic connectors with more robust military specification metallic connectors.
- Redesign battery pack to make battery refresh easier.
- Download time from Dosimeter to Laptop PC needs to speed up.
AFRL lab version takes 1-1/2 hours when no glitches
- dosimeter connectors need to be hermetically sealed

5.3 C-130 SERVICE APPLICATION

The service application was conducted on a C-130 stationed at the Air National Guard in Charlotte, North Carolina. Several aircraft in the C-130 fleet have experienced fatigue cracking in the lower flap-well-fairing skin immediately aft of the outboard engine. It is suspected that turbulent airflow from the engine exhaust and vortices from the prop-wash cause HCF damage in this region.

5.3-1 Structural Description

The region of interest is identified in figure 65. This figure shows the location of a skin panel under the flap well between Flap Stations 173.1 and 190.1. The region is located directly aft of the engine at Outer Wing Station 180.0. The region is just aft of the rear spar and is openly exposed to the environment whether the flaps are extended or not. Figure 66 shows a photograph of the region.
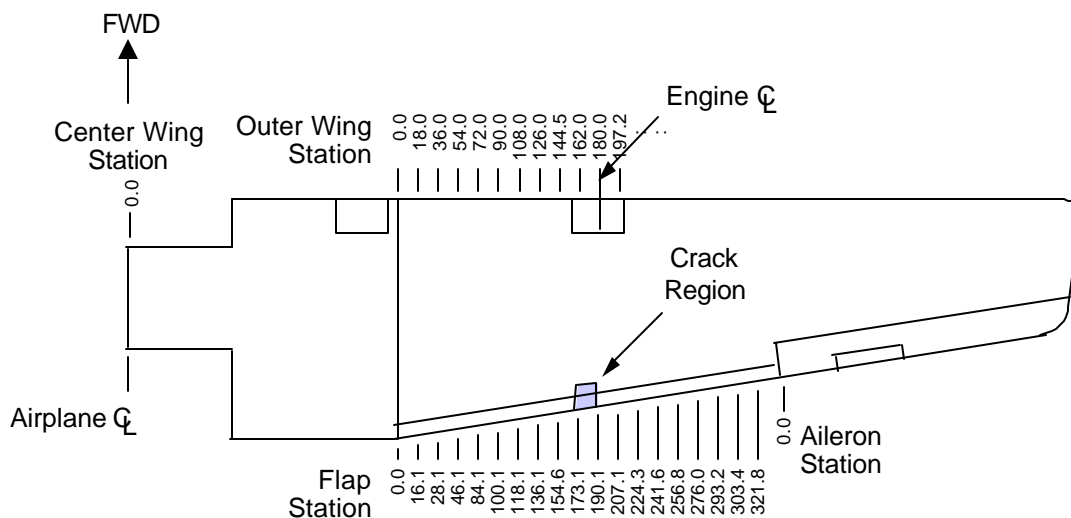

Figure 65. Cracking Region on C-130 Flap Well Skin Panel

Cracking within this region has been observed on several other C-130 aircraft. Figure 67 shows the location of the crack relative to surrounding substructure. The skin panel is bounded by hat stringers which run somewhat parallel to the aft spar of the wing. Additionally, the panel is bounded by an intermediate support structure on its in-board end, and by a rib on its out-board end. The dimensions of the skin panel are approximately 15 inches by 3 inches, with a skin thickness of approximately 0.02 inch. Figure 68 shows a photograph of the region.

Since the panel is located immediately aft of the outboard engine, it is subjected to prop wash, engine exhaust, engine noise, and high temperature environments. Any or all of these factors could be contributing to the HCF or sonic fatigue damage. In addition, since the flap well becomes somewhat of an open cavity while flaps are extended, the harsh environment may impact the upper fairing as well as the lower.

Figure 66. C-130 Outboard Wing and Engine (Opposite Side of Aircraft)
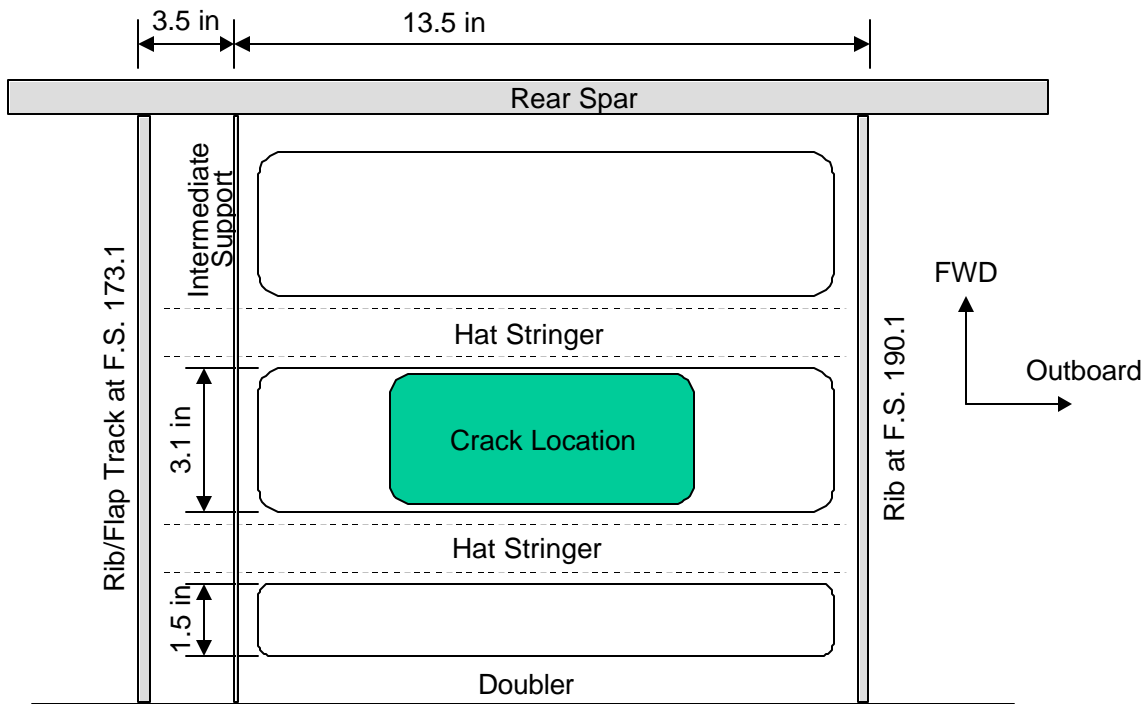

Figure 67. Cracking Location and Surrounding Substructure in C-130 Flap Well

Figure 68. Flap Well Skin Panel and Surrounding Substructure in C-130 Flap Well

5.3-2   Flight Data Collection and Analysis

The region of interest was instrumented with three strain gage sensors and one temperature sensor. The sensor layout is shown in figure 69. The strain sensors were positioned to detect bending strains associated with vibration modes in the two skin panels closest to the rear edge of the flap well fairing. As in all of the service confirmations, the panel surface was carefully prepared in order to ensure good bond strength for the instrumentation. The installed sensors are shown in figure 70. Lead wires from the sensors were soldered to the Dosimeter wiring cable which ran to the Dosimeter and battery pack. Once the lead wires were fixed in place, the instrumentation assembly was covered with RTV sealant (fig. 71). The fairly high mass loading of the sealant is judged to be acceptable because it is intended to evaluate the ratio of responses before and after Durability Patch installation, not absolute quantitative measurements.
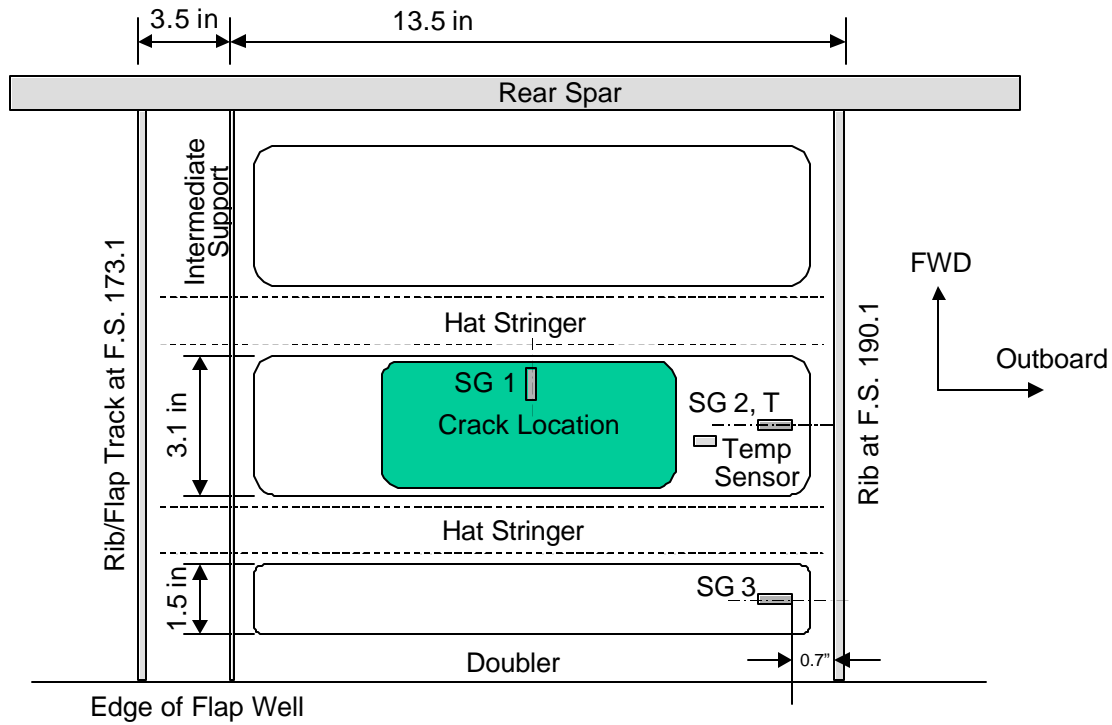
*Figure 69.   Strain Gage and Temperature Sensor Layout*

Figure 70. Strain Gage and Temperature Sensor Bonded in Place

77

Figure 71. Instrumentation Covered With Sealant.

The Dosimeter and battery mounting location was also in the flap well aft of the rear spar. It was four bays (approximately 6 ft) inboard of the strain gage location (fig. 72). Both Dosimeter and battery were mounted with nut plates to allow quick removal and reinstallation for download activities and battery replenishment.
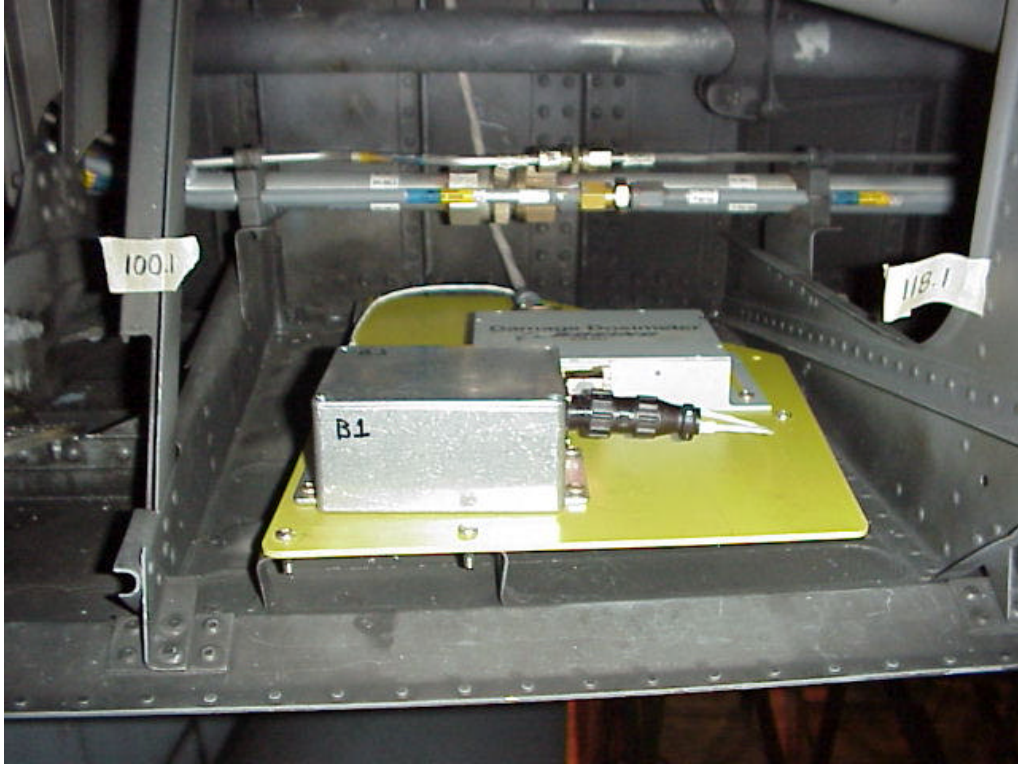
Figure 72. Dosimeter and Battery Pack Mounted in Flap Well

The original planned timeline for the C-130 application is shown in figure 73. The Dosimeter installation was completed on December 18th, 2000. Due to aircraft and sensor problems only a few flights were analyzed. While the Dosimeter did not perform as expected, it is judged that the set of data indicates the service conditions at which damage occurs.
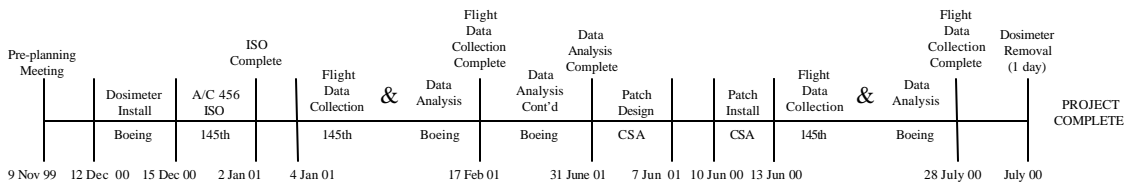

Figure 73. C-130 Durability Patch Program Timeline.

As described previously for Durability Patch design, third-octave-band distributions, strain PSDs, and normalized cumulative RMS plots should be analyzed for the vibration frequency at which damage occurs. These plots were generated from stored time history samples at or near the maximum RMS strain levels experience during any particular service record. If damage occurs between approximately 20 to 300 Hz, the frequency effects can be ignored and the tabulated properties in the VEM database (which are for 100 Hz) can be used directly. If this is not the case, temperatures of maximum material loss factors for the damaging vibration frequency must be read from the nomograms in the VEM database or other reliable source.

To determine the temperature at which damage occurs in service, strain versus temperature cross-plots and cumulative damage versus temperature were analyzed for the temperature at which damage occurs in service. The Cumulative Normalized Damage inherently takes this into consideration; furthermore, the temperature has been adjusted for the difference between ground level ambient for the particular service record and standard day temperature of 15 °C (59 °F). For the C-130, Figure 74 (the Temperature versus Strain Cross-Plot) indicates that, for this flight, damage occurs at approximately 95 °C; while the appendix indicates an ambient ground level air temperature of 30 °C. Thus, there is a temperature rise of approximately 65 °C above ambient. It is very important to have Dosimeter data when there is heating or cooling taking place for the intended application of damping, see also Figure 75.
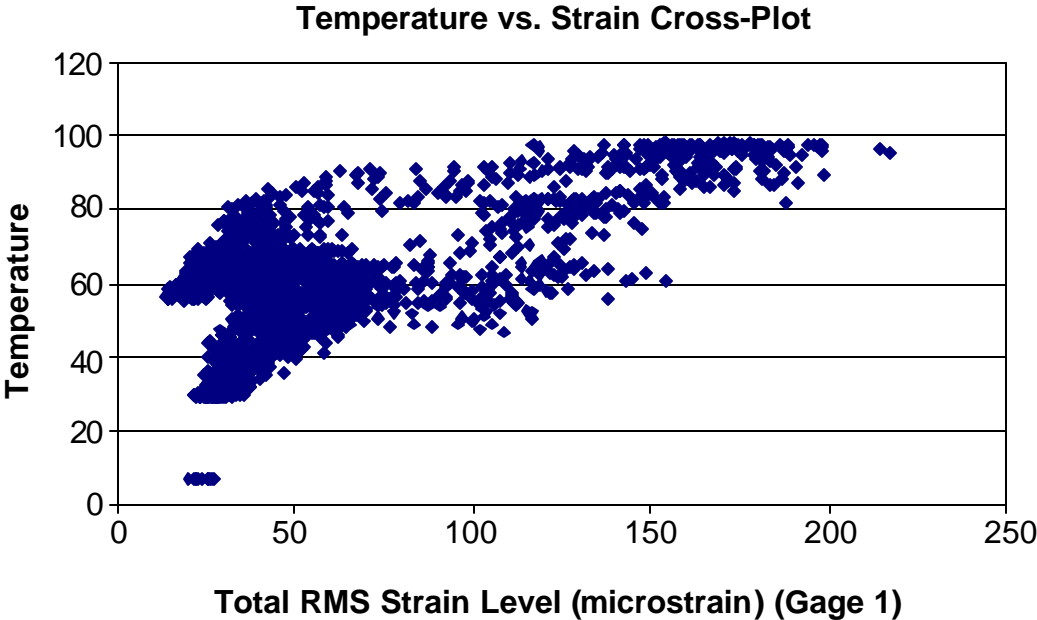

Figure 74. Cross-Plot of Temperature and Strain Activity (for Flight 1)
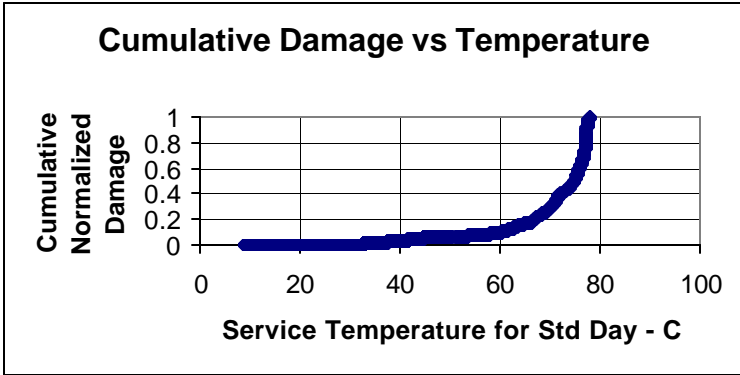
Figure 75. Determination of Service Temperature Damage (for Flight 1)

80
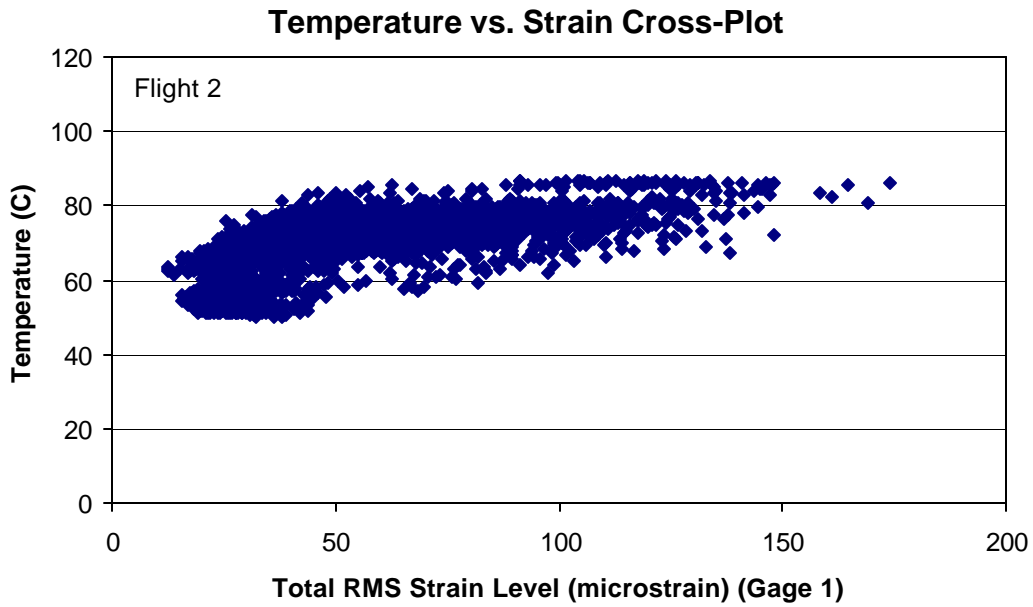
*Figure 76. Cross-Plot of Temperature and Strain Activity (for Flight 2)*
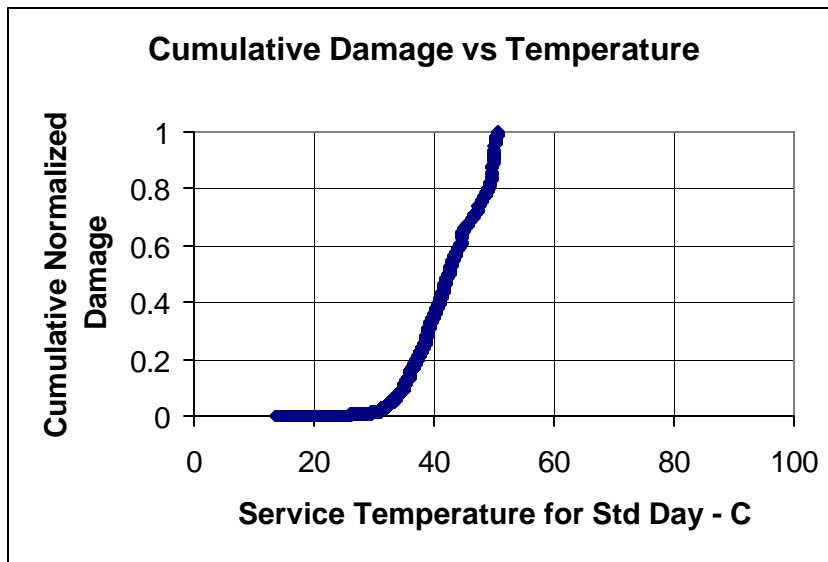
Figure 77. Determination of Service Temperature Damage (Flight 2)

In this application, for the second flight (as shown in figure 76 and 77) the temperature of maximum modal damping should be 15 °C (average ambient equal to standard day) plus 65 °C rise or 80 °C

(176 °F). From the VEM database table, Densil 2078 (or Densil 4078, the 0.004-inch-thick version) is selected for the C-130.

5.3-3   Problem Resolution

The skin cracking in the lower flap well fairing aft of the outboard engine appears to be due to resonant high cycle vibratory or sonic fatigue. It is exposed to high acoustic noise levels from prop wash and turbo jet engine exhaust as well as disturbed flow. As such, the Durability Patch appears to offer a cost effective alternative to conventional riveted sheet metal patching. The elastic repair/reinforcement and the additional vibration damping are judged to offer durability enhancement for the remaining life of the aircraft. The structure is subject to heating from the exhaust and there is a temperature rise above ambient of the structure. This rise is indicated to be 65 °C by the Damage Dosimeter data. By virtue of proper selection of the viscoelastic damping material, repair/reinforcement and damping are practical. The repaired/reinforced region of cracking and the augmented damping provided by the installation of a Durability Patch will have indefinite life.

5.3-4   Repair Design

For the application of the Durability Patch to the lower wing surface C-130 flap well fairing skin panel, and from scaling the skin panels as given in figure 63, the structural adhesive should measure 13.5 inches by 7.68 inches nominally. The VEM should be Densil 4078 (0.004- inch-thick version of 2078) and should be cut to 12.5 by 6.68 inches. The cutout should measure approximately 1.0 inch larger than any existing crack, or 5.0 inches if there is none. The other dimension should be about 2.0 inches. Ten layers of fiberglass prepreg should be installed in wedding cake fashion as shown in figure 78.
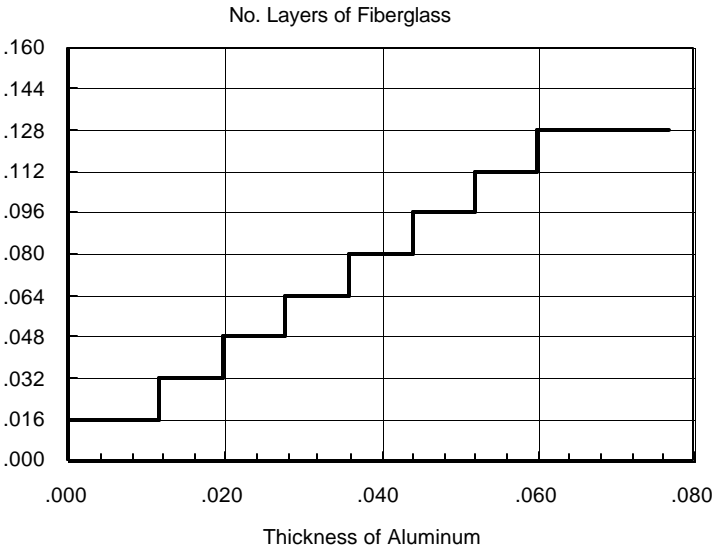

Figure 78. Fiberglass Thickness as Function of Aluminum Thickness

5.3-5 Design Verification

While the damping and repair structural analyses indicate that the Durability Patch will provide indefinite life due to the enhancement of static and dynamic capability of the lower flap well fairing skin and that the materials and processes will withstand the service environment indefinitely, without a service confirmation test, this cannot be guaranteed. Unknown factors such as Patch damage due to hydraulic fluid exposure or over-temperature conditions may reduce the Durability Patch useful service life. It is highly desirable to use the Damage Dosimeter to compare in service vibratory strain levels without and with a Durability Patch installed. These levels can be used to calculate longevity. Materials and processes have been selected to have indefinite life, but cannot be guaranteed without service exposure for some period of time.

6.0 CONCLUSIONS

The Durability Patch Program's goal was to develop a process that would help to define repair designs for secondary structure subjected to HCF loading. The intent was to facilitate collecting the required information that could be used to design a repair that would restore structural integrity and/or increase damping in the repair region. Increased damping leads to a reduction in resonant response and a repair that will survive the life of the aircraft. In order to design a repair with effective damping properties, the in-service structural dynamic characteristics and temperatures must be known. A rugged, small, and lightweight data acquisition unit called the damage dosimeter was developed to accomplish this task while causing minimal impact to the aircraft system. Running autonomously off of battery power, the damage dosimeter measures three channels of strain and a single channel of temperature.

The dosimeter met all if its design requirements. Twelve damage dosimeters were fabricated for the USAF per the contractual agreement. In service demonstration of the dosimeter and repair design process was proposed for each of three different aircraft platforms, a B-52, F-15, and C-130. Each of the demonstrations has been accomplished, and each showed that the damage dosimeter allows an engineer to easily instrument an in-service aircraft to obtain the structural characteristics necessary to properly select damping materials and design an arresting repair.

It was initially believed that the B-52 application would require a durability patch attached to the exterior surface of the fuselage skin. After assessment of the problem using data from the damage dosimeter, limited finite element analysis, and discussions with the B-52 SPO, a damping treatment installed on the interior skin surface of the airplane was determined to be the best treatment. This application highlights the advantage of having a diagnostic tool like the dosimeter t collect in-flight service data to help determine the most effective repair design. Although this application did not result in a structural repair, it was an excellent application as it showed through data collection and analysis, that only a damping treatment was necessary.

The second application was to evaluate the dynamic characteristics for an F-15 access panel on the underside of the airplane. This location had been previously evaluated and a durability patch had been installed. The purpose of this application was to confirm performance of the damage dosimeter and patch design process with prior known data. Additionally, this application evaluated the use of the dosimeter in a very severe fighter aircraft environment.

The third application focused on the edge of the flap well of a C-130 aircraft. Turbulent airflow from the prop-wash causes HCF in this region. It is expected that this evaluation will be a durability patch or surface attached damping treatment. Due to delays in flight, testing, this application is still under development. As this application is completed, the arresting repair design process will be documented.

In conclusion, the corner stone for the damped repair patch design process is the damage dosimeter. It has shown to be very simple to install, maintain, and use by flight line engineers and technicians. The fact that it does not interfere with the aircraft electrical power or cooling systems, make it a very attractive device for quick in-flight diagnostics of anomalous structural cracking. As a result of this USAF

contract, other service and commercial applications have requested similar devices. Delta airlines is very interested in using the dosimeter to evaluate what looks to be a high cycle fatigue problem with secondary structure on their MD-80 aircraft. Boeing is currently negotiating a cooperative research and development agreement (CRADA) with the Air Force Research Laboratory (AFRL) to allow Delta to use dosimeters developed under the subject contract. Additionally, the Space Shuttle is interested in using the dosimeter to address a vibration concern that is seen during its ferry on the back of a 747 aircraft. Boeing is currently funding an internal effort to modify the dosimeter technology to interface with a fiber optic corrosion sensor data acquisition card.

The dosimeter is a very valuable tool to facilitate the repair design process. It is cautioned, however, that the time to carry out a flight test should not be underestimated. This is very dependent on airplane scheduling and priorities. The diagnostics of secondary structure cracking can be somewhat low in priority. Therefore, mission readiness and asset deployment can result in significant delays in flight data collection using the dosimeter. This has been demonstrated for each of the service applications. Ultimately, however, the dosimeter weathered the prolonged installations and resulted in collecting very useful information.

APPENDIX A –STRAIN GAGE INSTALLATION PROCEDURE

The procedures for strain gage installation and temperature gage installation are very similar. Many of the steps are identical and can be performed at one time for both sensor types.

Gage Layout

1. Mark the major axes of the strain gage locations with a red or silver pencil (Colortex or equivalent).

2. Extend the lines well beyond the gage area so they can be redrawn after cleaning.

3. Gage layouts must show strain gage orientation.

Strain Gage Preparation

1. Make sure that 350-ohm resistance strain gages are used. Other gage resistances will not allow proper Dosimeter operation.

2. Remove the gage from it's acetate envelope and position it on a piece of glass.

3. Cut a 2 inch by ¾ inch piece of Kapton tape and apply it, centered, over the strain gage with the gage aligned with long direction of the tape.

4. Using a fine ball point pen, draw installation lines on the tape aligned with the gage installation marks.

   NOTE: The strain gages, as received from the manufacturer in sealed plastic packages, have been thoroughly cleaned and are ready for installation without additional cleaning. Avoid touching the gage with the fingers whenever possible, especially the bonding side of the gage. If the gage should become contaminated in this manner, clean with ethyl alcohol.

Surface Preparation

Degreasing

1. Clean a large area around the gaging location using ethyl acetate to remove any oils, grease, organic contaminants and any soluble chemical residues.

2. Use clean gauze pads saturated with the solvent.

   NOTE: Degreasing should be the first operation to avoid having subsequent abrading operations drive the contaminants into the surface material. An area covering 4 to 6 inches on all sides of the gage area should be cleaned. In addition to ethyl-acetate, other cleaning solvents can be used including methyl-ethyl-ketone, freon, ethyl-acetate or a mixture of ammonia and acetate.

Removal of Paint and Coatings

1. Using aluminum tape mask off an area considerably larger than required for gaging.

2. Abrade masked off area using 220-grit abrasive paper to remove any adherents such as scale, rust, paint, coatings, oxides, etc.

3. After paint and coatings have been removed, clean the masked off are using ethyl-acetate and gauze pads.

Scotchbrite pads or abrading cloth may be used to hasten penetration of the remover through thick coats of paint. For single gage locations it is usually quicker to abrade through the enamel with 100-grit cloth. An area the size of the strain gage plus ¼ inch minimum edge margin on all sides should be abraded, if room permits.

Baked enamel, anodizing, alclad, and electroplating may give the appearance of providing a satisfactory surface, but their presence can cause undesirable characteristics. Surface finishes should be removed unless drawings for the strain gage installations state otherwise.

If enamel coating is present, it may be advantageous to strip the coating with paint remover, and then finish sanding the base metal with 150- to 200-grit aluminum oxide cloth at individual gage locations. Acceptable strippers for metals are Turco 5292B, Turco 5351 and CeeBee A-228-D.

Finish Abrasion and Final Cleaning
1. Perform finish abrasion using 320-grit abrasive paper or cloth, followed by 400-grit abrasive paper or cloth.

2. Remove masking and using ethyl acetate and gauze pads clean area considerably larger than required for gaging.

Conditioner and Neutralizer Application
1. Scrub gaging area using M-prep Conditioner A and cotton tipped applicators.

   NOTE: Conditioner A should be applied repeatedly and the surface scrubbed with cotton-tipped applicators until a clean tip is no longer discolored by the scrubbing. Do not dip the contaminated applicator into the cleaning solution bottle. During the process the surface should be kept constantly wet with Conditioner A until the cleaning is completed.

2. When clean, the surface should be dried by wiping through the cleaned area with a gauze pad.

   NOTE: The stroke should begin inside the cleaned area to avoid dragging contaminants in from the boundary of the area. Then, with a fresh pad, a single slow stroke is made in the opposite direction. The pad should never be wiped back and forth, since this may redeposit the contaminants on the cleaned surface. Cleaning solutions should never be allowed to dry on the surface.

3. Scrub gaging area using M-prep Neutralizer 5 and cotton tipped applicators to neutralize the acidity of the Conditioner A.

   NOTE: The cleaned surface should be kept completely wet with Neutralizer 5 throughout this operation.

4. When neutralizer application is complete, the surface should be dried by wiping through the cleaned area with a gauze pad.

Strain Gage Application
Gage bonding must occur within 30 minutes of surface preparation.

All materials for bonding, and equipment for pressure application and for curing, should be already prepared so that the bonding procedures can continue without interruption.

Gage Positioning
1. Re-apply gage layout lines.

2. Carefully remove the gage/tape assembly from the glass, lifting the tape at a shallow angle, and apply it to the strain gage location aligning the layout lines on the tape with the layout lines on the part.

Adhesive Application
1. Mix adhesive per instructions.

2. Lifting at a shallow angle, peel back the tape assembly beginning from the grid end to raise the gage and terminal from the surface. By curling the tape back on itself and pressing it to the surface, the assembly will remain in position for application of adhesive.

3. Coat gage, terminal and specimen with prepared adhesive, and then immediately proceed to the next step.

4. Rotate the tape to approximately a 30-degree angle so that the gage is bridged over the installation area. While holding the tape slightly taut, slowly and firmly make a single wiping stroke over the gage/tape assembly with a piece of gauze, bringing the gage back down over the alignment marks on the specimen. A very thin uniform layer of adhesive is desired for optimum bond performance.

Cure

If controlled heat application is required, perform the first step under *Controlled Heat Application* prior to performing the *Pressure Application* steps.

Pressure Application
1. Build up a pressure application pad consisting of a 1/8-inch-thick Silicone gum pad, 2 layers of 1/8- to ¼-inch soft rubber, and a 1/16- to 1/8-inch Aluminum backup plate.

2. Position the pressure application pad over the gage and apply a cross pattern of 3M #Y434 Aluminum tape to secure in place.

3. Using a squeegee, press the tape down firmly around the pressure pad to apply pressure to the gage installation.

Controlled Heat Application (if necessary)
1. *Perform this step prior to Pressure Application.* Install two Type-E thermocouples near the gage using aluminum tape. Plug one thermocouple into the temperature controller and one thermocouple into a temperature indicator/read-out.

2. Install two heat lamps approximately 12 to 18 inches from the surface, and plug them into the temperature controller.

3. Adjust the controller to the desired temperature and cure the gage installation per the cure schedule for the selected adhesive. The table below provides a sample cure schedule for AE-10 adhesive. The controller should cycle the power to the lamps to maintain the selected temperature.

   NOTE: The distance between the lamps and the article can be reduced or the number of lamps can be increased to increase heating capability.

Glue Line Temp (Deg F)	Cure Time (Hours)
75	6
100	3
125	1.5
150	1.0
175	.5
200	.3

Cure Schedule for AE-10 Adhesive

Removal of Cure Apparatus
1. Turn off and remove the heat lamps and temperature controller apparatus.

2. Remove the aluminum tape and pressure pad buildup.

3. Remove the tape over the gage by pulling the tape directly back over itself, beginning at the grid end and working back towards the solder tab.

Verification Testing for Individual Gages

1. Measure the gage resistance and gage to part leakage resistance.

2. Verify that the gage resistance is 350 +/-2 ohms and the leakage resistance is greater than 10 giga-ohms.

Leadwire Installation

1. Position the prepared leadwire cable with the stripped ends over the solder tabs, trim as required and secure in place with Kapton tape.

2. Complete the solder joints at the solder tabs using a minimal amount of 361A-20R solder per figure 1.

```
7
1          Strain Gage #1
2

3          Strain Gage #2
4

5          Strain Gage #3
6
8

9    +     Temperature
10
```
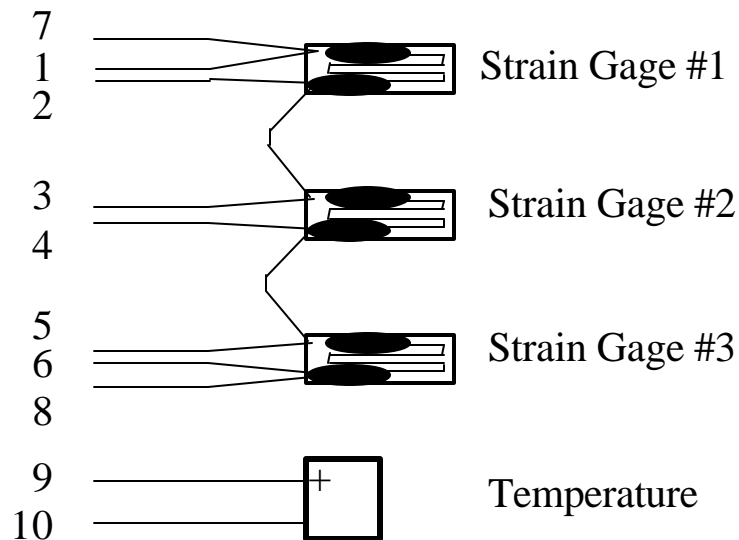
Figure 1

3. Measure the resistance at the Dosimeter connector per the Table 1.

pin	pin	resistance	tolerance
7	1	0	+/-1
7	2	350	+/-2
1	2	350	+/-2
1	3	350	+/-2
2	3	0	+/-1
2	4	350	+/-2
3	4	350	+/-2
3	5	350	+/-2
4	5	0	+/-1
5	6	350	+/-2
5	8	350	+/-2
6	8	0	+/-1
7	8	1050	+/-6

Table 1

90
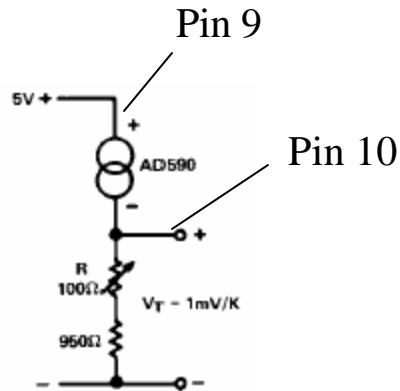
FIGURE 2

4. Apply +5 VDC +10/-0 to pin 9. Connect one end of a 1KΩ resistor to pin 10 and the other end to the return of the +5 VDC power source. Measure the voltage drop across the 1KΩ resistor. The voltage should equal one millvolt per degree Kelvin.

Weatherproofing

1. Apply M-coat D over the gage and solder tabs and allow to dry for a minimum of 30 minutes.

2. Cut a piece of the adhesive-backed Teflon provided in the M-coat J kit large enough to cover the gage and solder tab with approximately a .1-inch overlap. Make sure to form the Teflon tightly to the surface to prevent entrapment of air.

   NOTE: M-coat J is conductive. The M-coat D and the Teflon are used to provide electrical isolation. The Teflon also provides an additional humidity barrier.

3. Mix the M-coat J per instructions.

4. Apply the M-coat J over the gage, solder tabs, and a short length of the lead wire cable, making sure to work the coating under and around the cable to eliminate any moisture paths to the gage. Allow M-coat J to cure overnight.

   NOTE: Coatings are applied to strain gage installations for protection against moisture, mechanical damage or both. To be effective, there must be a continuous, impervious moisture seal from the gage to the end of the lead wires. The most vulnerable location for moisture entrance is at the contact surface between coating and lead wire. To obtain reliable sealing at the wire insulation, the vinyl insulation should be precoated with M-Coat B and Teflon insulation should be etched to a point beyond the edge of the coated area.

APPENDIX B –TEMPERATURE GAGE INSTALLATION PROCEDURE

The procedures for strain gage installation and temperature gage installation are very similar. Many of the steps are identical and can be performed at one time for both sensor types.

Surface Preparation
Surface preparation of the mounting area should be accomplished in the same manner as outlined for the strain gage installation. Follow the steps in Appendix A for:
- Degreasing
- Removal of Paint and Coatings
- Finish Abrasion and Final Cleaning Conditioner
- Neutralizer Application.

Temperature Gage Application
Gage bonding must occur within 30 minutes of surface preparation.

All materials for bonding, and equipment for pressure application and for curing, should be already prepared so that the bonding procedures can continue without interruption.

Procedure
1. Clean the bonding surface of the temperature sensor using isopropyl alcohol and a cotton-tipped applicator.
2. Mix adhesive per instructions.
3. Coat gage, terminal and specimen with prepared adhesive and then immediately proceed to the next step.
4. Firmly place the sensor on the specimen. A very thin uniform layer of adhesive is desired for optimum bond performance.

Cure
Cure of the temperature sensor bond should be accomplished in the same manner as outlined for the strain gage installation. Follow the steps in Appendix A for:
- Pressure Application
- Controlled Heat Application (if necessary).

Removal of Cure Apparatus
Removal of cure apparatus should follow the same procedures as outlined for the strain gage installation. Follow the steps in Appendix A for *Removal of Cure Apparatus*.

Leadwire Installation
1. Reference Figure 19 for temperature sensor wiring diagram.

2. Position the prepared leadwire cable with the stripped ends over the temperature sensor leads, trim as required, and secure in place with Kapton tape.

3. Complete the solder joints using a minimal amount of 361A-20R solder and a soldering iron.

4. Measure the gage resistance and gage to part leakage resistance at the end of the leadwire. Verify that the gage resistance is 350 +/-2 Ohms and the leakage resistance is greater than 10 Giga-Ohms.

Weatherproofing

Weatherproofing should be accomplished in the same manner as outlined for the strain gage installation. Follow the steps in Appendix A for *Weatherproofing*.

APPENDIX C – DETAILED DESCRIPTION OF DOSIMETER OPERATION

Detailed Operation Description for Acquisition Mode

To operate the Dosimeter in Acquisition Mode:
- Make sure that the RS-232 cable is *not* connected. This connection is reserved for Shop-Mode only.
- Connect strain and temperature instrumentation leads.
- Connect battery power supply.

Once the instrumentation leads and battery are connected the Dosimeter operates automatically as described below:

1. Following battery connection, the Dosimeter will power up after a short delay. The length of the delay will vary from 10.00 to 99.99 seconds depending on the status of the WDT and the preprogrammed IdleTime variable.
2. Upon power-up, the Dosimeter will then begin sampling data from the strain and temperature gages. For the first operation after memory has been reset, the Dosimeter will sample 20 sets of strain data from all three gages to determine a background noise level.
3. The background RMS noise level is multiplied by a preprogrammed factor to obtain the Noise Threshold.
4. Upon completion of the Noise Threshold calculation, the Dosimeter will power-down.
5. After a delay equal to the IdleTime, the Dosimeter will power-up again.
6. Upon power-up, the Dosimeter will once again begin sampling data. The gathered data will be immediately compared to the Noise Threshold. If the RMS strain level of the current data exceeds the Noise Threshold, then the data is recorded in memory and the Dosimeter continues operation. If the RMS strain level of the current data is less than the Noise Threshold, and remains below that threshold for several data gathering cycles, then the Dosimeter stops recording data and powers down.
7. The Dosimeter will remain powered down for a period of time equal to the IdleTime, after which time, the Dosimeter will power-up again and perform Step 6.
8. Once the Dosimeter has recorded approximately 12 hours of data, the available memory will have been filled. The Dosimeter will then stop recording data and power down. The Dosimeter will not begin recording data again until the memory has been reset in Shop-Mode.

Data Collection, Processing and Recording in Acquisition Mode

Data is collected at a rate of about one sample set every 1.3 seconds. A sample set consists of a single temperature measurement and 2048 samples at each of the three strain gages. Although the strain gage sample rate can be varied, all Dosimeters fabricated to date have the sample rate set at 7600 Hz. Thus, the collection of 2048 strain samples takes about 0.3 seconds. Subsequent processing and recording takes approximately 1.0 seconds per sample set.

The raw strain data for each of the three gages is processed through a Fast Fourier Transform (FFT) to generate a Power Spectral Density (PSD). The PSD is then integrated over 18 discrete frequency bands to obtain a course representation of the vibration environment. Each of the 18 frequency bands

has a width of 1/3-octave. The starting point of the 1/3-octave band distribution is a program variable. Practical limits on the starting point are between 15 Hz and 75 Hz. Below 15 Hz, the width of the 1/3-octave band is less than the frequency increment of 3.71 Hz (= 7600 Hz / 2048). Above 75 Hz, the final 1/3-octave band lies above the Nyquist frequency of 3800 Hz (= 7600 Hz / 2). The ending point of the final band is given by:

$$\text{End Frequency} = \text{Start Frequency } (2^{(18/3)})$$

The 1/3-octave band distributions for each strain gage are recorded to flash memory for each sample set. Each distribution requires 36 bytes of storage, totaling 106 bytes for all three distributions. In addition, the temperature and time are recorded as well as peak strains on all three gages. Together, these components comprise a SDR. The total memory require for one SDR is 122 bytes as shown in figure C-1. The total flash memory available for recording SDRs is approximately 3.6 Mbytes. Therefore, approximately 29,500 SDRs can be recorded before filling memory. At 1.3 seconds per SDR, this represents approximately 10.7 hours of data collection time.

In addition to recording SDRs, a limited number of strain time-histories are recorded. A strain time-history record consists of the 2048 data points which make up a single sample set for one strain gage. In its configuration at the time of this report, the Dosimeter was programmed to record the first 42 strain time-histories for all three strain gages. The strain time-history data can be used to accomplish a more detailed analysis of the vibration environment if desired. It can also be used to investigate anomalous SDRs.

Figure C-1 summarizes the components of the Standard Data Record and the Time-History Data Record. It also includes the memory address information as configured in the Dosimeter software at the time of this report.

Standard Data Record				Strain Time-History Record		
Element	**Size**			**Element**	**Size**	
Time	6	bytes		Time	10	bytes
Temperature	2	bytes		Unused	2	bytes
Strain Peaks	6	bytes		Temperature	2	bytes
1/3-Octave Bands Ch1	36	bytes		Strain Time-Hist Ch1	4096	bytes
1/3-Octave Bands Ch2	36	bytes		Strain Time-Hist Ch2	4096	bytes
1/3-Octave Bands Ch3	36	bytes		Strain Time-Hist Ch3	4096	bytes
Total Record Size	122	bytes		Total Record Size	12302	bytes
Memory First Address (hex)	10000			Memory First Address (hex)	380001	
Memory Last Address (hex)	380000			Memory Last Address (hex)	400000	
Total Memory	3604480	bytes		Total Memory	524287	bytes
Maximum Number of Records	29544			Maximum Number of Records	42	
Records per Second	1.3			Records per Second	1.3	
Maximum Recording Time	10.67	hours		Maximum Recording Time	54.60	seconds

Figure C-1. Contents and Size of Standard Data Record and Strain Time-History Record

Detailed Operation Description for Shop Mode

To operate the Dosimeter in Shop Mode:
1. Connect specialized RS-232 cable between Dosimeter and a computer containing the *DPD_Loader* software.
2. Connect an instrumentation load. An instrumentation load must be in place for the dosimeter to run properly in Shop Mode. This can be a dummy load or the actual strain and temperature instrumentation leads. If a dummy load is used, the strain gage portion of the load must emulate an Anderson loop configuration. Failure to properly connect an instrumentation load prior to applying power may permanently damage the Dosimeter.
3. Connect battery power supply.

Once the RS-232 cable, instrumentation load, and battery are connected, the Dosimeter operates automatically as described below:
1. Following battery connection, the Dosimeter will power up after a short delay. The length of the delay will vary from 10.00 to 99.99 seconds depending on the status of the WDT and the preprogrammed IdleTime variable.
2. Upon power-up, the Dosimeter will enter Shop Mode. At this time the computer can connect to the Dosimeter by using the software application named *DPD_Loader*. An electronic handshake is made between the Dosimeter and *DPD_Loader* using the CONNECT command. Figure C-2 shows a screen shot of the *DPD_Loader* interface window.
3. Once *DPD_Loader* has initiated the connection with the Dosimeter, the following *DPD_Loader* operations can be performed: (1) download SDR and time-history data from Dosimeter memory, (2) reset Dosimeter data memory, and (3) upload new software into Dosimeter program memory.
4. Once the user has performed the necessary operations with the *DPD_Loader* program, the program can be exited, and the serial cable can be disconnected.

It is worthwhile to note that during all Shop Mode operation, the Dosimeter power up and power down activity is governed by the WDT. When the Dosimeter powers up in Shop Mode, the WDT is initiated and begins to mark time. If the Dosimeter remains idle for a period of time equal to the IdleTime, the WDT will trigger the Dosimeter to power down. Execution of any command in *DPD_Loader* will serve to refresh the WDT, thereby resetting the time-out period. However, if no commands are executed before the IdleTime has elapsed, the Dosimeter will power down. Once the Dosimeter has powered down, the IdleTime must elapse again before the Dosimeter will power up again. Once the Dosimeter powers up again, the *DPD_Loader* connection must be reestablished. This can be a source of errors and frustration, especially when the IdleTime is short.
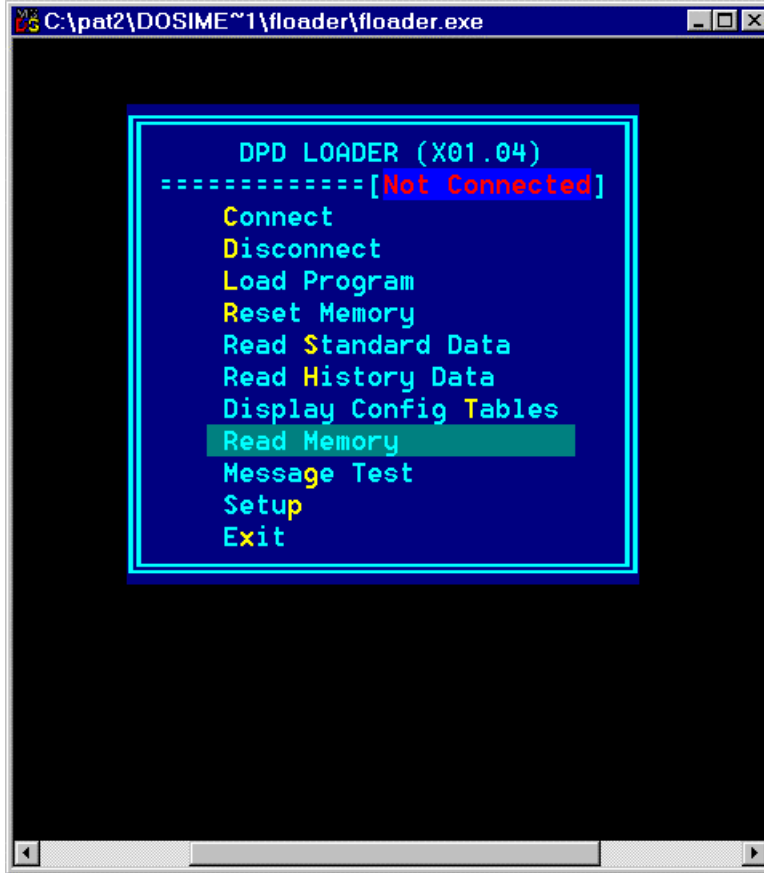
Figure C-2. DPD_Loader User Interface Window.

Appendix D

VEM DATABASE

LIST OF FIGURES

LIST OF TABLES

STRUCTURAL ADHESIVE DATABASE

Dexter EA9696 and Cytec FM 73 film structural adhesives were selected for use during this project; 3M AF163-2 would also be acceptable. All of these are a nominal 250 °F cure. Any of these may be cured at a somewhat lower temperature with a minimum reduction in properties. Curing at less than 212 °F eliminates concerns regarding entrapped moisture. The Australians cure FM73 at 80 °C (176 °F).

Per verbal discussions, the shear modulus for FM73 after a conventional cure at -67 °F is 132 ksi, RT 116 ksi, 140 °F 65 ksi, and 180 °F is 31 ksi. It was learned from David LeGrand of Dexter Hysol Aerospace Products that the typical shear modulus for EA9696 at 82 °F is 115ksi; 180 °F-84ksi; 220 °F-57ksi; and 250 °F-10ksi. Figure 1 shows a comparison of shear modulus, as function of temperature, for Cytec FM73 and Dexter Hysol EA9696.
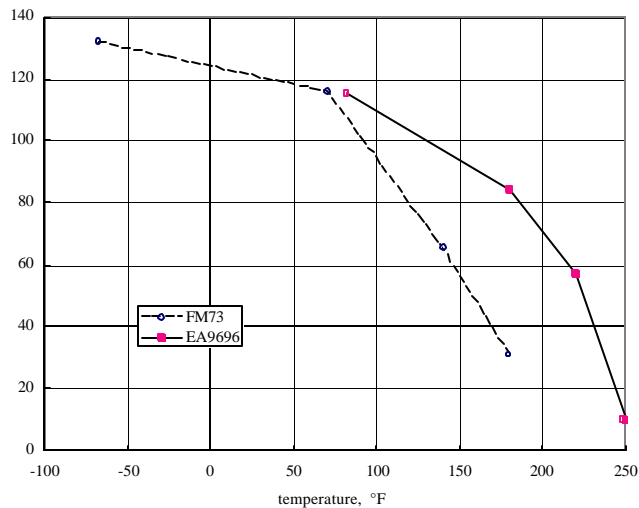
Figure 1. Shear Modulus Versus Temperature for Candidate Film Adhesives, 250°F Cure

The state of the art of design for HCF in structural adhesives has been investigated. Specifications require experimental fatigue specimens to be exposed to constant amplitude sinusoidal average stress of 750 psi for 1e6 cycles, at the end of which the test is terminated.

An expert employed by Cytec has indicated that adhesives behave better under high strain rates (within reason); as a consequence, there is a qualitative indication that properties at higher frequency vibration would be favorable.

99

FIBERGLASS DATABASE

Fiberite MXB-7701/7781 fiberglass prepreg was selected for use during this program; the 7701 indicates the resin and 7781 the weave style. Weave style 1582, 0.013 thick, and 1583, 0.016, are also available with 7701 resin and have similar modulus, but may not be available with the same lead times as 7781. This information is from Rick Byrens (714-744-5626; fax 714-532-4096) of Fiberite Orange Product Technology. A higher modulus resin 7701 prepreg is available.

During this program, a laminate of 10 layers of Fiberite MXB-7701/7781 fiberglass prepreg was assembled and cured at 250 °F under vacuum. A beam was cut from the laminate with a high-speed diamond saw. The thickness was measured as 0.125 inch, from which the average cured ply thickness is 0.0125 inch, which compares with 0.009 to 0.010 inch projected by the fiberglass prepreg supplier and can vary depending on resin content percentage. From the first two measured natural frequencies of the free-free beam, the Young's modulus was calculated as 2.6 msi, which compares with a nominal 3.3 msi projected by the supplier.

VEM DATABASE

For the best accuracy in predictions of modal damping and frequency values and related characteristics, the intended batch of production materials and their processing should be followed meticulously in fabricating test specimens. Different batches of materials will in general have different mechanical properties. The present section presents the design database properties of experimental complex modulus for 10 VEMs in both un-cocured and co-cured condition.

Table 1. Comparison of cocured and un-cocured for candidate VEMs

VEM	temperature peak damping, 100 Hz		peak loss factor		modulus (psi) at peak damping		thickness	material
	not cocured	cocured	not cocured	cocured	not cocured	cocured	inches	
3M 9469	68°F	86°F	1.2	0.6	165	1500	0.005	acrylic
3M 468	68°F	91°F	1.2	0.7	150	750	0.005	acrylic
Dyad601	53°F	53°F	1.3	1.3	1100	420	0.020	polyurethane
Dyad606	98°F	97°F	1.2	1.2	1000	1100	0.020	polyurethane
Dyad609	136°F	135°F	1.0	1.1	1300	1800	0.020	polyurethane
Avery3099	92°F	83°F	2.5	2.3	120	190	0.022	rubber-based
Avery1125	53°F	na	2.0	na	420	na	0.005	acrylic
Avery1191	82°F	na	2.4	na	125	na	0.011	rubber-based
3M 9245	na	na	0.5	0.6	13000	7000	0.020	acrylic/epoxy
Densil2078	260°F	162°F	1.3	0.5	20	900	0.002	silicone

Complex modulus data was taken for those VEMs listed in *Table* . As received, VEM's were placed in test blocks in conventional fashion. Cocured VEM's were first processed into laminates as follows:

Table 2. Layup of Cocured Laminates

Cocured Laminates:
Layer 1: fiberglass prepreg
Layer 2: VEM
Layer 3: structural adhesive film
Layer 4: structural adhesive film
Layer 5: VEM
Layer 6: fiberglass prepreg

The fiberglass prepreg was Fiberite MXB-7701/7781, and the structural adhesive was Dexter Hysol Aerospace EA9696. The structural adhesive and the fiberglass prepreg were cured at 250 °F for 1 hour with surface-to-surface contact with the VEM. Specimens (2.0- by 1.5-inches) were cut with a high-speed diamond saw from this symmetric laminate. The area is based on stiffness requirements of

101

the measurement system. These specimens were secondarily bonded to the blocks and were used to measure the complex shear modulus using impedance techniques. An analysis was performed which indicated that the shear stiffness of the structural adhesive in this laminate would not affect the values determined for the VEM.

The expectation is that any and all 250 °F amine-cure (not anhydride-cure) epoxy resins for fiberglass prepreg, meeting Boeing BMS 8-79, will be compatible.

In *Table* , the peak material loss factor, the corresponding shear modulus, and the temperature of peak loss factor for 100 Hz for both cocured and un-cocured conditions is given. From this information, estimates of effects of cocuring may be inferred.

Other projects have used a separator layer between the VEM and the adhesive or prepreg.

Wicket plots and/or nomograms, as appropriate, are included in Figure 2 through Figure 22.
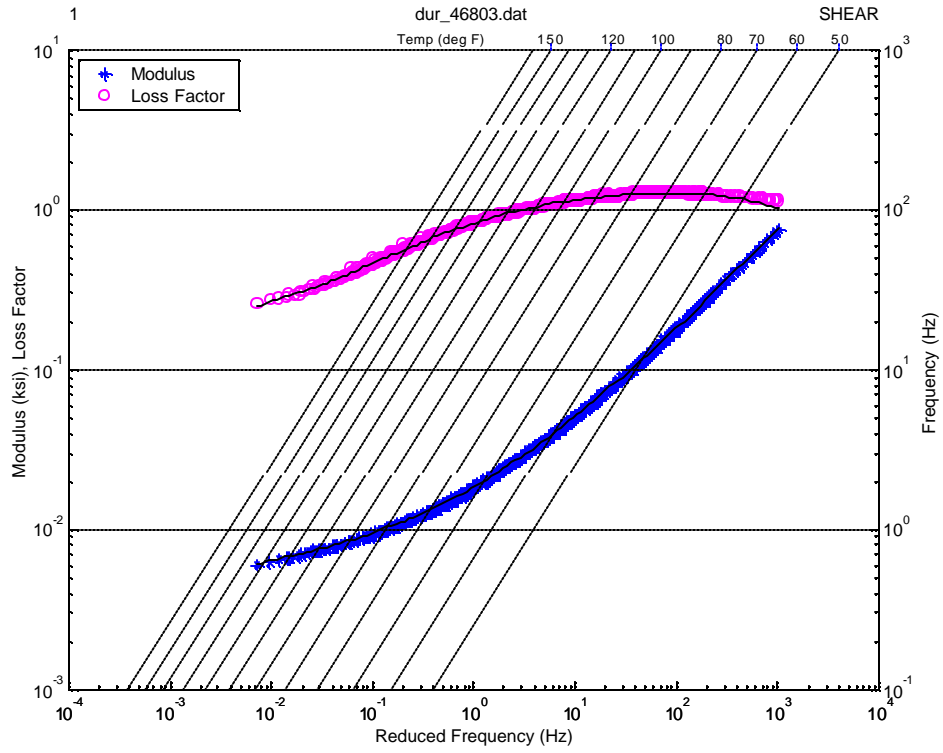
Figure 2. Nomogram for 3M 468
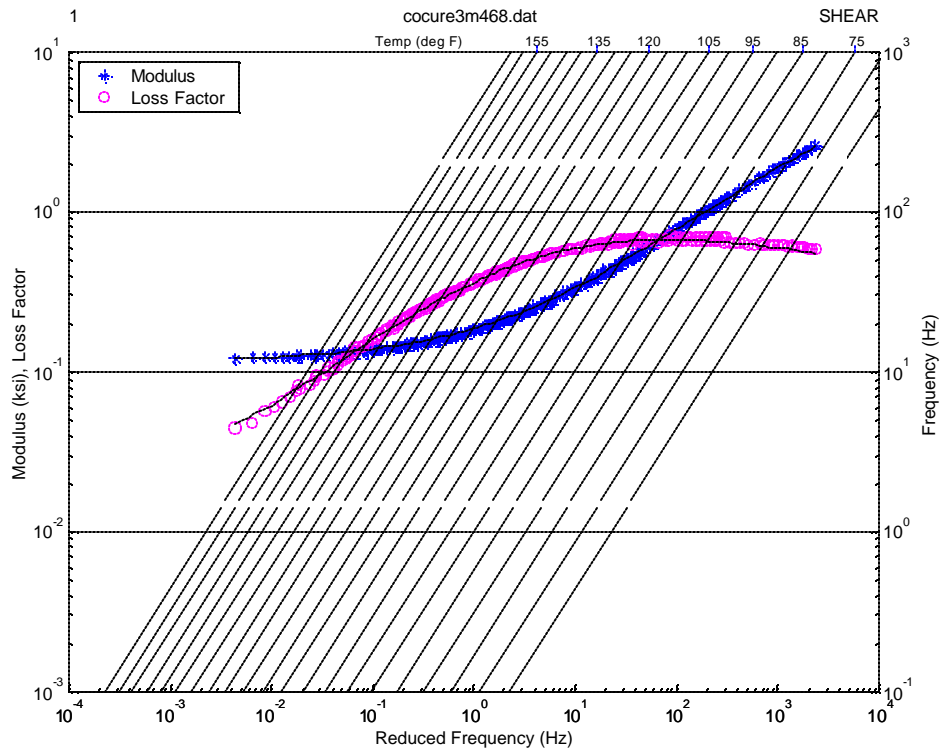
*Figure 3. Nomogram for Cocured 3M 468*

103
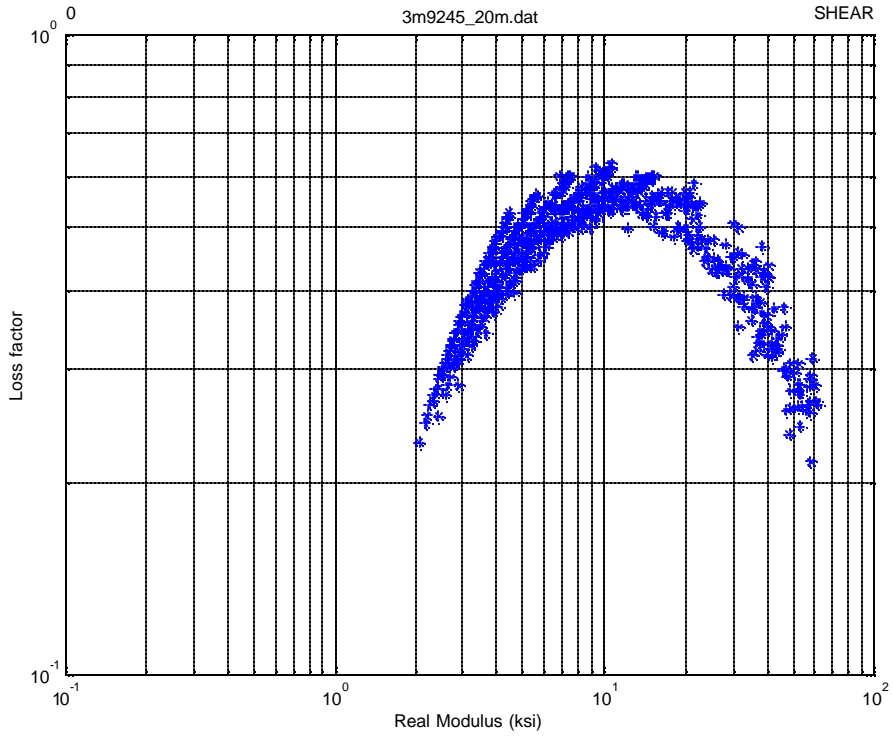
*Figure 4. Wicket Plot for 3M 9245*
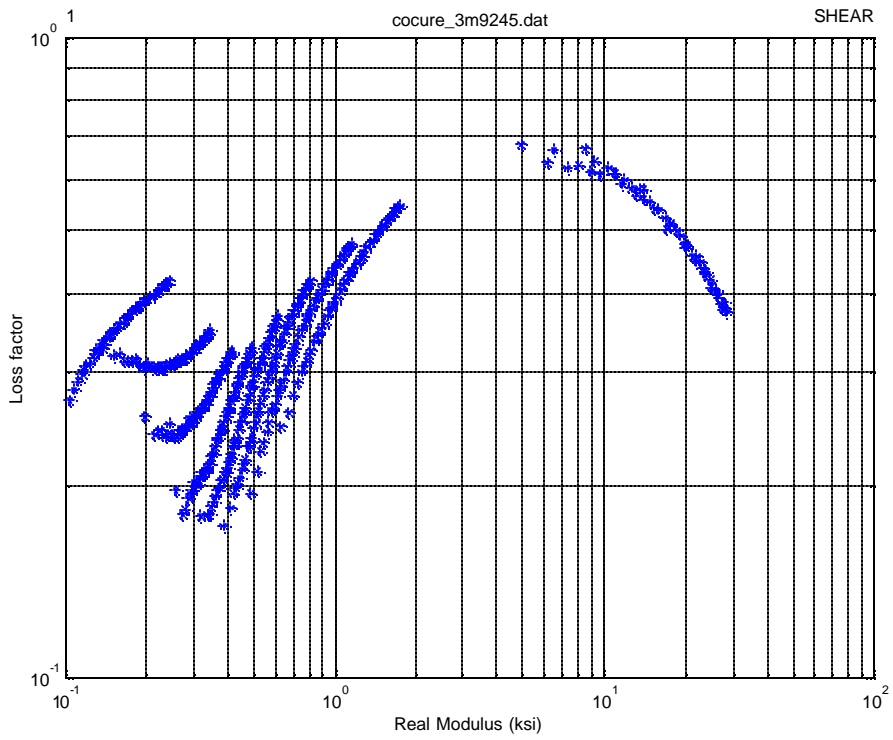
Figure 5. Wicket Plot for Cocured 3M 9245
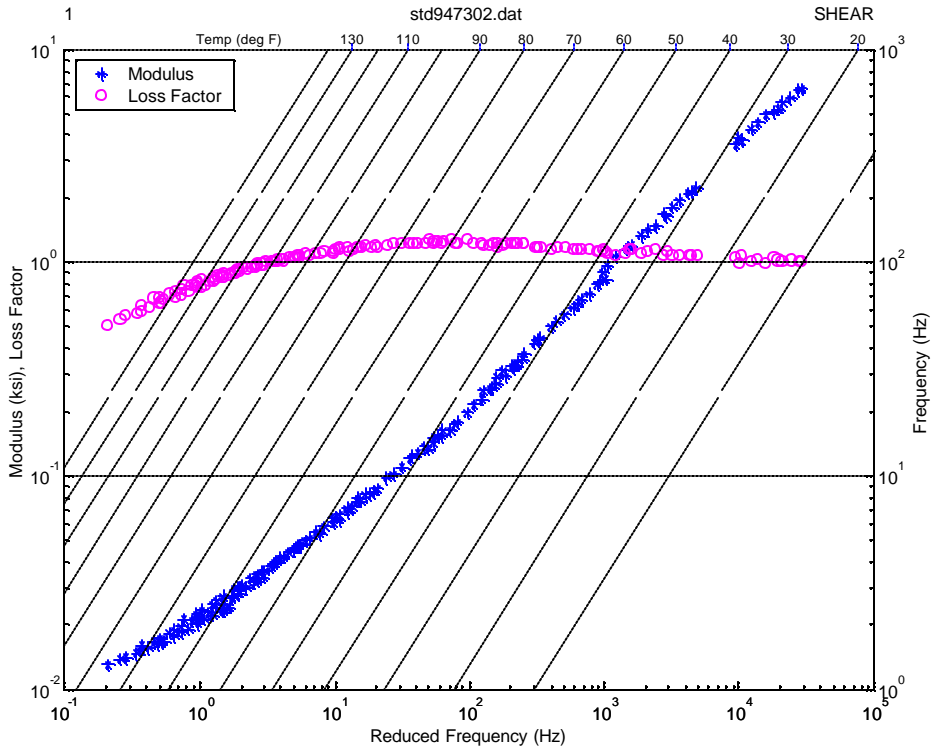
*Figure 6. Nomogram for 3M 9469*
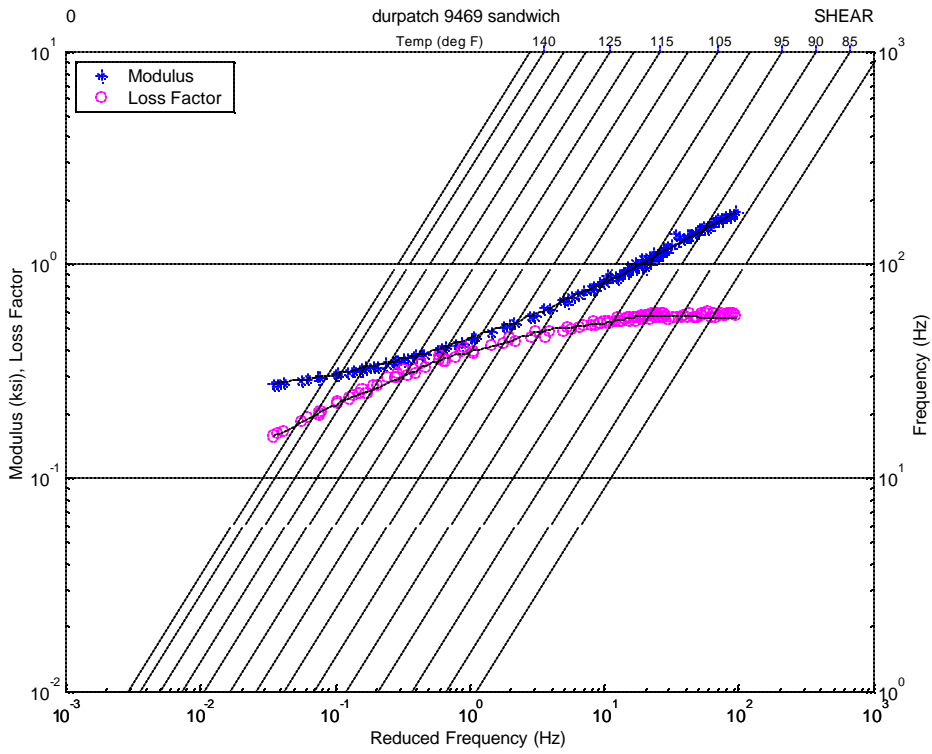
*Figure 7. Nomogram for Cocured 3M 9469*
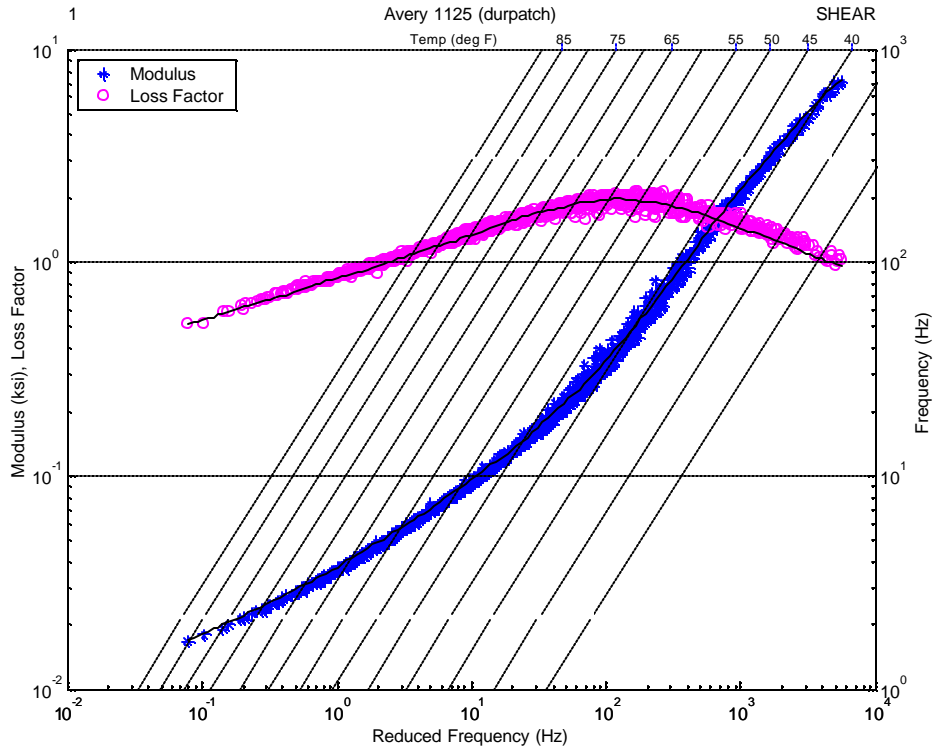
Figure 8. Nomogram for Avery 1125
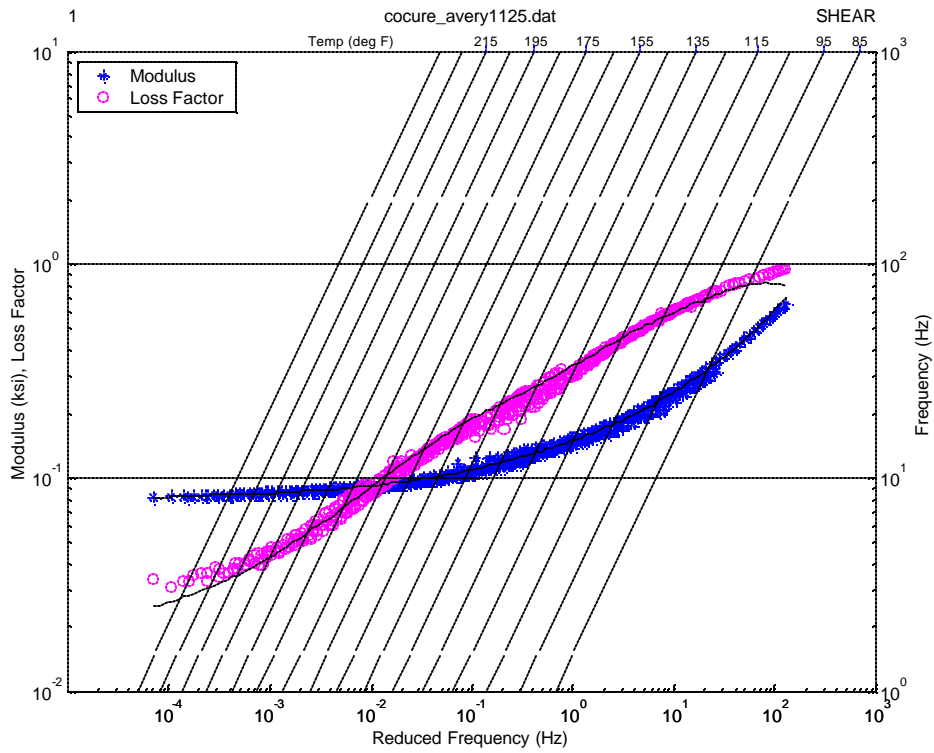
Figure 9. Nomogram for Cocured Avery 1125
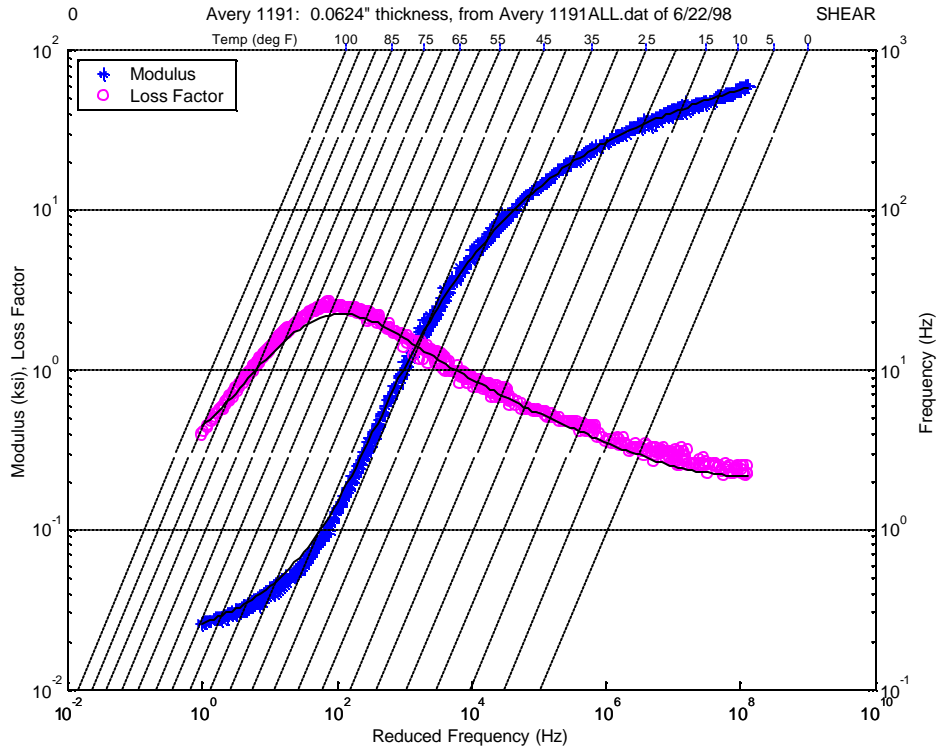
Figure 10. Nomogram for Avery 1191
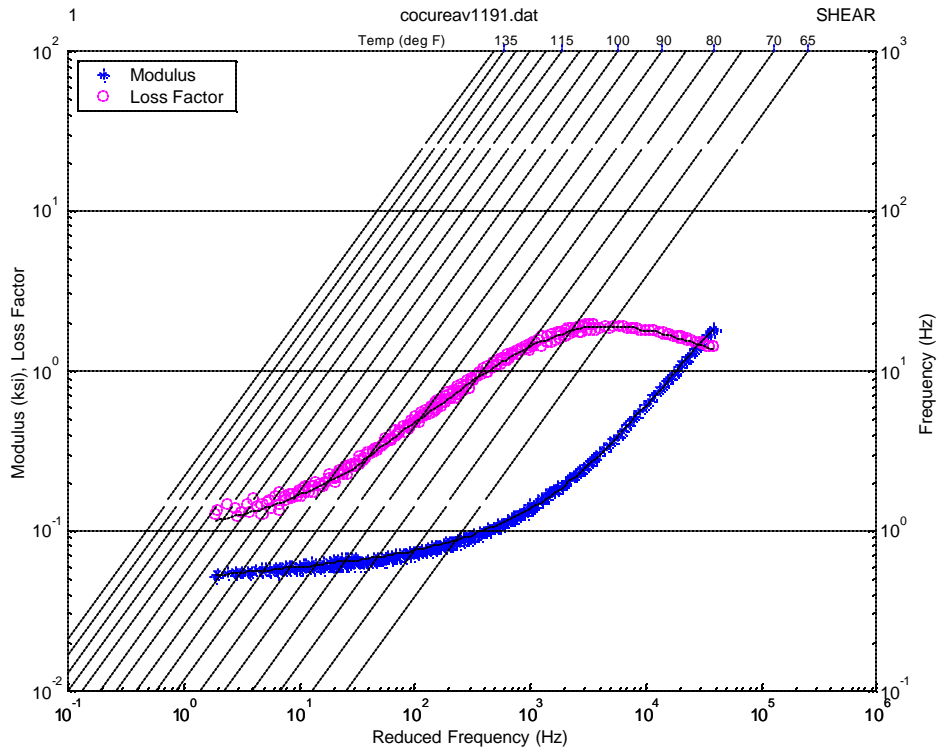
Figure 10a. Nomogram for cocured Avery 1191

107
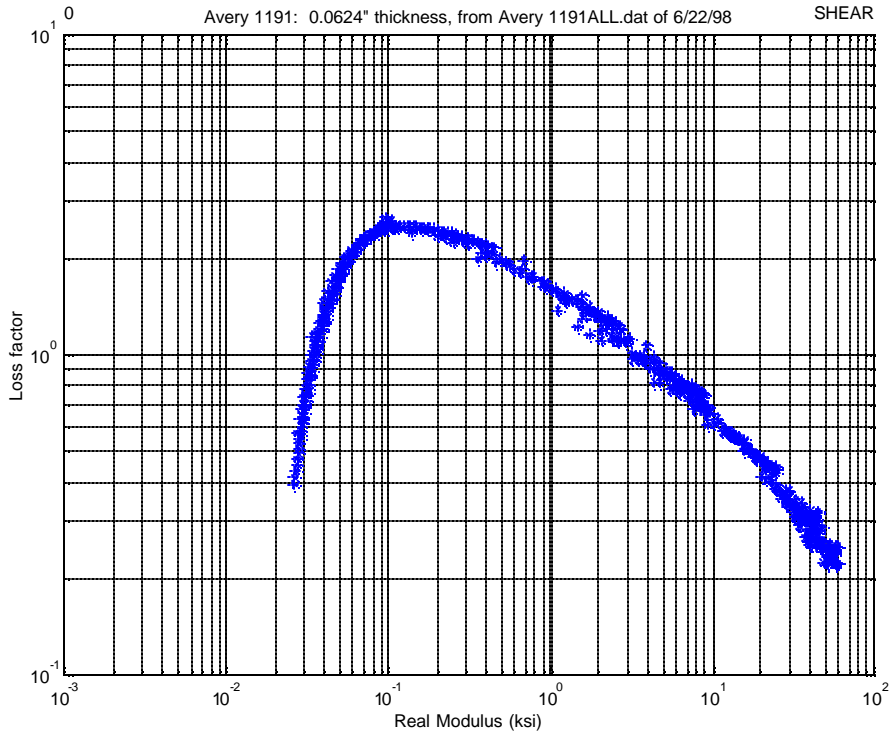
Figure 11. Wicket Plot for Avery 1191
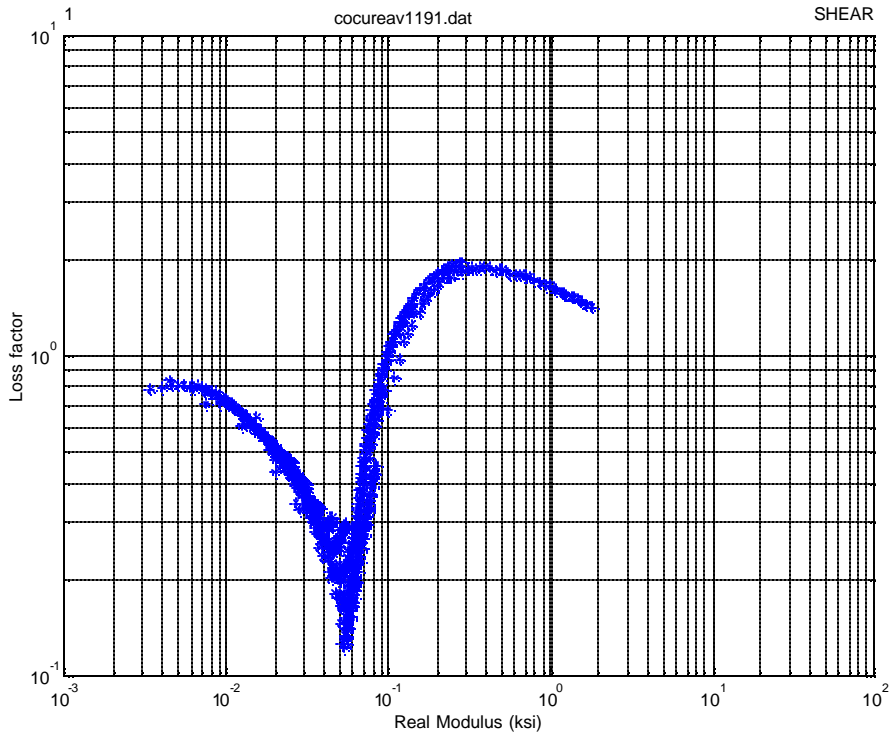
Figure 12. Wicket Plot for Cocured Avery 1191
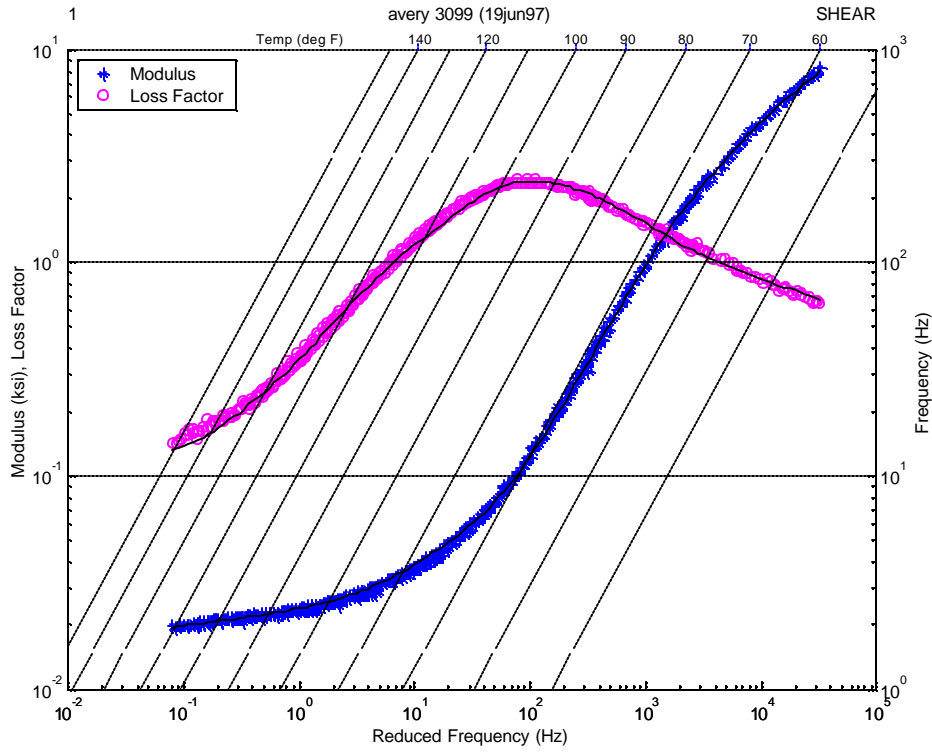
Figure 13. Nomogram for Avery 3099
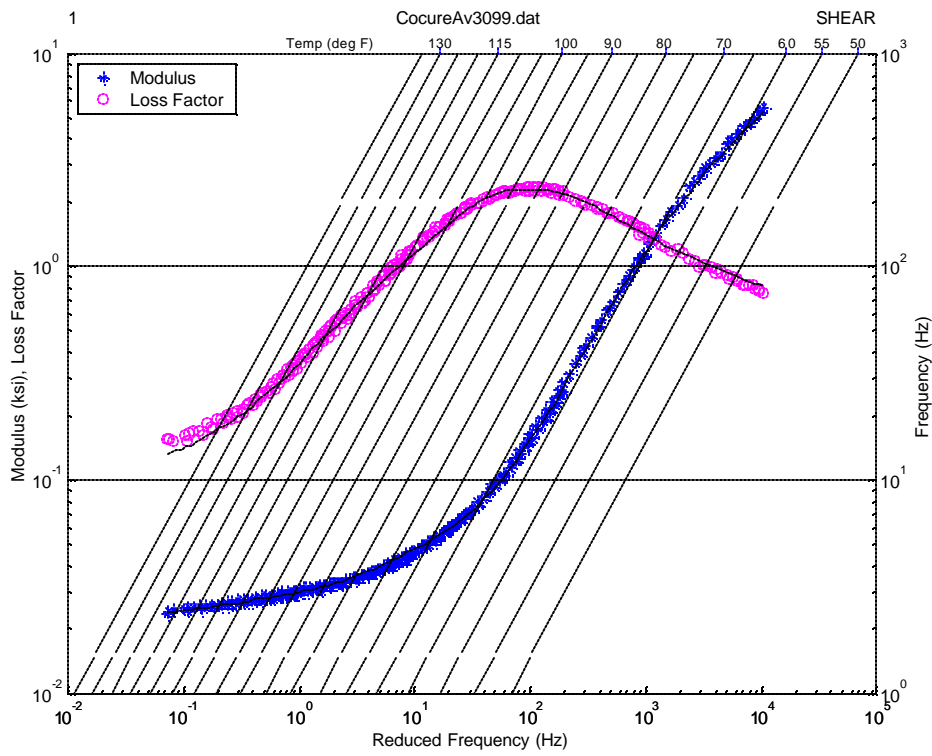
Figure 14. Nomogram for Cocured Avery 3099

109
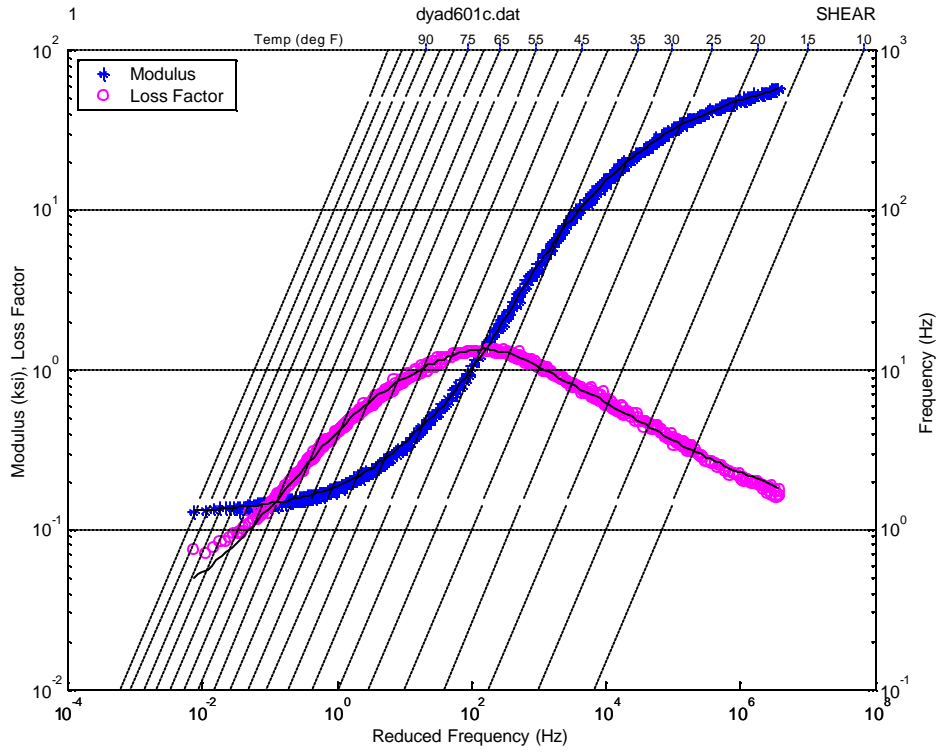
Figure 15. Nomogram for Soundcoat Dyad601
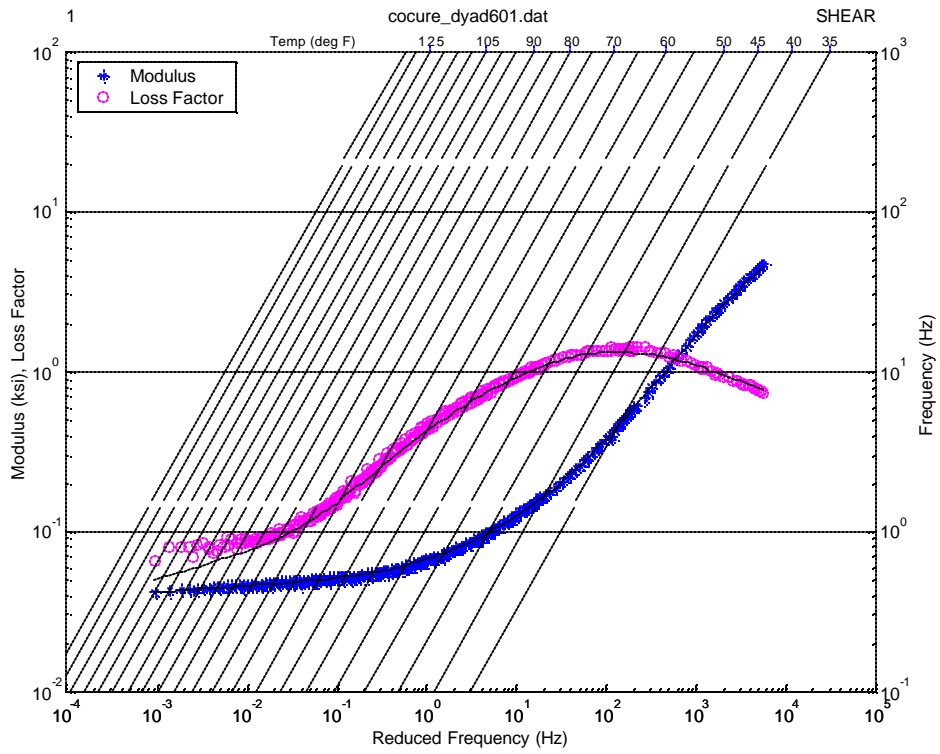
Figure 16. Nomogram for Cocured Soundcoat Dyad601

110
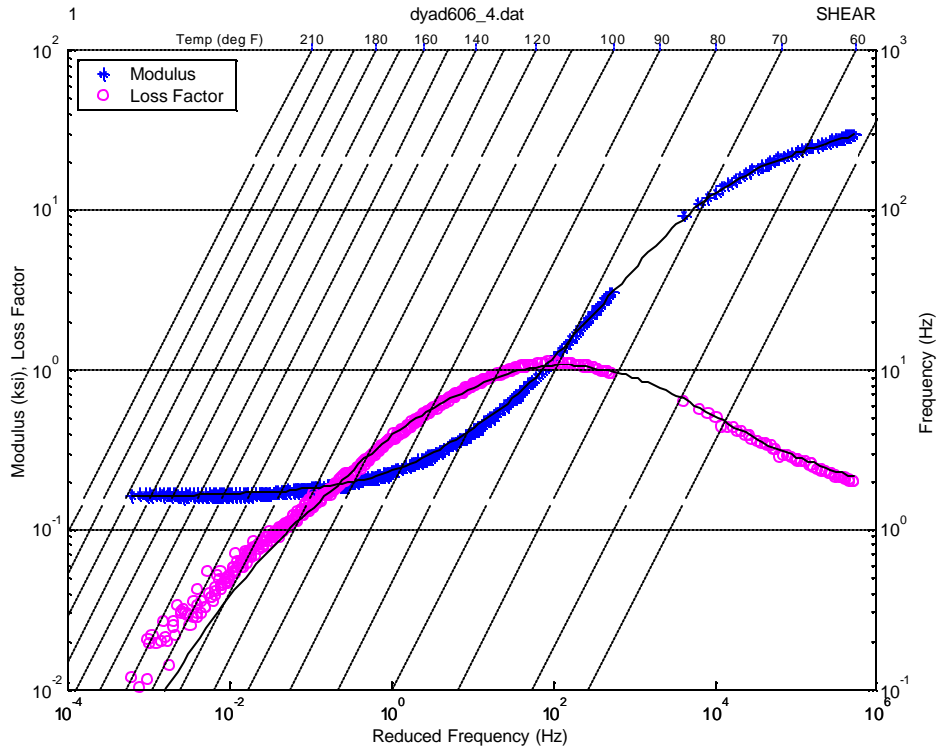
Figure 17. Nomogram for Soundcoat Dyad606
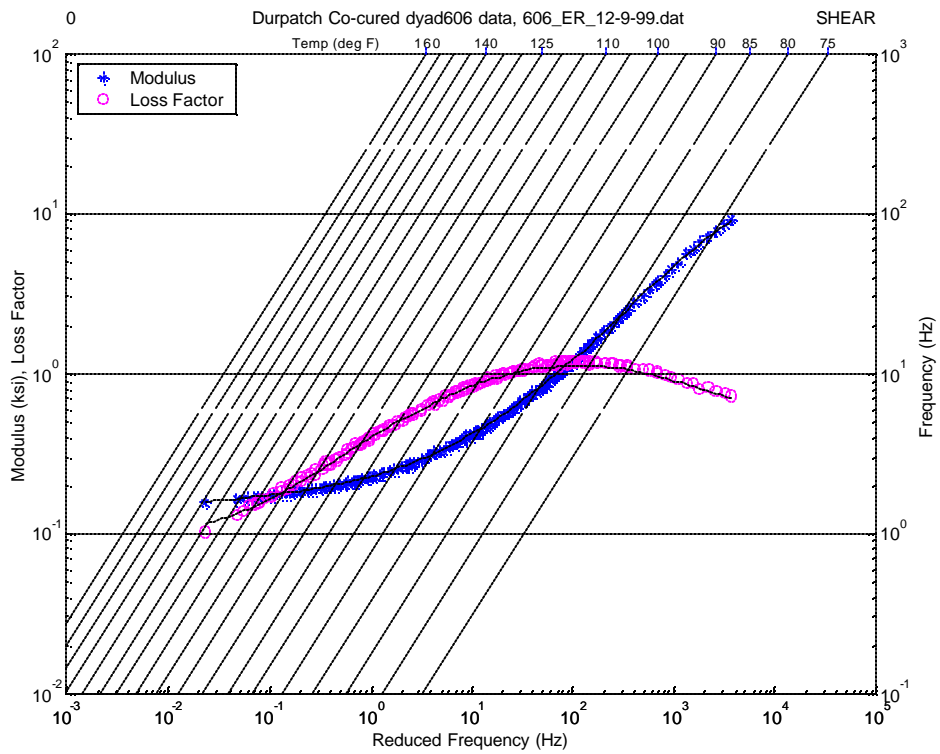
Figure 18. Nomogram for Cocured Soundcoat Dyad606

111
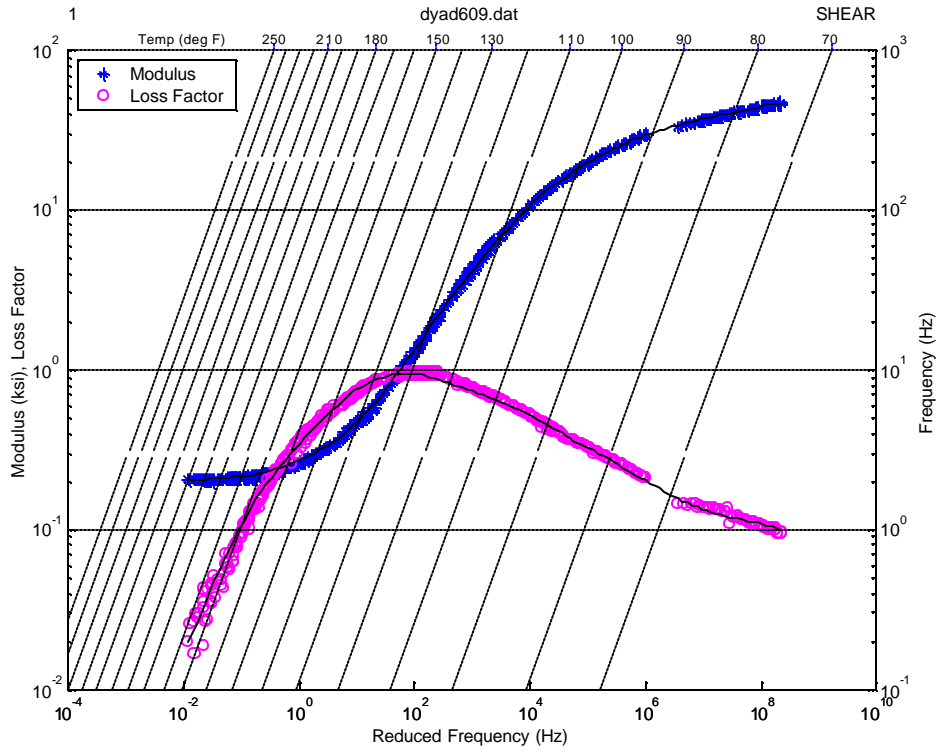
Figure 19. Nomogram for Soundcoat Dyad609
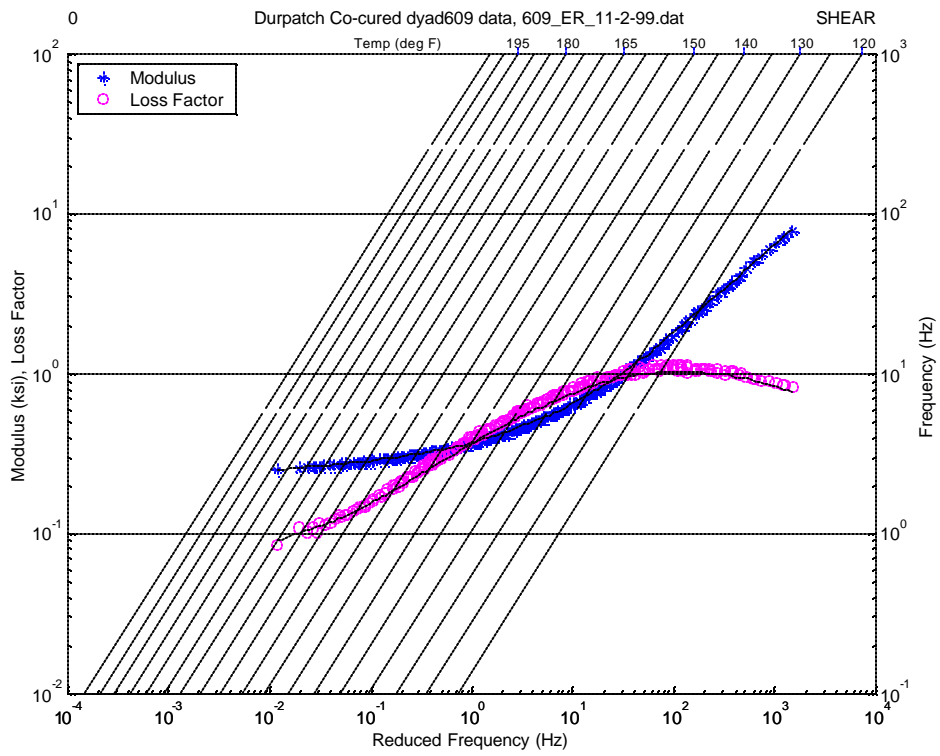
Figure 20. Nomogram for Cocured Soundcoat Dyad609

112
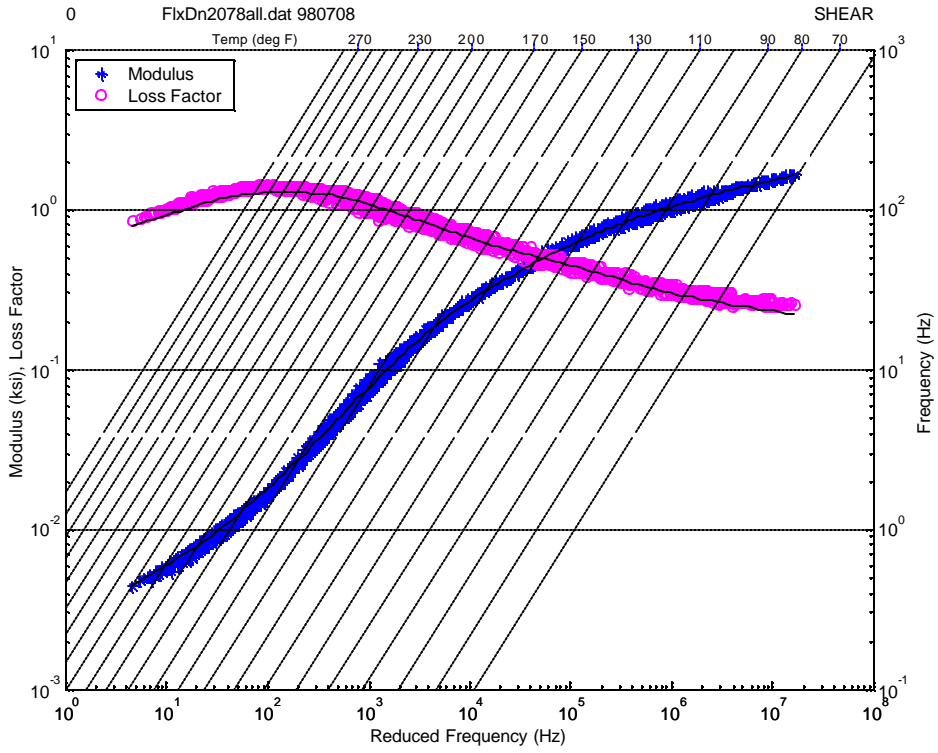
Figure 21. Nomogram for Flexcon Densil
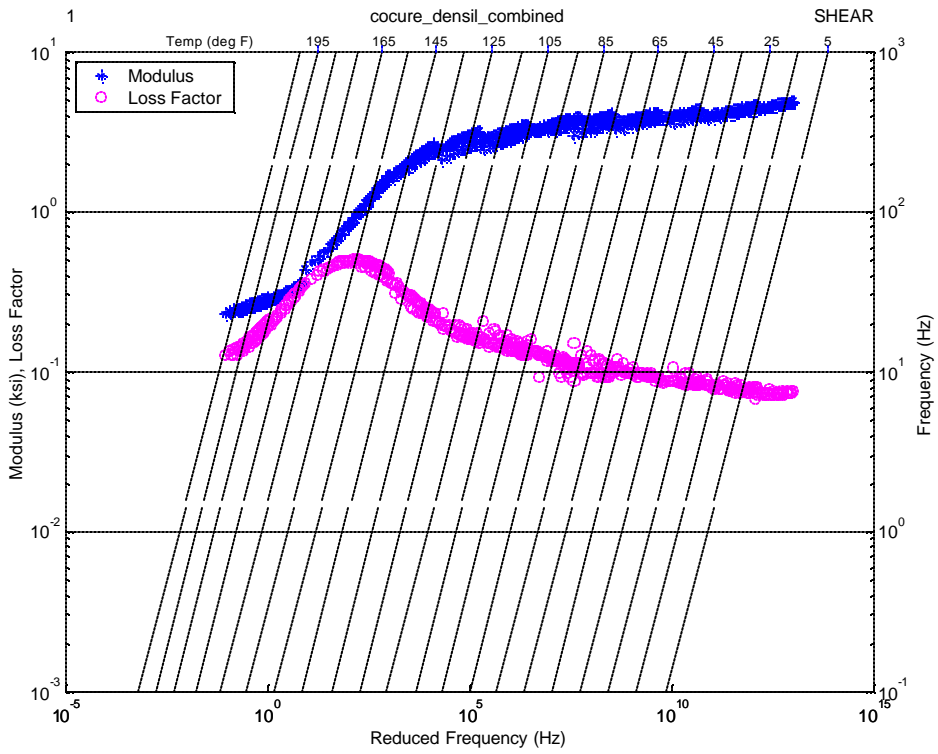
Figure 22. Nomogram for Cocured Flexcon Densil

113

APPENDIX E

DURABILITY PATCH
INSTALLATION PROCEDURES
&
SILANE SURFACE PREPARATION PROCESS

(These procedures are adapted from those developed by WL/MLSE and WR-ALC/TIEDD)

1. MATERIALS   The basic list of materials required for the process are as follows:

Solvent (MEK, reagent grade acetone, Citra Safe, X-Caliber or isopropyl alcohol.)
Markers
Sanding Disks
Rubber Gloves
Dust Masks
Duralace Wipes
Oil-Free Nitrogen
Scotchbrite, 3M Company
Aluminum Oxide Grit (50 Micron)
Vacuum Bagging Material
Tape (masking, flash breaker, Teflon)
Silane (Z 6040)
Distilled Water
Glass Beaker/Flask
Mixing Magnet
Cotton Gloves
Acid Brushes
Porous Teflon Coated Fiberglass or Release Bleeder B
Nonporous Teflon Coated Fiberglass or Perforated Red Release Film
Breather Material
Bleeder Material
Parachute Chord
Divinycell
BR-127 Primer
Dexter EA 9696, Cytec FM 73, or equivalent, Adhesive
Fiberite MXB-7701/7781 woven fiberglass prepreg (or equivalent)
VEM (Visco Elastic damping Material)

2. EQUIPMENT The basic list of equipment for the process are as follows:

CAUTION
CHECK THAT ALL HEAT BLANKETS, INFRARED LAMPS AND QUARTZ HEATERS ARE SAFE FOR USE. CHECK CONDITION OF INSULATION, WIRING AND BLANKETS FOR SIGNS OF CRACKING AND DEGRADATION.

High Speed Grinder
Grit Blast Gun
Adhesive Primer Spray Gun
Infrared Lamps or Quartz Heaters
Isoscope
Hot Bonder – Briskheat 6000 or 9000
Heater Blanket
J-Type Thermocouples

3.0 AIRCRAFT PREPARATION

Bonding to secondary structure may possibly accommodate less stringent procedures.

3.1 FUEL SYSTEMS. *The fuel status of the aircraft shall be thoroughly discussed with the appropriate safety personnel to assure that the aircraft is in the safest condition for the repair with the equipment used.   Modifications shall be made to this procedure as different applications, repair locations and aircraft occur. These procedures shall be approved by the appropriate safety personnel and filed units prior to the initiation of any work.*

CAUTION
FUEL AND SAFETY CONDITION INSPECTIONS SHALL BE COMPLETED BY THE REPAIR TEAM CHIEF PRIOR TO INITIATION OF ANY WORK!!

3.1.1   C-141. All tanks shall be drained and depuddled for any fuel tank repair. For field work, all tanks shall be continuously air purged. The Lower Explosive Limit (LEL) shall be 1.4% or less for all tanks in which access is required and 5% or less for all other fuel tanks.

3.1.2   C-130. For field repair efforts on the lower wing surface aft of the engines, all aircraft fuel tanks shall be completely full and topped off. See WR-ALC/SEG letter (on file) of 31 July 1998. All fuel tanks shall remain closed. The aircraft shall be placed in an approved fuel cell hanger. No work is to be accomplished inside any fuel tanks or fuel cell in the fueled condition.

3.1.2.1 If work is being accomplished inside the engine dry bays, visually check for signs of fuel and check that the LEL is 1.5% or less. Air purge as necessary to maintain the LEL of 1.5% or less.

3.1.2.2 Visually check for any signs of fuel drainage from any drain channel. Vacuum or air purge the drain channels as necessary until the LEL is 20% or less.

__3.2 AIRCRAFT POSITIONING__. The aircraft shall be positioned and jacked or no-loaded as appropriate for the repair being accomplished. This position shall be coordinated with the appropriate SPO engineer.

4.0 SURFACE PREPARATION

NOTE

Timing throughout the process is critical. Preplanning as to thermocouple locations, heat sinks, bagging, equipment condition, etc. can save a lot of confusion and panic later and possibly avoid a lot of wasted time through having to restart the effort due to problems that could have been easily avoided. Think it through FIRST, then ACT!!

4.1 SURFACE CONTAMINATE REMOVAL

CAUTION
RUBBER(OR EQUIVALENT) GLOVES & EYE PROTECTION MUST BE WORN DURING THIS OPERATION.

4.1.1 Solvent wipe an area extending a minimum of 2 inches in all directions outside the repair area with one of the following solvents: MEK (Methyl Ethyl Ketone), acetone, Citra Safe, X-Caliber, or isopropyl alcohol. Use Duralace or cheesecloth and wipe in only one direction, frequently turning the wipe to a clean surface. The above list is order of preference. Choose a solvent that is approved at the repair location.

4.1.2 Identify and mark riser, weephole, crack, *corrosion pits*, etc. and patch center locations using an approved marker and extend perpendicular lines from the patch center point to one foot outside repair area in all directions. Check the actual patch against the location and check for size, possible interference and location of fasteners. Contact engineering if there are any problems.

4.1.3 Remove all surface coatings down to bare metal using locally approved procedures to an area 1 inch larger than the patch in all directions. Be sure that the patch position is known and center point is marked prior to this step.

CAUTION
RUBBER GLOVES & EYE PROTECTION MUST BE WORN DURING THIS OPERATION.

4.1.4 Solvent wipe repair area per directions of paragraph 4.1.1.

4.1.5 Connect high speed grinder to 90 psi oil-free nitrogen, *or equivalent approved highly filtered air,* and abrade the repair area using a fine grit Scotchbrite disk. Visually check for any signs of corrosion, nicks, or scratches and carefully blend out removing only the minimum metal possible. If there are any questions as to severity of the damage, contact engineering for resolution.

NOTE

Only verified oil-free water pumped nitrogen, *or equivalent approved highly filtered air*, is to be used in this entire repair process or contamination of the bond surface could result. Only dedicated nozzles, hoses, etc. will be used with the nitrogen *or highly filtered air*.

NOTE

From this point forward, extreme care must be taken to ensure that the repair area is not touched by anything, including fingers, except as outlined below.

WARNING

FROM THIS POINT ON, THE REPAIR PROCESS CANNOT BE STOPPED UNTIL, AS A MINIMUM, THE PRIMER IS CURED. PREFERABLY, THE PROCESS WILL NOT BE STOPPED PRIOR TO PATCH CURING.

4.2   SILANE MIXING

4.2.1   In a clean glass or polyethylene beaker or flask, mix a solution of 99 parts (weight or volume) of distilled water and 1 part (+1/-0) parts of Dow Corning Z6040 silane. A 100ml of solution is sufficient to treat a 60 square inch repair area.

4.2.2. Place a clean mixing magnet in beaker, cover to keep from contamination, and agitate on a magnetic mixer for a minimum of 1 hour prior to use. Continue agitating until the solution is actually used.

NOTE

MAXIMUM SOLUTION LIFE IS 4 HOURS AFTER THE 1 HOUR MIX TIME.

4.3 GRIT BLASTING OPERATION

4.3.1. Solvent wipe the repair area using Duralace wipes moistened with reagent grade MEK or acetone. Wipe until all residue is removed (new Duralace wipes remain clean after wiping). Be careful not to drag contaminants into the repair area from the surrounding structure. On the last wipe, remove the solvent with a second clean wipe prior to its evaporation.

WARNING
DUE TO THE ABRASIVE NATURE OF ALUMINUM OXIDE
AND ITS AFFECT ON FUEL SYSTEM COMPONENTS,
STRICT ACCORDANCE TO GRIT BLAST CONTAINMENT
PROCEDURES MUST BE FOLLOWED.

4.3.2. Grit blasting will be in accordance with "TI GRIT BLASTING CONTAINMENT PROCEDURES", dated 3 April 1996. See Appendix A. In addition, all applicable sections of LJ specification 94-LJLE-017, SPECIFICATION FOR ALUMINUM OXIDE GRIT BLAST CONTAINMENT, FUEL TANK INSPECTION AND CLEANING PROCEDURE, C-141 AIRCRAFT' , will be followed. See Appendix B.

4.3.3. Grit blast an area one inch in all directions greater than the repair patch with 50 micron aluminum oxide grit using 30-100 psi oil-free nitrogen pressure. Adjust the blast pressure as necessary to produce a uniform fine mat finish, *45 PSI is recommended,* with no signs of buffing marks. Blow the area clean of excess grit with oil-free nitrogen.

4.4 SILANE APPLICATION

4.4.1. Rinse off a clean natural bristle brush with distilled water and use it to apply the silane solution to the repair area for a minimum of 10 minutes after the entire repair area is wet.

NOTE
Inspect for water breaks

WARNING
IF A WATER BREAK FREE SURFACE IS NOT ACHIEVED, THE
PROCESS MUST BE RESTARTED AT PARA 4.0

Apply silane solution to the repair area continuously to maintain a film of solution on the surface throughout the 10 minute time period. Brush the silane from the center of the repair area. Do not allow the surface to dry. Clean the brush thoroughly with distilled water and wrap in a clean plastic bag.

NOTE
Ensure that the brush does not touch the surrounding uncleaned
structure.

4.4.2. Connect an air nozzle to oil-free nitrogen, *or approved highly filtered air,* and remove the silane solution from the repair area by starting at the center of the repair area and working outward in all directions.

NOTE
Do not allow anything to be blown onto the silaned area from the
surrounding areas.

4.5 SILANE CURE PROCESS

4.5.1. Place one or more thermocouples around the perimeter of the silaned area but not touching under the area to be patched. The thermocouple ends must be in contact with the skin and must be taped with high temperature tape (such as Teflon tape). A map of the thermocouple locations must be made. Plug thermocouples into hot bonder or thermocouple reading device.

NOTE

In some cases when repairing on a wing surface, a continuous air purge of the fuel tanks is required to maintain proper LEL levels. In this case assure that the air supply is not set on airconditioning or blowing directly on the repair site which will make attaining proper cure temperature very difficult. Additional insulation at the repair site may be required

4.5.2. Insulate as necessary around the repair area to achieve good thermal distribution. Insulation materials must be temperature resistant to at least one and a half times the curing temperature. Approved materials are polyester breather and Divinycell.

4.5.3.   Center infrared lamp over the repair area and raise until baffles are within 1/4 inch from the skin in all directions. Do not allow the baffles to touch the surface of the aircraft.

WARNING

FOR C-130 REPAIRS ON THE LOWER WING SURFACE, ASSURE THAT THE TEMPERATURE OVER ANY FUEL BLADDER NEVER EXCEEDS 200°F. IF THE HEATER OR HEAT BLANKET IS WITHIN 4 INCHES OF A BLADDER, PLACE A THERMOCOUPLE ON THE WING SURFACE OVER THE BLADDER AND MONITOR THROUGHOUT THE CURE CYCLE.

4.5.4. Plug infrared lamp into the variac power supply, set the power at 50% and apply heat to the repair area until highest thermocouple is 205 ± 5 °F (the power setting will need to be adjusted to ensure thermocouples attain the desired temperatures). When all thermocouples are in a range of 170°F to 210°F, maintain heat for 60+5,-0 minutes, monitoring the thermocouples and adjusting the power setting as necessary. Record temperatures throughout the cure cycle. Prevent cross ventilation to the repair area as much as possible. It may be necessary to build a temporary screen or curtain from bagging material to prevent wind from crossing the repair site and causing problems with contamination and thermal cooling.

WARNING
IF SILANE CURE TEMPERATURE EXCEEDS 215 ° F,
PROCESS MUST BE STARTED OVER FROM PARA 3.0.

NOTE

THE RECOMMENDED TIME ALLOWED BETWEEN SILANE
DRYING AND APPLICATION OF HEAT IS 30 MINUTES. IN
NO CASE CAN THE TIME EXCEED 60 MINUTES.

4.5.4. After 1 hour silane cure, turn off power supply, remove infrared lamp and allow the repair area
to cool to 90°F or ambient whichever is higher.

4.6 CORROSION INHIBITING PRIMER APPLICATION

NOTE

The primer must be warmed to ambient temperature prior to opening
the container. A good indicator of this is when moisture no longer
condenses on the can.

CAUTION

RESPIRATOR AND PROTECTIVE CLOTHING BE WORN
WHEN APPLYING PRIMER.

4.6.1. Connect spray gun to oil-free nitrogen, *or approved highly filtered air,* and spray BR-127
adhesive primer onto the repair area to obtain a cured thickness of 0.0001 to 0.0004 inches (0.1 to 0.4
mil).   Assure that the primer in the spray cup is agitated continuously during application to assure
uniform distribution of the chromates over the surface.

4.6.2. Allow primer to air dry for a minimum of 30 minutes.

4.6.3. Center infrared lamp over the repair area and raise until baffles are within 1/4 inch from the skin
in all directions. Do not allow the baffles to touch the surface of the aircraft.

4.6.4. Plug infrared lamp into the variac power supply and set the power setting to 60%. Apply heat
until the highest thermocouple is 250±5°F. Cure time is based on the lowest thermocouple reading as
shown below (the power setting may need to be adjusted to ensure thermocouples attain the desired
temperatures). Record temperatures throughout the cure cycle. Prevent cross ventilation to the repair
area as much as possible. It may be necessary to build a temporary screen or curtain from bagging
material to prevent wind from crossing the repair site and causing problems with contamination and
thermal cooling.

BR-127 Adhesive Primer Cure Schedule

Lowest Thermocouple Reading (°F)	Minimum Cure Time (Minutes)
200-239	90
240-265	60

4.6.5. After primer cure, turn off power. Remove infrared lamp and allow the repair area to cool to 90°F or ambient whichever is higher.

NOTE

The repair process can be stopped at this point if the surface is covered with a clean bagging film or clean kraft paper to protect it from contamination.

5.0 DURABILITY PATCH INSTALLATION

NOTE

Normally the patches will be pre-cured at depot in the autoclave and then adhesively bonded. In some situations due to geometry and/or damage location, the patches will have to be co-cured on site. In this situation the bagging and cure cycle will have to be modified per engineering for the specific application. Bonded repair/reinforcement of sonic fatigue crack locations in secondary structure is much less stringent than bonded repair of primary structure. Elaborate processes necessary for minimization of porosity and temperature gradients in patches for primary structure may not be required for secondary structure. Co-curing of a layer of structural film adhesive, a layer of VEM, and multiple layers of fiberglass prepreg may be acceptable on site.

NOTE

Prior to opening the bag containing the adhesive, it must be warmed to ambient temperature. A good indicator of this is when moisture no longer condenses on the bag.

5.1A PATCH LOCATION (PRE-CURED)

5.1A.1. Remove the peel ply from the patch and apply the layer of VEM (do not touch patch bonding surface) to the pre-cured patch.

5.1A.2. Remove the peel ply from the VEM and apply the adhesive (do not touch patch bonding surface).

5.1A.3. Mark perpendicular center lines on the outer surface of the patch.

5.1A.4. Remove adhesive separator backing sheet and apply patch to the repair area.

NOTE

Due to tackiness of the VEM and the adhesive, ensure correct patch alignment before contacting the repair area.

5.1B PATCH LOCATION (CO-CURED)

5.1B.1. Cut layer of structural adhesive film to proper size, i.e., such that it barely touches the edge of the fasteners associated with the "figure 8.".

5.1B.2. Cut layer of VEM 0.5 inch smaller on the perimeter than the structural adhesive. Cut the opening in the VEM. Install a one piece release liner on one side of the VEM and a split and folded release liner on the other side.

5.1B.3. Cut layer of fiberglass prepreg to the same size and shape as structural adhesive. Cut subsequent layers 0.125 inch smaller on the perimeter.

5.1B.4. Leave liner on only one side of adhesive and put in place. Note: Due to tackiness of the adhesive, ensure correct alignment before contacting the repair area.

5.1B.5. Remove liner from adhesive.

5.1B.6. Position VEM with split and folded release liner in contact with the adhesive. Holding one end of the VEM at a time in position, lift other end and remove one piece of the split liner. Repeat on other end.

5.1B.7. With liner on only one side, position a layer of fiberglass. Note: Due to tackiness of the adhesive, ensure correct alignment before contacting the repair area.

5.1B.8. Remove liner.

5.1B.9. Vacuum bag and de-bulk.

Repeat steps 7 through 9 until all of the layers of fiberglass are installed.

5.2   VACUUM BAGGING SCHEDULE

5.2.1. Install flashbreaker tape around the perimeter of the patch.

5.2.2. Place one or more thermocouples around the perimeter of the patch 1/4 inch from edge of the patch. The thermocouples ends should be in contact with parent material and should be taped with Teflon tape.   Check the ends of the thermocouples for any signs of cracks or breaks in the welds, if broken reweld or replace.

5.2.3. Install a breather chain around the periphery of the patch and out to the vacuum source. Breather chain should be within 1 inch of the patch.   Breather chain material can be chain link chain, parachute chord or rolled up polyester breather. Ensure chain link chain does not puncture vacuum bag by installing protective breather over chain.

5.2.4. Cover repair area, 4 inches beyond patch, with perforated release film.

5.2.5. Cover repair area and breather chain with 2 plies of bleeder *A* release material. Bleeder should extend 2 inches beyond heat blanket.

5.2.6. Cover repair area, 1 inch beyond patch, with 1 ply of nonporous release film.

5.2.7. Center heater blanket over the repair area and tape into place.

NOTE

It is strongly recommended that the heat blankets be checked by thermography prior to use to assure uniform heating and no dead circuits

NOTE

The heat blanket should extend a <u>minimum</u> of 4 inches beyond the repair patch in each direction.

5.2.8. Cover the entire repair area with 2 plies of polyester breather material.   Assure that breather is over the bleeder chain at the vacuum port.

5.2.9. Install vacuum bag and pull vacuum of 22 +/- 2 inches of mercury. Include a vacuum gage on the side of the repair area opposite the vacuum inlet to monitor part pressure.

5.2.10. Remove vacuum line and monitor vacuum. Vacuum should not drop more than one inch of mercury per minute. If this is not obtained, find vacuum leak and repeat this step. *The vacuum leak shall not be under the patch or in a location that a vacuum or air path will be through or over the patch. If it can be clearly identified that the leak is outside the parch area and the leak path will not be across the patch, then the leak is acceptable as long as adequate pressure can be maintained.*

6.0.   ADHESIVE CURE CYCLE

6.1. PROGRAM HOT BONDER

<u>WARNING</u>
DO NOT EXCEED ESTABLISHED VACUUM PRESSURES FOR CURING. IF REQUIRED VACUUM PRESSURE IS EXCEEDED, THERE IS A STRONG LIKELYHOOD OF TRAPPING AIR UNDER THE PATCH - ESPECIALLY ON THE LARGER REPAIRS.

6.1.1. Set vacuum pressure at 15 to 19 inches of mercury at vacuum bag.

The Double Ramp cure cycle SHALL be used for all larger patches and all patches where there is a wide variation in substructure thickness. *Contact engineering when in doubt.*

6.1.2. Program hot bonder; Double ramp (preferred method)

Ramp 1 -   Ramp up rate 3°F per minute up to 185°F, highest thermocouple.
               Hold for 30 minutes

Ramp 2 -   Ramp up rate 3° F per minute up to 260°F, highest thermocouple.
               Hold for soak time based on lowest thermocouple reading from 250°F
               adhesive cure table in para 5.3.
               Cool down at 15°F per minute until 150°F.

6.1.3.   Program hot bonder; Single ramp

Ramp 1 -   Ramp up rate 3°F per minute up to 260°F, highest thermocouple.
               Hold for soak time based on lowest thermocouple reading from 250°F
               adhesive cure table in para 5.3.
               Cool down at 15°F per minute until 150°F.

6.2   HOT BONDER CONTROL

NOTE

Assure that a thorough map of all thermocouple locations is completed. Based on thermocouple locations, heater blanket placement and known substructure, preplan for which thermocouples should be lagging and leading as to temperature.

6.2.1. Place 1 thermocouple in the control and 1 thermocouple in limit and set the printer on. Turn the hot bonder on and monitor all thermocouples to determine which one is recording the hottest temperature during the heat up. Change this thermocouple with the control thermocouple so that the control thermocouple is the hottest temperature (an alarm will sound when the thermocouples are unplugged and shut down will occur if the temperature difference is too great making restarting of the program necessary). Record temperatures throughout the cure cycle.   Save all cure tapes for engineering review.

6.3. 250° F Adhesive Cure Schedule

EA 9628. AF-163-2K, FM-73
(all .085 PSF weight)

Lowest Thermocouple Reading (° F)	Soak Time (Hours)
200	6
220	4
240	2

6.4   COOL DOWN AND CLEAN UP

6.4.1. Do not break vacuum until all thermocouples are below 150° F. When all thermocouples read under 150° F remove vacuum, bagging and curing materials from over the patch and any insulation.

6.4.2. Remove excess flash around patch with Scotchbrite pads.

7.0. THERMOGRAPHIC INSPECTION

7.0.1.   *For C-141 repairs*, perform nondestructive inspection of repair patch in accordance with LJ specification 93-LJLE-021, "QUALITY SPECIFICATION FOR INSTALLATION OF COMPOSITE REPAIRS ON C-141 AIRCRAFT".

7.0.2   For C-130 repairs, thermographic inspection shall be performed by a level 1 or greater certified inspector. No delaminations or disbonds 1.5 inches of the ends (load transfer ends) of the patch and .5 inches of any non load transfer side. Maximum single disbond or delamination is 0.5 inches diameter, maximum cluster of smaller bubbles /delaminations/disbonds is 2 inches in diameter. If cracks are repaired, no delamination or disbond within 1 inch of the crack site.

8.0. CORROSION PROTECTION AND FINISH

8.0.1. *For both C-141 and C-130*, apply corrosion protection and finish to areas around the patch in accordance with LJ specification 93-LJLE-022, "FINISH AND SEALING PROCEDURES FOR COMPOSITE WEEPHOLE CRACK REPAIRS, C-141 LOWER INNER WING".

Attachment 1

Specific on Materials Required
for
Durability Patch Installation
and
Silane Surface Preparation

Solvent (MEK, reagent grade acetone)
Markers
Sanding Disks
Rubber Gloves
Dust Mask
Duralace
Oil-Free Nitrogen
Scotchbrite, 3M Company
Aluminum Oxide Grit (50 micron)
Vacuum Bagging Material
Tape (masking, flash breaker, Teflon)
Silane (Z 6040)
Distilled Water
Glass Beaker/Flask
Mixing Magnet
Cotton Gloves
Acid Brushes
Porous Teflon Coated Fiberglass or Release Bleeder B
Nonporous Teflon Coated Fiberglass or Perforated Red Release Film
Breather Material
Bleeder Material
Divinycell
BR-127 Primer
Dexter EA 9696, Cytec FM 73, or equivalent, Adhesive
Fiberite MXB-7701/7781 woven fiberglass prepreg (or equivalent)
VEM (Visco Elastic damping Material)

Attachment 2

Specific on Equipment Required
for
Durability Patch Installation
and
Silane Surface Preparation

High Speed Grinder
Grit Blast Spray Gun
Adhesive Primer Spray Gun
infrared Lamps or Quartz Heaters
Isoscope
Hot Bonder-Briskheat 6000 or 9000
Heater Blankets
J-Type Thermocouples

LIST OF ACRONYMS

Acronym	Description
ADC	Analog-to-digital converter
ADH	Adhesive
ATIS	Aircraft Test Instrumentation System
BC	Boundary condition
CFT	Conformal fuel tank
COTS	Commercial off the shelf
CTE	Coefficient of thermal expansion
DFT	Discrete Fourier transform
DSP	Digital signal processor
EMI	Electromagnetic interference
FEA	Finite element analysis
FEM	Finite element model
FFT	Fast Fourier transform
FG	Fiber glass
FRF	Frequency response function
HCF	High-cycle fatigue
LCT/RCT	Left/right conformal tank
LIF	Life improvement factor
MSE	Modal strain energy
PSA	Pressure-sensitive adhesive
PSD	Power spectral density
RC	Resistor/capacitor
RMS	Root mean square
RN	Record number
SDR	Standard data records
SIF	Stress improvement factor

SPO	Special Program Office
VDC	Direct current voltage
VEM	Viscoelastic material
WDT	Watchdog timer

REFERENCES

1. Rudder, F.F., Jr. and Plumblee, H.E., Jr., "Sonic Fatigue Design Guide for Military Aircraft," USAF AFFDL-TR-74-112, May 1975 (Available from Defense Technical Information Center as ADB 004600). {ASIAC 6915}

2. Byrne, K.P., "On the Growth Rate of Bending Induced Edge Cracks in Panels Excited by Convected Random Pressure Fields," J. Sound Vib. (1980) 68(2), pp 161-171.

3. Soovere, J., and M.L. Drake, "Aerospace Structures Technology Damping Design Guide," USAF-AFWAL-TR-84-3089, 3 Vols., Dec. 1985.

4. Clarkson, B.L. , "Review of Sonic Fatigue Technology," NASA Contractor Report 4587, NASA Langley Research Center, Hampton, VA, April 1994.

5. Wolfe, H.F., Shroyer, C.A., Brown, D.L., and Simmons, L.W., "An Experimental Investigation of Nonlinear Behavior of Beams and Plates Excited to High Levels of Dynamic Response," USAF-WL-TR-96-3057, October 1995.

6. Baker, A.A., and R. Jones, eds., {Bonded Repair of Aircraft Structures}, Martinus Nijhoff Publishers, 1988.

7. Fredell, Robert S., USAF/DFEM, Academy Department of Engineering Mechanics, "Damage Tolerant Repair Techniques for Pressurized Aircraft Fuselages" 2E WL-TR-94-3134, 1994.

8. Composite Repair of Military Aircraft Structures, AGARD CP 550, Oct.\ 1994.

9. Rogers, L.C., R.W. Gordon, and C.D. Johnson "Seminar on Damped Laminated Beams," unpublished, WPAFB OH, 19 March 1980.

10. Johnson, C.D., Kienholz, D.A., Rogers, L.C. "Finite Element Prediction of Damping in Beams with Constrained Viscoelastic Layers," {em Shock and Vibration Bulletin}, No. 51, pp 71-81, May 1981.

11. Johnson, C.D., Kienholz, D.A., "Finite Element Prediction of Damping in Structures with Constrained Viscoelastic Layers," {AIAA Journal}, Vol. 20, No. 9, September 1982.

12. Rogers, L.C. and Fowler, B.L., "Smoothing, Interpolating and Modeling Complex Modulus Data," CSA Rpt, to be published.

13. L. Rogers, et al, "Durability patch: application of passive damping to high cycle fatigue cracking on aircraft," SPIE Smart Structures and Materials - Passive Damping and Isolation Conference - San Diego CA, Paper no. 3045-28, Mar 1997.

14. S.Liguore, R.Perez, and K.Walters, "Damped Composite Bonded Repairs for Acoustic Fatigue," AIAA Structures, Dynamics and Materials Conference, 1997.

15. R.Callinan, L. Rose, C. Wang, "Three Dimensional Stress Analysis of Crack Patching," ICF9, International Conference on Fracture, Sydney Australia, June 1997.

16. R. Callinan, S. Galea, S. Sanderson, "Composite Bonded Repair of Cracked Panels Subject to Acoustic Fatigue," ICCM-11, Melbourne Australia, July 1997.

17. Rogers, L. C. and Searle I. R., "Durability Patch: repair and life extension of high cycle fatigue damage on secondary structure of aging aircraft" DOD/FAA/NASA Conference on Aging Aircraft, July 8-10 1997, Ogden UT

18. Anderson, K. F., "Practical Applications of Current Loop Signal Conditioning", Technical Memorandum: NASA-TM-4636, Jan 1995, NASA Dryden Flight Research Facility, Edwards CA.

19. Wong, J., "A Collection of Amp Applications", Application Note AN-106, Analog Devices, Norwood, Ma

20. Klonowski, P., "Use of the AD590 Temperature Transducer in a Remote Sensing Application", Application Note AN-273, Analog Devices, Norwood, MA.

21. Schreier, Paul, Editor, "For data collection at rugged or remote sites, loggers still rule", Cover Story, Personal Engineering & Instrumentation News, August 1997, Vol 14, No 8.

22. Dallas Semiconductor, "Watchdog Timekeeper" Application Note 66, Dallas Semiconductor, Dallas, TX.

23. O'Byrne, M. A., *Electromagnetic Interference Control Requirements*, Boeing Document Number D6-16050-4, July 7, 1991.

24. MIL-STD-461D, Requirements for the Control of Electromagnetic Interference Emissions and Susceptibility, August 4, 1986.

25. Kinlock, Tony, "Adhesives and Adhesion".